



**Related U.S. Application Data**

continuation of application No. 11/582,206, filed on Oct. 16, 2006, now Pat. No. 7,460,852, which is a continuation of application No. 10/922,135, filed on Aug. 18, 2004, now Pat. No. 7,123,898, which is a continuation of application No. 10/267,531, filed on Oct. 8, 2002, now Pat. No. 6,804,502.

(60) Provisional application No. 60/328,353, filed on Oct. 10, 2001.

(51) **Int. Cl.**

- H04M 1/00** (2006.01)
- H04B 1/40** (2015.01)
- H01P 1/15** (2006.01)
- H03K 17/06** (2006.01)
- H03K 17/10** (2006.01)
- H03K 17/693** (2006.01)
- H03K 19/0185** (2006.01)
- H03K 19/0944** (2006.01)
- H03K 17/08** (2006.01)

(52) **U.S. Cl.**

CPC ..... **H03K 17/102** (2013.01); **H03K 17/693** (2013.01); **H03K 19/018521** (2013.01); **H03K 19/0944** (2013.01); **H03K 2017/0803** (2013.01)

(56) **References Cited**

U.S. PATENT DOCUMENTS

3,699,359	A	10/1972	Shelby
3,731,112	A	5/1973	Smith
3,878,450	A	4/1975	Greatbatch
3,942,047	A	3/1976	Buchanan
3,943,428	A	3/1976	Whidden
3,955,353	A	5/1976	Astle
3,975,671	A	8/1976	Stoll
3,988,727	A	10/1976	Scott
4,047,091	A	9/1977	Hutchines et al.
4,053,916	A	10/1977	Cricchi et al.
4,061,929	A	12/1977	Asano
4,068,295	A	1/1978	Portmann
4,079,336	A	3/1978	Gross
4,106,086	A	8/1978	Holbrook et al.
4,139,826	A	2/1979	Pradal
4,145,719	A	3/1979	Hand et al.
4,186,436	A	1/1980	Ishiwatari
4,241,316	A	12/1980	Knapp
4,244,000	A	1/1981	Ueda et al.
4,256,977	A	3/1981	Hendrickson
4,316,101	A	2/1982	Minner
4,317,055	A	2/1982	Yoshida et al.
4,321,661	A	3/1982	Sano
4,367,421	A	1/1983	Baker
4,390,798	A	6/1983	Kurafuji
4,460,952	A	7/1984	Risinger
RE31,749	E	11/1984	Yamashiro
4,485,433	A	11/1984	Topich
4,621,315	A	11/1986	Vaughn et al.
4,633,106	A	12/1986	Backes et al.
4,638,184	A	1/1987	Kimura
4,679,134	A	7/1987	Bingham
4,703,196	A	10/1987	Arakawa
4,736,169	A	4/1988	Weaver et al.
4,739,191	A	4/1988	Puar
4,746,960	A	5/1988	Valeri et al.
4,748,485	A	5/1988	Vasudev
4,752,699	A	6/1988	Cranford et al.
4,769,784	A	9/1988	Doluca et al.
4,777,577	A	10/1988	Bingham et al.
4,809,056	A	2/1989	Shirato et al.
4,810,911	A	3/1989	Noguchi
4,825,145	A	4/1989	Tanaka et al.

4,839,787	A	6/1989	Kojima et al.
4,847,519	A	7/1989	Wahl et al.
4,849,651	A	7/1989	Estes, Jr.
4,890,077	A	12/1989	Sun
4,891,609	A	1/1990	Eilley
4,893,070	A	1/1990	Milberger et al.
4,897,774	A	1/1990	Bingham et al.
4,906,587	A	3/1990	Blake
4,929,855	A	5/1990	Ezzeddine
4,939,485	A	7/1990	Eisenberg
4,984,040	A	1/1991	Yap
4,985,647	A	1/1991	Kawada
4,999,585	A	3/1991	Burt et al.
5,001,528	A	3/1991	Bahraman
5,012,123	A	4/1991	Ayasli et al.
5,023,494	A	6/1991	Tsukii et al.
5,029,282	A	7/1991	Ito
5,032,799	A	7/1991	Milberger et al.
5,038,325	A	8/1991	Douglas et al.
5,041,797	A	8/1991	Belcher et al.
5,061,907	A	10/1991	Rasmussen
5,061,911	A	10/1991	Weidman et al.
5,068,626	A	11/1991	Takagi et al.
5,081,371	A	1/1992	Wong
5,081,706	A	1/1992	Kim
5,095,348	A	3/1992	Houston
5,107,152	A	4/1992	Jain et al.
5,111,375	A	5/1992	Marshall
5,124,762	A	6/1992	Childs et al.
5,125,007	A	6/1992	Yamaguchi et al.
5,126,590	A	6/1992	Chern
5,138,190	A	8/1992	Yamazaki et al.
5,146,178	A	9/1992	Nojima et al.
5,148,393	A	9/1992	Furuyama
5,157,279	A	10/1992	Lee
5,182,529	A	1/1993	Chern
5,193,198	A	3/1993	Yokouchi
5,208,557	A	5/1993	Kersh, III
5,212,456	A	5/1993	Kovalcik et al.
5,272,457	A	12/1993	Heckaman et al.
5,274,343	A	12/1993	Russell et al.
5,283,457	A	2/1994	Matloubian
5,285,367	A	2/1994	Keller
5,306,954	A	4/1994	Chan et al.
5,313,083	A	5/1994	Schindler
5,317,181	A	5/1994	Tyson
5,319,604	A	6/1994	Imondi et al.
5,345,422	A	9/1994	Redwine
5,349,306	A	9/1994	Apel
5,350,957	A	9/1994	Cooper et al.
5,375,256	A	12/1994	Yokoyama et al.
5,375,257	A	12/1994	Lampen
5,392,186	A	2/1995	Alexander et al.
5,392,205	A	2/1995	Zavaleta
5,405,795	A	4/1995	Beyer et al.
H1435	H	5/1995	Cherne et al.
5,416,043	A	5/1995	Burgener et al.
5,422,586	A	6/1995	Tedrow et al.
5,422,590	A	6/1995	Coffman et al.
5,442,327	A	8/1995	Longbrake et al.
5,446,418	A	8/1995	Hara et al.
5,448,207	A	9/1995	Kohama
5,455,794	A	10/1995	Javanifard et al.
5,465,061	A	11/1995	Dufour
5,477,184	A	12/1995	Uda et al.
5,488,243	A	1/1996	Tsuruta et al.
5,492,857	A	2/1996	Reedy et al.
5,493,249	A	2/1996	Manning
5,519,360	A	5/1996	Keeth
5,535,160	A	7/1996	Yamaguchi
5,548,239	A	8/1996	Kohama
5,553,021	A	9/1996	Kubono et al.
5,553,295	A	9/1996	Pantelakis et al.
5,554,892	A	9/1996	Norimatsu
5,559,368	A	9/1996	Hu et al.
5,572,040	A	11/1996	Reedy et al.
5,576,647	A	11/1996	Sutardja et al.
5,578,853	A	11/1996	Hayashi et al.
5,581,106	A	12/1996	Hayashi et al.

(56)

## References Cited

## U.S. PATENT DOCUMENTS

5,589,793	A	12/1996	Kassapian	5,969,560	A	10/1999	Kohama et al.
5,594,371	A	1/1997	Douseki	5,969,571	A	10/1999	Swanson
5,596,205	A	1/1997	Reedy et al.	5,973,363	A	10/1999	Staab et al.
5,597,739	A	1/1997	Sumi et al.	5,973,382	A	10/1999	Burgener et al.
5,600,169	A	2/1997	Burgener et al.	5,973,636	A	10/1999	Okubo et al.
5,600,588	A	2/1997	Kawashima	5,986,518	A	11/1999	Dougherty
5,610,533	A	3/1997	Arimoto et al.	5,990,580	A	11/1999	Weigand
5,629,655	A	5/1997	Dent	6,020,778	A	2/2000	Shigehara
5,663,570	A	9/1997	Reedy et al.	6,020,781	A	2/2000	Fujioka
5,670,907	A	9/1997	Gorecki et al.	6,020,848	A	2/2000	Wallace et al.
5,672,992	A	9/1997	Nadd	6,049,110	A	4/2000	Koh
5,677,649	A	10/1997	Martin	6,057,555	A	5/2000	Reedy et al.
5,681,761	A	10/1997	Kim	6,057,723	A	5/2000	Yamaji et al.
5,689,144	A	11/1997	Williams	6,061,267	A	5/2000	Houston
5,694,308	A	12/1997	Cave	6,063,686	A	5/2000	Masuda et al.
5,698,877	A	12/1997	Gonzalez	6,064,253	A	5/2000	Faulkner et al.
5,699,018	A	12/1997	Yamamoto et al.	6,064,275	A	5/2000	Yamauchi
5,717,356	A	2/1998	Kohama	6,064,872	A	5/2000	Vice
5,729,039	A	3/1998	Beyer et al.	6,066,993	A	5/2000	Yamamoto et al.
5,731,607	A	3/1998	Kohama	6,081,165	A	6/2000	Goldman
5,734,291	A	3/1998	Tasdighi et al.	6,081,443	A	6/2000	Morishita et al.
5,748,016	A	5/1998	Kurosawa	6,081,694	A	6/2000	Matsuura et al.
5,748,053	A	5/1998	Kameyama et al.	6,084,255	A	7/2000	Ueda et al.
5,753,955	A	5/1998	Fechner	6,087,893	A	7/2000	Oowaki et al.
5,757,170	A	5/1998	Pinney	6,094,088	A	7/2000	Yano
5,760,652	A	6/1998	Yamamoto et al.	6,100,564	A	8/2000	Bryant et al.
5,767,549	A	6/1998	Chen et al.	6,104,061	A	8/2000	Forbes et al.
5,774,411	A	6/1998	Hsieh et al.	6,107,885	A	8/2000	Migueluez et al.
5,774,792	A	6/1998	Tanaka et al.	6,111,778	A	8/2000	MacDonald et al.
5,777,530	A	7/1998	Nakatuka	6,114,923	A	9/2000	Mizutani
5,784,311	A	7/1998	Assaderaghi et al.	6,118,343	A	9/2000	Winslow
5,784,687	A	7/1998	Itoh et al.	6,122,185	A	9/2000	Utsunomiya et al.
5,786,617	A	7/1998	Merrill et al.	6,130,570	A	10/2000	Pan et al.
5,793,246	A	8/1998	Costello et al.	6,130,572	A	10/2000	Ghilardelli et al.
5,801,577	A	9/1998	Tailliet	6,133,752	A	10/2000	Kawagoe
5,804,858	A	9/1998	Hsu et al.	6,137,367	A	10/2000	Ezzedine et al.
5,807,772	A	9/1998	Takemura	6,160,292	A	12/2000	Flaker et al.
5,808,505	A	9/1998	Tsukada	6,169,444	B1	1/2001	Thurber, Jr.
5,812,939	A	9/1998	Kohama	6,172,378	B1	1/2001	Hull et al.
5,814,899	A	9/1998	Okumura et al.	6,173,235	B1	1/2001	Maeda
5,818,099	A	* 10/1998	Burghartz ..... 257/548	6,177,826	B1	1/2001	Mashiko et al.
5,818,278	A	10/1998	Yamamoto et al.	6,188,247	B1	2/2001	Storino et al.
5,818,283	A	10/1998	Tonami et al.	6,188,590	B1	2/2001	Chang et al.
5,818,289	A	10/1998	Chevallier et al.	6,191,449	B1	2/2001	Shino
5,818,766	A	10/1998	Song	6,191,653	B1	2/2001	Camp, Jr. et al.
5,821,769	A	10/1998	Douseki	6,195,307	B1	2/2001	Umezawa et al.
5,821,800	A	10/1998	Le et al.	6,201,761	B1	3/2001	Wollesen
5,825,227	A	10/1998	Kohama et al.	RE37,124	E	4/2001	Monk et al.
5,861,336	A	1/1999	Reedy et al.	6,215,360	B1	4/2001	Callaway, Jr.
5,863,823	A	1/1999	Burgener	6,218,248	B1	4/2001	Hwang et al.
5,864,328	A	1/1999	Kajimoto	6,218,890	B1	4/2001	Yamaguchi et al.
5,874,836	A	2/1999	Nowak et al.	6,218,892	B1	4/2001	Soumyanath et al.
5,874,849	A	2/1999	Marotta et al.	6,222,394	B1	4/2001	Allen et al.
5,877,978	A	3/1999	Morishita et al.	6,225,866	B1	5/2001	Kubota et al.
5,878,331	A	3/1999	Yamamoto et al.	6,239,649	B1	5/2001	Bertin et al.
5,880,620	A	3/1999	Gitlin et al.	6,239,657	B1	5/2001	Bauer
5,883,396	A	3/1999	Reedy et al.	6,249,027	B1	6/2001	Burr
5,883,541	A	3/1999	Tahara et al.	6,249,029	B1	6/2001	Bryant et al.
5,889,428	A	3/1999	Young	6,249,446	B1	6/2001	Shearon et al.
5,892,260	A	4/1999	Okumura et al.	6,281,737	B1	8/2001	Kuang et al.
5,892,382	A	4/1999	Ueda et al.	6,288,458	B1	9/2001	Berndt
5,892,400	A	4/1999	van Sadars et al.	6,297,687	B1	10/2001	Sugimura
5,895,957	A	4/1999	Reedy et al.	6,297,696	B1	10/2001	Abdollahian et al.
5,903,178	A	5/1999	Miyatsuji et al.	6,300,796	B1	10/2001	Troutman et al.
5,912,560	A	6/1999	Pasternak	6,304,110	B1	10/2001	Hirano
5,917,362	A	6/1999	Kohama	6,308,047	B1	10/2001	Yamamoto et al.
5,920,093	A	7/1999	Huang et al.	6,310,508	B1	10/2001	Westerman
5,920,233	A	7/1999	Denny	6,316,983	B1	11/2001	Kitamura
5,926,466	A	7/1999	Ishida et al.	6,320,225	B1	11/2001	Hargrove et al.
5,930,605	A	7/1999	Mistry et al.	6,337,594	B1	1/2002	Hwang
5,930,638	A	7/1999	Reedy et al.	6,341,087	B1	1/2002	Kunikiyo
5,945,867	A	8/1999	Uda et al.	6,356,536	B1	3/2002	Repke
5,945,879	A	8/1999	Rodwell et al.	6,365,488	B1	4/2002	Liao
5,953,557	A	9/1999	Kawahara	6,380,793	B1	4/2002	Bancal et al.
5,959,335	A	9/1999	Bryant et al.	6,380,802	B1	4/2002	Pehike et al.
				6,387,739	B1	5/2002	Smith
				6,392,440	B2	5/2002	Nebel
				6,392,467	B1	5/2002	Oowaki et al.
				6,396,325	B2	5/2002	Goodell

(56)

## References Cited

## U.S. PATENT DOCUMENTS

6,396,352	B1	5/2002	Muza	6,882,210	B2	4/2005	Asano et al.
6,400,211	B1	6/2002	Yokomizo et al.	6,891,234	B1	5/2005	Connelly et al.
6,407,427	B1	6/2002	Oh	6,897,701	B2	5/2005	Chen et al.
6,407,614	B1	6/2002	Takahashi	6,898,778	B2	5/2005	Kawanaka
6,411,156	B1	6/2002	Borkar et al.	6,903,596	B2	6/2005	Geller et al.
6,411,531	B1	6/2002	Nork et al.	6,908,832	B2	6/2005	Farrens et al.
6,414,353	B2	7/2002	Maeda et al.	6,917,258	B2	7/2005	Kushitani et al.
6,414,863	B1	7/2002	Bayer et al.	6,933,744	B2	8/2005	Das et al.
6,429,487	B1	8/2002	Kunikiyo	6,934,520	B2	8/2005	Rozsypal
6,429,632	B1	8/2002	Forbes et al.	6,947,720	B2	9/2005	Razavi et al.
6,429,723	B1	8/2002	Hastings	6,954,623	B2	10/2005	Chang et al.
6,433,587	B1	8/2002	Assaderaghi et al.	6,969,668	B1	11/2005	Kang et al.
6,433,589	B1	8/2002	Lee	6,975,271	B2	12/2005	Adachi et al.
6,449,465	B1	9/2002	Gailus et al.	6,978,122	B2	12/2005	Kawakyu et al.
6,452,232	B1	9/2002	Adan	6,978,437	B1	12/2005	Rittman et al.
6,461,902	B1	10/2002	Xu et al.	7,023,260	B2	4/2006	Thorp et al.
6,466,082	B1	10/2002	Krishnan	7,042,245	B2	5/2006	Hidaka
6,469,568	B2	10/2002	Toyoyama et al.	7,045,873	B2	5/2006	Chen et al.
6,486,511	B1	11/2002	Nathanson et al.	7,056,808	B2	6/2006	Henley et al.
6,486,729	B2	11/2002	Imamiya	7,057,472	B2	6/2006	Fukamachi et al.
6,496,074	B1	12/2002	Sowlati	7,058,922	B2	6/2006	Kawanaka
6,498,058	B1	12/2002	Bryant et al.	7,068,096	B2	6/2006	Chu
6,498,370	B1	12/2002	Kim et al.	7,082,293	B1	7/2006	Rofougaran et al.
6,504,212	B1	1/2003	Allen et al.	7,088,971	B2	8/2006	Burgener et al.
6,504,213	B1	1/2003	Ebina	7,092,677	B1	8/2006	Zhang et al.
6,509,799	B1	1/2003	Franca-Neto	7,109,532	B1	9/2006	Lee et al.
6,512,269	B1	1/2003	Bryant et al.	7,123,898	B2	10/2006	Burgener et al.
6,518,645	B2	2/2003	Bae et al.	7,129,545	B2	10/2006	Cain
6,518,829	B2	2/2003	Butler	7,132,873	B2	11/2006	Hollmer
6,521,959	B2	2/2003	Kim et al.	7,138,846	B2	11/2006	Suwa et al.
6,537,861	B1	3/2003	Kroell et al.	7,161,197	B2	1/2007	Nakatsuka et al.
6,559,689	B1	5/2003	Clark	7,173,471	B2	2/2007	Nakatsuka et al.
6,563,366	B1	5/2003	Kohama	7,199,635	B2	4/2007	Nakatsuka et al.
6,608,785	B2	8/2003	Chuang et al.	7,202,712	B2	4/2007	Athas
6,608,789	B2	8/2003	Sullivan et al.	7,202,734	B1	4/2007	Raab
6,617,933	B2	9/2003	Ito et al.	7,212,788	B2	5/2007	Weber et al.
6,631,505	B2	10/2003	Arai	7,248,120	B2	7/2007	Burgener et al.
6,632,724	B2	10/2003	Henley et al.	7,266,014	B2	9/2007	Wu et al.
6,642,578	B1	11/2003	Arnold et al.	7,269,392	B2	9/2007	Nakajima et al.
6,646,305	B2	11/2003	Assaderaghi et al.	7,307,490	B2	12/2007	Kizuki
6,653,697	B2	11/2003	Hidaka et al.	7,345,342	B2	3/2008	Challa
6,670,655	B2	12/2003	Lukes et al.	7,345,521	B2	3/2008	Takahashi et al.
6,677,641	B2	1/2004	Kocon	7,355,455	B2	4/2008	Hidaka
6,677,803	B1	1/2004	Chiba	7,359,677	B2	4/2008	Huang et al.
6,684,055	B1	1/2004	Blackaby et al.	7,391,282	B2	6/2008	Nakatsuka et al.
6,684,065	B2	1/2004	Bult	7,404,157	B2	7/2008	Tanabe
6,693,326	B2	2/2004	Adan	7,405,982	B1	7/2008	Flaker et al.
6,693,498	B1	2/2004	Sasabata et al.	7,432,552	B2	10/2008	Park
6,698,082	B2	3/2004	Crenshaw et al.	7,457,594	B2	11/2008	Theobold et al.
6,698,498	B1	3/2004	Ziegelaar et al.	7,460,852	B2	12/2008	Burgener et al.
6,703,863	B2	3/2004	Gion	7,515,882	B2	4/2009	Kelcourse et al.
6,704,550	B1	3/2004	Kohama et al.	7,546,089	B2	6/2009	Bellantoni
6,711,397	B1	3/2004	Petrov et al.	7,551,036	B2	6/2009	Berroth et al.
6,714,065	B2	3/2004	Komiya et al.	7,561,853	B2	7/2009	Miyazawa
6,717,458	B1	4/2004	Potanin	7,616,482	B2	11/2009	Prall
6,762,477	B2	7/2004	Kunikiyo	7,659,152	B2	2/2010	Gonzalez et al.
6,774,701	B1	8/2004	Heston et al.	7,710,189	B2	5/2010	Toda
6,781,805	B1	8/2004	Urakawa	7,719,343	B2	5/2010	Burgener et al.
6,788,130	B2	9/2004	Pauletti et al.	7,733,156	B2	6/2010	Brederlow et al.
6,790,747	B2	9/2004	Henley et al.	7,733,157	B2	6/2010	Brederlow et al.
6,801,076	B1	10/2004	Merritt	7,741,869	B2	6/2010	Hidaka
6,803,680	B2	10/2004	Brindle et al.	7,756,494	B2	7/2010	Fujioka et al.
6,804,502	B2	10/2004	Burgener et al.	7,786,807	B1	8/2010	Li et al.
6,816,000	B2	11/2004	Miyamitsu	7,796,969	B2	9/2010	Kelly et al.
6,816,001	B2	11/2004	Khouri et al.	7,808,342	B2	10/2010	Prikhodko et al.
6,816,016	B2	11/2004	Sander et al.	7,817,966	B2	10/2010	Prikhodko et al.
6,819,938	B2	11/2004	Sahota	7,860,499	B2	12/2010	Burgener et al.
6,825,730	B1	11/2004	Sun	7,868,683	B2	1/2011	Iklov
6,830,963	B1	12/2004	Forbes	7,890,891	B2	2/2011	Stuber et al.
6,831,847	B2	12/2004	Perry	7,910,993	B2	3/2011	Brindle et al.
6,833,745	B2	12/2004	Hausmann et al.	7,928,759	B2	4/2011	Hidaka
6,836,172	B2	12/2004	Okashita	7,936,213	B2	5/2011	Shin et al.
6,870,241	B2	3/2005	Nakatani et al.	7,960,772	B2	6/2011	Englekirk
6,871,059	B1	3/2005	Piro et al.	7,982,265	B2	7/2011	Challa et al.
6,879,502	B2	4/2005	Yoshida et al.	8,081,928	B2	12/2011	Kelly
				8,103,226	B2	1/2012	Andrys et al.
				8,111,104	B2	2/2012	Ahadian et al.
				8,129,787	B2	3/2012	Brindle et al.
				8,131,225	B2	3/2012	Botula et al.

(56)

## References Cited

## U.S. PATENT DOCUMENTS

8,131,251	B2	3/2012	Burgener et al.
8,195,103	B2	6/2012	Waheed et al.
8,232,627	B2	7/2012	Bryant et al.
8,253,494	B2	8/2012	Blednov
8,405,147	B2	3/2013	Brindle et al.
8,427,241	B2	4/2013	Ezzeddine et al.
8,527,949	B1	9/2013	Pleis et al.
8,536,636	B2	9/2013	Englekirk
8,559,907	B2	10/2013	Burgener et al.
8,583,111	B2	11/2013	Burgener et al.
8,649,754	B2	2/2014	Burgener et al.
8,729,948	B2	5/2014	Sugiura
8,742,502	B2	6/2014	Brindle et al.
8,954,902	B2	2/2015	Stuber et al.
9,087,899	B2	7/2015	Brindle et al.
9,130,564	B2	9/2015	Brindle et al.
2001/0015461	A1	8/2001	Ebina
2001/0031518	A1	10/2001	Kim et al.
2001/0040479	A1	11/2001	Zhang
2001/0045602	A1	11/2001	Maeda et al.
2002/0029971	A1	3/2002	Kovacs
2002/0079971	A1	6/2002	Vathulya
2002/0115244	A1	8/2002	Park et al.
2002/0126767	A1	9/2002	Ding et al.
2002/0195623	A1	12/2002	Horiuchi et al.
2003/0002452	A1	1/2003	Sahota
2003/0032396	A1	2/2003	Tsuchiya et al.
2003/0141543	A1	7/2003	Bryant et al.
2003/0160515	A1	8/2003	Yu et al.
2003/0181167	A1	9/2003	Iida
2003/0201494	A1	10/2003	Maeda et al.
2003/0205760	A1	11/2003	Kawanaka et al.
2003/0222313	A1	12/2003	Fechner
2003/0224743	A1	12/2003	Okada et al.
2003/0227056	A1	12/2003	Wang et al.
2004/0021137	A1	2/2004	Fazan et al.
2004/0061130	A1	4/2004	Morizuka
2004/0080364	A1	4/2004	Sander et al.
2004/0121745	A1	6/2004	Meck
2004/0129975	A1	7/2004	Koh et al.
2004/0204013	A1	10/2004	Ma et al.
2004/0227565	A1	11/2004	Chen et al.
2004/0242182	A1	12/2004	Hidaka et al.
2005/0077564	A1	4/2005	Forbes
2005/0079829	A1	4/2005	Ogawa et al.
2005/0121699	A1	6/2005	Chen et al.
2005/0122163	A1	6/2005	Chu
2005/0127442	A1	6/2005	Veeraraghavan et al.
2005/0167751	A1	8/2005	Nakajima et al.
2005/0212595	A1	9/2005	Kusunoki et al.
2005/0264341	A1	12/2005	Hikita et al.
2006/0009164	A1	1/2006	Kataoka
2006/0022526	A1	2/2006	Cartalade
2006/0077082	A1	4/2006	Shanks
2006/0161520	A1	7/2006	Brewer et al.
2006/0194558	A1	8/2006	Kelly
2006/0194567	A1	8/2006	Kelly et al.
2006/0267093	A1	11/2006	Tang
2006/0270367	A1	11/2006	Burgener et al.
2006/0281418	A1	12/2006	Huang et al.
2007/0018247	A1	1/2007	Brindle et al.
2007/0023833	A1	2/2007	Okhonin et al.
2007/0045697	A1	3/2007	Cheng et al.
2007/0279120	A1	12/2007	Brederlow et al.
2007/0290744	A1	12/2007	Adachi et al.
2008/0073719	A1	3/2008	Fazan et al.
2008/0076371	A1	3/2008	Dribinsky et al.
2008/0191788	A1	8/2008	Chen et al.
2008/0303080	A1	12/2008	Bhattacharyya
2009/0029511	A1	1/2009	Wu
2010/0330938	A1	12/2010	Yin
2011/0092179	A1	4/2011	Burgener et al.
2011/0163779	A1	7/2011	Hidaka
2011/0169550	A1	7/2011	Brindle et al.
2011/0299437	A1	12/2011	Mikhemar et al.
2012/0007679	A1	1/2012	Burgener et al.
2012/0169398	A1	7/2012	Brindle et al.
2012/0267719	A1	10/2012	Brindle et al.
2013/0015717	A1	1/2013	Dykstra
2013/0293280	A1	11/2013	Brindle et al.
2014/0028521	A1	1/2014	Bauder et al.
2014/0085006	A1	3/2014	Mostov et al.
2014/0087673	A1	3/2014	Mostov et al.
2014/0165385	A1	6/2014	Englekirk
2014/0167834	A1	6/2014	Stuber et al.
2014/0179249	A1	6/2014	Burgener et al.
2014/0306767	A1	10/2014	Burgener et al.
2014/0312422	A1	10/2014	Brindle et al.
2015/0015321	A1	1/2015	Dribinsky et al.

## FOREIGN PATENT DOCUMENTS

DE	19832565	8/1999
DE	112011103554	9/2013
EP	0385641	9/1990
EP	0622901	11/1994
EP	782267	7/1997
EP	0788185	8/1997
EP	0851561	1/1998
EP	913939	5/1999
EP	625831	11/1999
EP	1006584	6/2000
EP	1451890	2/2011
EP	2348532	7/2011
EP	2348533	7/2011
EP	2348534	7/2011
EP	2348535	7/2011
EP	2348536	7/2011
EP	2387094	11/2011
EP	1774620	10/2014
EP	2884586	6/2015
JP	A-55-75348	6/1980
JP	1-254014	10/1989
JP	A-02-161769	6/1990
JP	04-34980	2/1992
JP	4-183008	6/1992
JP	5299995	11/1993
JP	6112795	4/1994
JP	06-314985	11/1994
JP	A-06-334506	12/1994
JP	7046109	2/1995
JP	07-070245	3/1995
JP	07106937	4/1995
JP	8023270	1/1996
JP	8070245	3/1996
JP	8-148949	6/1996
JP	11163704	6/1996
JP	8251012	9/1996
JP	A-08-307305	11/1996
JP	8330930	12/1996
JP	09-008621	1/1997
JP	9008627	1/1997
JP	9041275	2/1997
JP	9055682	2/1997
JP	9092785	4/1997
JP	9148587	6/1997
JP	09163721	6/1997
JP	9163721	6/1997
JP	09-200021	7/1997
JP	9181641	7/1997
JP	9186501	7/1997
JP	9200074	7/1997
JP	9238059	9/1997
JP	9243738	9/1997
JP	9270659	10/1997
JP	9284170	10/1997
JP	9298493	10/1997
JP	A-09-284114	10/1997
JP	9326642	12/1997
JP	10079467	3/1998
JP	10-93471	4/1998
JP	10-242477	9/1998
JP	10242826	9/1998
JP	A-10-242829	9/1998

(56)

## References Cited

## FOREIGN PATENT DOCUMENTS

JP	10-344247	12/1998
JP	10335901	12/1998
JP	11026776	1/1999
JP	11112316	4/1999
JP	A-11-13611	5/1999
JP	11163642	6/1999
JP	11205188	7/1999
JP	11274804	10/1999
JP	2000031167	1/2000
JP	2000183353	6/2000
JP	2000188501	7/2000
JP	2000208614	7/2000
JP	2000223713	8/2000
JP	2000243973	9/2000
JP	2000277703	10/2000
JP	2000294786	10/2000
JP	2000311986	11/2000
JP	2001007332	1/2001
JP	2001089448	3/2001
JP	2001-119281	4/2001
JP	2001157487	5/2001
JP	2001156182	6/2001
JP	2001274265	10/2001
JP	2004515937	5/2002
JP	200216441	6/2002
JP	2003-060451 A	2/2003
JP	2003060451	2/2003
JP	2003101407	4/2003
JP	2003143004	5/2003
JP	2003167615	6/2003
JP	2003-198248 A	7/2003
JP	2003189248	7/2003
JP	2003332583	11/2003
JP	2002156602	12/2003
JP	2004-147175	5/2004
JP	2004-515937 A	5/2004
JP	2004166470	6/2004
JP	2004199950	7/2004
JP	2004288978	10/2004
JP	2005-203643	7/2005
JP	2005-251931	9/2005
JP	2003-347553	12/2008
JP	4659826	1/2011
JP	4892092	12/2011
JP	2010-506156	12/2012
JP	5215850	3/2013
JP	5591356	8/2014
JP	5678106	1/2015
KR	1994027615	12/1994
WO	WO 95/23460 A1	8/1995
WO	WO9523460	8/1995
WO	WO9806174	2/1998
WO	WO9935695	7/1999
WO	WO 02/27920 A1	4/2002
WO	WO0227920	4/2002
WO	2007008934	1/2007
WO	WO2007008934	1/2007
WO	WO2007033045 A2	3/2007
WO	WO2012054642	4/2012

## OTHER PUBLICATIONS

Suh, et al., "A Physical Charge-Based Model for Non-Fully Depleted SOI MOSFET's and Its Use in Assessing Floating-Body Effects in SOI CMOS Circuits", IEEE Transactions on Electron Devices, vol. 42, No. 4, Apr. 1995, pp. 728-737.

Wang, et al., "A Robust Large Signal Non-Quasi-Static MOSFET Model for Circuit Simulation", IEEE 2004 Custom Integrated Circuits Conference, pp. 2-1-1 through 2-1-4.

Tinella, Carlo, "Study of the potential of CMOS-SOI technologies partially abandoned for radiofrequency applications", Thesis for obtaining the standard of Doctor of INPG, National Polytechnic of Grenoble, Sep. 25, 2003, 187 pgs.

Terauchi, et al., "A 'Self-Body-Bias' SOI MOSFET: A Novel Body-Voltage-Controlled SOI MOSFET for Low Voltage Applications", The Japan Society of Applied Physics, vol. 42 (2003), pp. 2014-2019, Part 1, No. 4B, Apr. 2003.

Dehan, et al., "Dynamic Threshold Voltage MOS in Partially Depleted SOI Technology: A Wide Frequency Band Analysis", Solid-State Electronics 49 (2005), pp. 67-72.

Kuroda, et al., "A 0.9-V, 150-MHz, 10-mW, 4 mm<sup>2</sup>, 2-D Discrete Cosine Transform Core Processor with Variable Threshold-Voltage (VT) Scheme", IEEE Journal of Solid-State Circuits, vol. 31, No. 11, Nov. 1996, pp. 1770-1779.

Kuroda, et al., "A 0.9-V, 150-MHz, 10-mW, 4 mm<sup>2</sup>, 2-D Discrete Cosine Transform Core Processor with Variable-Threshold-Voltage Scheme", Technical Paper, 1996 IEEE International Solid-State Circuits Conference, 1996 Digest of Technical Papers, pp. 166-167.

Cathelin, et al., "Antenna Switch Devices in RF Modules for Mobile Applications", ST Microelectronics, Front-End Technology and Manufacturing, Crolles, France, Mar. 2005, 42 pgs.

Cristoloveanu, Sorin, "State-of-the-art and Future of Silicon on Insulator Technologies, Materials, and Devices", Microelectronics Reliability 40 (2000), pp. 771-777.

Sivaram, et al., "Silicon Film Thickness Considerations in SOI-DTMOs", IEEE Device Letters, vol. 23, No. 5, May 2002, pp. 276-278.

Drake, et al., "Analysis of the Impact of Gate-Body Signal Phase on DTMOs Inverters in 0.13um PD-SOI", Department of EECS, University of Michigan, Ann Arbor, MI, Sep./Oct. 2003, 4 pgs.

Drake, et al., "Analysis of the Impact of Gate-Body Signal Phase on DTMOs Inverters in 0.13um PD-SOI", Department of EECS, University of Michigan, Ann Arbor, MI, Sep./Oct. 2003, 16 pgs.

Drake, et al., Evaluation of Dynamic-Threshold Logic for Low-Power VLSI Design in 0.13um PD-SOI, University of Michigan, Ann Arbor, MI, Dec. 2003, 29 pgs.

Casu, Mario Roberto, "High Performance Digital CMOS Circuits in PD-SOI Technology: Modeling and Design", Tesi di Dottorato di Ricerca, Gennaio 2002, Politecnico di Torino, Corso di Dottorato di Ricerca in Ingegneria Elettronica e delle Comunicazioni, 200 pgs.

Dehan, et al., "Alternative Architectures of SOI MOSFET for Improving DC and Microwave Characteristics", Microwave Laboratory, Universite catholique de Louvain, Sep. 2001, 4 pgs.

Colinge, Jean-Pierre, "An SOI Voltage-Controlled Bipolar-MOS Device", IEEE Transactions on Electron Devices, vol. ED-34, No. 4, Apr. 1987, pp. 845-849.

Pellella, et al., "Analysis and Control of Hysteresis in PD/SOI CMOS", University of Florida, Gainesville, FL., 1999 IEEE, pp. 34.5.1 through 34.5.4.

Adriaensen, et al., "Analysis and Potential of the Bipolar- and Hybrid-Mode Thin-Film SOI MOSFETs for High-Temperature Applications", Laboratoire de Microelectronique, Universite catholique de Louvain, May 2001, 5 pgs.

Gentinne, et al., "Measurement and Two-Dimensional Simulation of Thin-Film SOI MOSFETs: Intrinsic Gate Capacitances at Elevated Temperatures", Solid-State Electronics, vol. 39, No. 11, pp. 1613-1619, 1996.

Su, et al., "On the Prediction of Geometry-Dependent Floating-Body Effect in SOI MOSFETs", IEEE Transactions on Electron Devices, vol. 52, No. 7, Jul. 2005, pp. 1662-1664.

Fung, et al., "Present Status and Future Direction of BSIM SOI Model for High-Performance/Low-Power/RF Application", IBM Microelectronics, Semiconductor Research and Development Center, Apr. 2002, 4 pgs.

Weigand, Christopher, "An ASIC Driver for GaAs FET Control Components", Technical Feature, Applied Microwave & Wireless, 2000, pp. 42-48.

Lederer, et al., "Frequency degradation of SOI MOS device output conductance", Microwave Laboratory of UCL, Belgium, IEEE 2003, pp. 76-77.

Lederer, et al., "Frequency degradation of SOI MOS device output conductance", Microwave Laboratory of Universite catholique de Louvain, Belgium, Sep./Oct. 2003, 1 pg.

Cheng, et al., "Gate-Channel Capacitance Characteristics in the Fully-Depleted SOI MOSFET", IEEE Transactions on Electron Devices, vol. 48, No. 2, Feb. 2001, pp. 388-391.

(56)

## References Cited

## OTHER PUBLICATIONS

- Ferlet-Cavrois, et al., "High Frequency Characterization of SOI Dynamic Threshold Voltage MOS (DTMOS) Transistors", 1999 IEEE International SOI Conference, Oct. 1999, pp. 24-25.
- Yeh, et al., "High Performance 0.1um Partially Depleted SOI CMOSFET", 2000 IEEE International SOI Conference, Oct. 2000, pp. 68-69.
- Bawedin, et al., "Unusual Floating Body Effect in Fully Depleted MOSFETs", IMEP, Enserg, France and Microelectronics Laboratory, UCL, Belgium, Oct. 2004, 22 pgs.
- Flandre, et al., "Design of EEPROM Memory Cells in Fully Depleted CMOS SOI Technology", Catholic University of Louvain Faculty of Applied Science, Laboratory of Electronics and Microelectronics, Academic Year 2003-2004, 94 pgs.
- Takamiya, et al., "High-Performance Accumulated Back-Interface Dynamic Threshold SOI MOSFET (AB-DTMOS) with Large Body Effect at Low Supply Voltage", Japanese Journal of Applied Physics, vol. 38 (1999), Part 1, No. 4B, Apr. 1999, pp. 2483-2486.
- Drake, et al., "Evaluation of Dynamic-Threshold Logic for Low-Power VLSI Design in 0.13um PD-SOI", IFIP VLSI-SoC 2003, IFIP WG 10.5 International Conference on Very Large Scale Integration of System-on-Chip, Darmstadt, Germany, Dec. 1-3, 2003.
- Huang, et al., "Hot Carrier Degradation Behavior in SOI Dynamic-Threshold-Voltage nMOSFET's (n-DTMOSFET) Measured by Gated-Diode Configuration", Microelectronics Reliability 43 (2003), pp. 707-711.
- Goo, et al., "History-Effect-Conscious SPICE Model Extraction for PD-SOI Technology", 2004 IEEE International SOI Conference, Oct. 2004, pp. 156-158.
- Workman, et al., "Dynamic Effects in BTG/SOI MOSFETs and Circuits Due to Distributed Body Resistance", Proceedings 1997 IEEE International SOI Conference, Oct. 1997, pp. 28-29.
- Ernst, et al., "Detailed Analysis of Short-Channel SOI DT-MOSFET", Laboratoire de Physique des Composants a Semiconducteurs, Enserg, France, Sep. 1999, pp. 380-383.
- Huang, et al., "Device Physics, Performance Simulations and Measured Results of SOI MOS and DTMOS Transistors and Integrated Circuits", Beijing Microelectronics Technology Institute, 1998 IEEE, pp. 712-715.
- Bernstein, et al., "Design and CAD Challenges in sub-90nm CMOS Technologies", IBM Thomas J. Watson Research Center, NY, Nov. 11-13, 2003, pp. 129-136.
- Wiatr, et al., "Impact of Floating Silicon Film on Small-Signal Parameters of Fully Depleted SOI-MOSFETs Biased into Accumulation", Solid-State Electronics 49 (2005), Received Sep. 11, 2030, revised on Nov. 9, 2004, pp. 779-789.
- Gritsch, et al., "Influence of Generation/Recombination Effects in Simulations of Partially Depleted SOI MOSFETs", Solid-State Electronics 45 (2001), Received Dec. 22, 2000, accepted Feb. 14, 2001, pp. 621-627.
- Chang, et al., "Investigations of Bulk Dynamic Threshold-Voltage MOSFET with 65 GHz "Normal-Mode" Ft and 220GHz "Over-Drive Mode" Ft for RF Applications", Institute of Electronics, National Chiao-Tung University, Taiwan, 2001 Symposium on VLSI Technology Digest of Technical Papers, pp. 89-90.
- Le TMOS en technologie SOI, 3.7.2.2 Pompage de charges, pp. 110-111.
- Horiuchi, Masatada, "A Dynamic-Threshold SOI Device with a J-FET Embedded Source Structure and a Merged Body-Bias-Control Transistor—Part I: A J-FET Embedded Source Structure Properties", IEEE Transactions on Electron Devices, vol. 47, No. 8, Aug. 2000, pp. 1587-1592.
- Horiuchi, Masatada, "A Dynamic-Threshold SOI Device with a J-FET Embedded Source Structure and a Merged Body-Bias-Control Transistor—Part II: Circuit Simulation", IEEE Transactions on Electron Devices, vol. 47, No. 8, Aug. 2000, pp. 1593-1598.
- F. Hameau and O. Rozeau, "Radio-Frequency Circuits Integration Using CMOS SOI 0.25um Technology", 2002 RF IC Design Workshop Europe, Mar. 19-22, 2002, Grenoble, France.
- O. Rozeau et al., "SOI Technologies Overview for Low-Power Low-Voltage Radio-Frequency Applications," Analog Integrated Circuits and Signal Processing, 25, pp. 93-114, Boston, MA, Kluwer Academic Publishers, Nov. 2000.
- C. Tinella et al., "A High-Performance CMOS-SOI Antenna Switch for the 2.55-GHz Band," IEEE Journal of Solid-State Circuits, vol. 38, No. 7, Jul. 2003.
- H. Lee et al., "Analysis of body bias effect with PD-SOI for analog and RF applications," Solid State Electron., vol. 46, pp. 1169-1176, 2002.
- J.-H. Lee, et al., "Effect of Body Structure on Analog Performance of SOI NMOSFETs," Proceedings, 1998 IEEE International SOI Conference, Oct. 5-8, 1998, pp. 61-62.
- C. F. Edwards, et al., The Effect of Body Contact Series Resistance on SOI CMOS Amplifier Stages, IEEE Transactions on Electron Devices, vol. 44, No. 12, Dec. 1997 pp. 2290-2294.
- S. Maeda, et al., Substrate-bias Effect and Source-drain Breakdown Characteristics in Body-tied Short-channel SOI MOSFET's, IEEE Transactions on Electron Devices, vol. 46, No. 1, Jan. 1999 pp. 151-158.
- F. Assaderaghi, et al., "Dynamic Threshold-voltage MOSFET (DTMOS) for Ultra-low Voltage VLSI," IEEE Transactions on Electron Devices, vol. 44, No. 3, Mar. 1997, pp. 414-422.
- G. O. Workman and J. G. Fossum, "A Comparative Analysis of the Dynamic Behavior of BTG/SOI MOSFETs and Circuits with Distributed Body Resistance," IEEE Transactions on Electron Devices, vol. 45, No. 10, Oct. 1998 pp. 2138-2145.
- T.-S. Chao, et al., "High-voltage and High-temperature Applications of DTMOS with Reverse Schottky Barrier on Substrate Contacts," IEEE Electron Device Letters, vol. 25, No. 2, Feb. 2004, pp. 86-88.
- Wei, et al., "Measurement of Transient Effects in SOI DRAM/SRAM Access Transistors", IEEE Electron Device Letters, vol. 17, No. 5, May 1996.
- Kuang, et al., "SRAM Bitline Circuits on PD SOI: Advantages and Concerns", IEEE Journal of Solid-State Circuits, vol. 32, No. 6, Jun. 1997.
- Sleight, et al., "Transient Measurements of SOI Body Contact Effectiveness", IEEE Electron Device Letters, vol. 19, No. 12, Dec. 1998.
- Chung, et al., "SOI MOSFET Structure with a Junction-Type Body Contact for Suppression of Pass Gate Leakage", IEEE Transactions on Electron Devices, vol. 48, No. 7, Jul. 2001.
- Lee, et al., "Effects of Gate Structures on the RF Performance in PD SOI MOSFETs", IEEE Microwave and Wireless Components Letters, vol. 15, No. 4, Apr. 2005.
- Hirano, et al., "Impact of Actively Body-bias Controlled (ABC) SOI SRAM by using Direct Body Contact Technology for Low-Voltage Application" IEEE, 2003, pp. 2.4.1-2.4.4.
- Lee, et al., "Harmonic Distortion Due to Narrow Width Effects in Deep sub-micron SOI-CMOS Device for analog-RF applications", 2002 IEEE International SOI Conference, Oct. 2002.
- Kuo, et al., "Low-Voltage SOI CMOS VLSI Devices and Circuits", 2001, Wiley Interscience, New York, XP001090589, pp. 57-60 and 349-354.
- Peregrine Semiconductor Corporation, Response filed in the EPO dated May 16, 2011 for related appln. No. 11153227.1, 5 pgs.
- Chinese Patent Office, translation of an Office Action received from the Chinese Patent Office dated Jul. 31, 2009 for related appln. No. 200680025128.7, 3 pgs.
- Brindle, Chris, et al, Translation of a Response filed in the Chinese Patent Office dated Nov. 30, 2009 for related appln. No. 200680025128.7, 3 pgs.
- Sedra, Adel A., et al., "Microelectronic Circuits", Fourth Edition, University of Toronto, Oxford University Press, 1982, 1987, 1991 and 1998, pp. 374-375.
- Suehle, et al., "Low Electric Field Breakdown of Thin SiO2 Films Under Static and Dynamic Stress", IEEE Transactions on Electron Devices, vol. 44, No. 5, May 1997.
- Bolam, et al., "Reliability Issues for Silicon-on-Insulator", IBM Microelectronics Division, IEEE 2000, pp. 6.4.1-6.4.4.
- Hu, et al., "A Unified Gate Oxide Reliability Model", IEEE 37th Annual International Reliability Physics Symposium, San Diego, CA 1999, pp. 47-51.

(56)

**References Cited**

## OTHER PUBLICATIONS

- Nguyen, Tram Hoang, Office Action received from the USPTO dated Sep. 19, 2008 for related U.S. Appl. No. 11/484,370, 7 pgs.
- Brindle, Christopher, Response filed in the USPTO dated Jan. 20, 2009 for related U.S. Appl. No. 11/484,370, 7 pgs.
- Nguyen, Tram Hoang, Office Action received from the USPTO dated Apr. 23, 2009 for related U.S. Appl. No. 11/484,370, 11 pgs.
- Brindle, Christopher, Response filed in the USPTO dated Aug. 24, 2009 for related U.S. Appl. No. 11/484,370, 8 pgs.
- Nguyen, Tram Hoang, Office Action received from the USPTO dated Jan. 6, 2010 for related U.S. Appl. No. 11/484,370, 46 pgs.
- Brindle, Christopher, Amendment filed in the USPTO dated Jul. 6, 2010 for related U.S. Appl. No. 11/484,370, 32 pgs.
- Nguyen, Tram Hoang, Notice of Allowance received from the USPTO dated Nov. 12, 2010 for related U.S. Appl. No. 11/484,370, 21 pgs.
- Iperione, Analia, International Search Report received from the EPO dated Nov. 7, 2006 for related appln. No. PCT/US2006/026965, 19 pgs.
- Peregrine Semiconductor Corporation, Response filed in the EPO dated May 16, 2011 for related appln. No. 11153313.9, 8 pgs.
- Peregrine Semiconductor Corporation, Response filed in the EPO dated May 16, 2011 for related appln. No. 11153281.8, 7 pgs.
- Peregrine Semiconductor Corporation, Response filed in the EPO dated May 16, 2011 for related appln. No. 11153241.2, 5 pgs.
- Peregrine Semiconductor Corporation, Response filed in the EPO dated May 16, 2011 for related appln. No. 11153247.9, 6 pgs.
- Kurusu, Masakazu, Japanese Office Action received from the Japanese Patent Office dated Apr. 17, 2012 for related appln. No. 2010-506156, 4 pgs.
- Peregrine Semiconductor Corporation, Response filed in the EPO dated May 15, 2012 for related appln. No. 10011669.8, 19 pgs.
- Patel, Reema, Notice of Allowance received from the USPTO dated May 24, 2012 for related U.S. Appl. No. 13/046,560, 15 pgs.
- Oliveros, Toscano, Communication under Rule 71(3) EPC received from the EPO dated Apr. 25, 2014 for appln. No. 05763216.8, 47 pgs.
- Peregrine Semiconductor Corporation, Response filed in the JPO dated Apr. 28, 2015 for appln. No. 2013-006353, 12 pgs.
- European Patent Office, Communication received from the EPO dated May 2, 2014 for appln. No. 07794407.2, 1 pg.
- Tran, Pablo, Office Action received from the USPTO dated May 8, 2014 for U.S. Appl. No. 14/052,680, 5 pgs.
- European Patent Office, Brief Communication received from the EPO dated May 8, 2014 for appln. No. 02800982.7, 2 pgs.
- Peregrine Semiconductor Corporation, Reply filed in the EPO dated May 8, 2014 for appln. No. 02800982.7, 79 pgs.
- Tat, Binh C., Office Action received from the USPTO dated May 23, 2014 for U.S. Appl. No. 13/948,094, 7 pgs.
- Peregrine Semiconductor Corporation, Translation of Response filed in the JPO dated Jul. 3, 2014 for appln. No. 2013-003388, 14 pgs.
- Japanese Patent Office, Notice of Allowance received from the JPO dated Jul. 8, 2014 for appln. No. 2013-006353, 3 pgs.
- Peregrine Semiconductor Corporation, Response filed in the EPO dated Jul. 11, 2014 for appln. No. 07794407.2, 32 pgs.
- Tat, Binh C., Notice of Allowance received from the USPTO dated Jul. 18, 2014 for U.S. Appl. No. 13/028,144, 29 pgs.
- Tran, Pablo N., Office Action received from the USPTO dated Aug. 7, 2014 for U.S. Appl. No. 14/177,062, 7 pgs.
- European Patent Office, Brief Communication received from the EPO dated Aug. 14, 2014 for appln. No. 02800982.7, 2 pgs.
- Patel, Reema, Office Action received from the USPTO dated Aug. 15, 2014 for U.S. Appl. No. 14/028,357, 8 pgs.
- Nguyen, Niki Hoang, Notice of Allowance received from the USPTO dated Aug. 20, 2014 for U.S. Appl. No. 14/198,315, 11 pgs.
- European Patent Office, Decision to Grant a European patent pursuant to Article 97(1) EPC received from the EPO dated Sep. 4, 2014 for appln. No. 05763216.8, 2 pgs.
- Tat, Binh C., Notice of Allowance received from the USPTO dated Oct. 1, 2014 for U.S. Appl. No. 13/028,144, 15 pgs.
- Brindle, et al., Amendment filed in the USPTO dated Oct. 2, 2014 for U.S. Appl. No. 13/850,251, 13 pgs.
- Peregrine Semiconductor Corporation, Response filed in the EPO dated Oct. 14, 2014 for appln. No. 10011669.8, 30 pgs.
- Stuber, et al., Response/Amendment filed in the USPTO dated Oct. 23, 2014 for U.S. Appl. No. 13/948,094, 28 pgs.
- European Patent Office, Brief Communication received from the EPO dated Oct. 24, 2014 for appln. No. 02800982.7, 2 pgs.
- La Casta, Munoa, Interlocutory decision in opposition proceedings received from the EPO dated Oct. 31, 2014 for appln. No. 02800982.7, 77 pgs.
- Burgener, et al., Amendment filed in the USPTO dated Nov. 10, 2014 for U.S. Appl. No. 14/052,680, 13 pgs.
- Burgener, et al., Response filed in the USPTO dated Nov. 6, 2014 for U.S. Appl. No. 14/177,062, 15 pgs.
- Peregrine Semiconductor Corporation, Response file din the EPO dated Dec. 4, 2014 for U.S. Appl. No. 14/182,150.4, 6 pgs.
- Tat, Binh C., Notice of Allowance received from the USPTO dated Dec. 5, 2014 for U.S. Appl. No. 13/028,144, 13 pgs.
- Stuber, et al., Comments on Examiner's Statement of Reasons for Allowance filed in the USPTO dated Dec. 8, 2014 for U.S. Appl. No. 13/028,144, 4 pgs.
- Tat, Binh C., Office Action received from the USPTO dated Jan. 2, 2015 for U.S. Appl. No. 13/948,094, 187 pgs.
- Nguyen, Niki Hoang, Final Office Action received from the USPTO dated Jan. 22, 2015 for U.S. Appl. No. 13/850,251, 245 pgs.
- Nguyen, Niki Hoang, Notice of Allowance received from the USPTO dated Feb. 3, 2015 for U.S. Appl. No. 14/198,315, 215 pgs.
- Tran, Pablo N., Office Action received from the USPTO dated Feb. 24, 2015 for U.S. Appl. No. 14/177,062, 5 pgs.
- Stuber, et al., Response/Amendment filed in the USPTO dated Mar. 2, 2015 for U.S. Appl. No. 13/948,094, 11 pgs.
- European Patent Office, Invitation pursuant to Rule 63(1) EPC received from the EPO dated Mar. 3, 2015 for appln. No. 14182150.4, 3 pgs.
- Tat, Binh C., Office Action received from the USPTO dated Mar. 27, 2015 for U.S. Appl. No. 13/948,094, 23 pgs.
- Gu, et al., "Low Insertion Loss and High Linearity PHEMT SPDT and SP3T Switch Ics for WLAN 802.11a/b/g Application", 2004 IEEE Radio Frequency Integrated Circuits Symposium, 2004, pp. 505-508.
- Koudymov, et al., "Low Loss High Power RF Switching Using Multifinger AlGaIn/GaN MOSHFETs", University of South Carolina Scholar Commons, 2002, pp. 449-451.
- Abidi, "Low Power Radio Frequency IC's for Portable Communications", IEEE, 1995, pp. 544-569.
- De La Houssaye, et al., "Microwave Performance of Optically Fabricated T-Gate Thin Film Silicon on Sapphire Based MOSFET's", IEEE Electron Device Letters, 1995, pp. 289-292.
- Smuk, et al., "Monolithic GaAs Multi-Throw Switches with Integrated Low Power Decoder/Driver Logic", 1997, IEEE Radio Frequency Integrated Circuits.
- McGrath, et al., "Multi Gate FET Power Switches", Applied Microwave, 1991, pp. 77-88.
- Smuk, et al., "Multi-Throw Plastic MMIC Switches up to 6GHz with Integrated Positive Control Logic", IEEE, 1999, pp. 259-262.
- Razavi, "Next Generation RF Circuits and Systems", IEEE, 1997, pp. 270-282.
- Gould, et al., "NMOS SPDT Switch MMIC with >48dB Isolation and 30dBm IIP3 for Applications within GSM and UMTS Bands", Bell Labs, 2001, pp. 1-4.
- Caverly, "Nonlinear Properties of Gallium Arsenide and Silicon FET-Based RF and Microwave Switches", IEEE, 1998, pp. 1-4.
- McGrath, et al., "Novel High Performance SPDT Power Switches Using Multi-Gate FET's", IEEE, 1991, pp. 839-842.
- Suematsu, "On-Chip Matching SI-MMIC for Mobile Communication Terminal Application", IEEE, 1997, pp. 9-12.
- Caverly, et al., "On-State Distortion in High Electron Mobility Transistor Microwave and RF Switch Control Circuits", IEEE Transactions on Microwave Theory and Techniques, 2000, pp. 98-103.
- "Radiation Hardened CMOS Dual DPST Analog Switch", Intersil, 1999, pp. 1-2.

(56)

## References Cited

## OTHER PUBLICATIONS

- Newman, "Radiation Hardened Power Electronics", Intersil Corporation, 1999, pp. 1-4.
- "RF & Microwave Device Overview 2003—Silicon and GaAs Semiconductors", NEC, 2003.
- "RF Amplifier Design Using HFA3046, HFA3096, HFA3127, HFA3128 Transistor Arrays", Intersil Corporation, 1996, pp. 1-4.
- "SA630 Single Pole Double Throw (SPDT) Switch", Philips Semiconductors, 1997.
- Narendra, et al., "Scaling of Stack Effects and its Application for Leakage Reduction", ISLPED 2001, 2001, pp. 195-200.
- Huang, "Schottky Clamped MOS Transistors for Wireless CMOS Radio Frequency Switch Application", University of Florida, 2001, pp. 1-167.
- Botto, et al., "Series Connected Soft Switched IGBTs for High Power, High Voltage Drives Applications: Experimental Results", IEEE, 1997, pp. 3-7.
- Baker, et al., "Series Operation of Power MOSFETs for High Speed Voltage Switching Applications", American Institute of Physics, 1993, pp. 1655-1656.
- Lovelace, et al., "Silicon MOSFET Technology for RF ICs", IEEE, 1995, pp. 1238-1241.
- "Silicon Wave SiW1502 Radio Modem IC", Silicon Wave, 2000, pp. 1-21.
- Johnson, et al., "Silicon-On-Sapphire MOSFET Transmit/Receive Switch for L and S Band Transceiver Applications", Electronic Letters, 1997, pp. 1324-1326.
- Reedy, et al., "Single Chip Wireless Systems Using SOI", IEEE International SOI Conference, 1999, pp. 8-11.
- Stuber, et al., "SOI CMOS with High Performance Passive Components for Analog, RF and Mixed Signal Designs", IEEE International SOI Conference, 1998, pp. 99-100.
- Fukuda, et al., "SOI CMOS Device Technology", Special Edition on 21st Century Solutions, 2001, pp. 54-57.
- Kusunoki, et al., "SPDT Switch MMIC Using E/D Mode GaAs JFETs for Personal Communications", IEEE GaAs IC Symposium, 1992, pp. 135-138.
- Caverly, et al., "SPICE Modeling of Microwave and RF Control Diodes", IEEE, 2000, pp. 28-31.
- Baker, et al., "Stacking Power MOSFETs for Use in High Speed Instrumentation", American Institute of Physics, 1992, pp. 5799-5801.
- Sanders, "Statistical Modeling of SOI Devices for the Low Power Electronics Program", AET, Inc., 1995, pp. 1-109.
- Karandikar, et al., "Technology Mapping for SOI Domino Logic Incorporating Solutions for the Parasitic Bipolar Effect", ACM, 2001, pp. 1-14.
- Huang, et al., "TFSOI Can It Meet the Challenge of Single Chip Portable Wireless Systems", IEEE International SOI Conference, 1997, pp. 1-3.
- Devlin, "The Design of Integrated Switches and Phase Shifters", 1999.
- Hess, et al., "Transformerless Capacitive Coupling of Gate Signals for Series Operation of Power MOS Devices", IEEE, 1999, pp. 673-675.
- "uPG13xG Series L-Band SPDT Switch GaAs MMIC", NEC, 1996, pp. 1-30.
- Reedy, et al., "UTSi CMOS: A Complete RF SOI Solution", Peregrine Semiconductor, 2001, pp. 1-6.
- Hittite Microwave, "Wireless Symposium 2000 is Stage for New Product Introductions", Hittite Microwave, 2000, pp. 1-8.
- Montoriol, et al., "3.6V and 4.8V GSM/DCS1800 Dual Band PA Application with DECT Capability Using Standard Motorola RFICs", 2000, pp. 1-20.
- Ajjkuttira, et al., "A Fully Integrated CMOS RFIC for Bluetooth Applications", IEEE International Solid-State Circuits Conference, 2001, pp. 1-3.
- Apel, et al., "A GaAs MMIC Transceiver for 2.45 GHz Wireless Commercial Products", Microwave and Millimeter-Wave Monolithic Circuits Symposium, 1994, pp. 15-18.
- Caverly, et al., "CMOS RF Circuits for Integrated Wireless Systems", IEEE, 1998, pp. 1-4.
- Devlin, et al., "A 2.4 GHz Single Chip Transceiver", Microwave and Millimeter-Wave Monolithic Circuits Symposium, 1993, pp. 23-26.
- Fiorenza, et al., "RF Power Performance of LDMOSFETs on SOI: An Experimental Comparison with Bulk Si MOSFETs", IEEE Radio Frequency Integrated Circuits Symposium, 2001, pp. 43-46.
- Giffard, et al., "Dynamic Effects in SOI MOSFETs", IEEE SOS/SOI Technology Conference, Oct. 1991, pp. 160-161.
- Imai, et al., "Novel High Isolation FET Switches", IEEE Transactions on Microwave Theory and Techniques, 1996, pp. 685-691.
- Ishida, et al., "A Low Power GaAs Front End IC with Current Reuse Configuration Using 0.15um Gate GaAs MODFETs", IEEE, 1997, pp. 669-672.
- Iwata, et al., "Gate Over Driving CMOS Architecture for 0.5V Single Power Supply Operated Devices", IEEE, 1997, pp. 290-291, 473.
- Kumar, et al., "A Simple High Performance Complementary TFSOI BiCMOS Technology with Excellent Cross-Talk Isolation", 2000 IEEE International SOI Conference, 2000, pp. 142-143.
- Kwok, "An X-Band SOS Resistive Gate Insulator Semiconductor (RIS) Switch", IEEE Transactions on Electron Device, 1980, pp. 442-448.
- Lee, "CMOS RF: (Still) No Longer an Oxymoron (Invited)", IEEE Radio Frequency Integrated Circuits Symposium, 1999, pp. 3-6.
- Madhian, et al., "A 2-V, 1-10GHz BiCMOS Transceiver Chip for Multimode Wireless Communications Networks", IEEE, 1997, pp. 521-525.
- McRory, et al., "Transformer Coupled Stacked FET Power Amplifier", IEEE Journal of Solid State Circuits, vol. 34, No. 2, Feb. 1999, pp. 157-161.
- Nagayama, et al., "Low Insertion Loss DP3T MMIC Switch for Dual Band Cellular Phones", IEEE Journal of Solid State Circuits, 1999, pp. 1051-1055.
- Nishijima, et al., "A High Performance Transceiver Hybrid IC for PHS Hand Set Operating with Single Positive Voltage Supply", Microwave Symposium Digest, 1997, pp. 1155-1158.
- O, et al., "CMOS Components for 802.11b Wireless LAN Applications", IEEE Radio Frequency Integrated Circuits Symposium, 2002, pp. 103-106.
- Peczalski, "RF/Analog/Digital SOI Technology GPS Receivers and Other Systems on a Chip", IEEE Aerospace Conference Proceedings, 2002, pp. 2013-2017.
- Shifrin, et al., "A New Power Amplifier Topology with Series Biasing and Power Combining of Transistors", IEEE 1992 Microwave and Millimeter-Wave Monolithic Circuits Symposium, 1992, pp. 39-41.
- Shimura, et al., "High Isolation V-Band SPDT Switch MMIC for High Power Use", IEEE MTT-S International Microwave Symposium Digest, 2001, pp. 245-248.
- Uda, et al., "A High Performance and Miniaturized Dual Use (antenna/local) GaAs SPDT Switch IC Operating at +3V/0V", Microwave Symposium Digest, 1996, pp. 141-144.
- Uda, et al., "High Performance GaAs Switch IC's Fabricated Using MESFETs with Two Kinds of Pinch Off Voltages and a Symmetrical Pattern Configuration", IEEE Journal of Solid-State Circuits, 1994, pp. 1262-1269.
- Ippoushi, "SOI Structure Avoids Increases in Chip Area and Parasitic Capacitance Enables Operational Control of Transistor Threshold Voltage", Renesas Edge, vol. 2004.5, Jul. 2004, p. 15.
- Park, "A Regulated, Charge Pump CMOS DC/DC Converter for Low Power Application", 1998, pp. 1-62.
- Hittite Microwave, Floating Ground SPNT MMIC Switch Driver Techniques, 2001.
- Caverly, et al., "Gallium Nitride-Based Microwave and RF Control Devices", 2001.
- Sedra, et al., "Microelectronic Circuits", University of Toronto, Oxford University Press, Fourth Edition, 1982, 1987, 1991, 1998, pp. 374-375.
- Bahl, "Lumped Elements for RF and Microwave Circuits", Artech House, 2003, pp. 353-394.
- "Positive Bias GaAs Multi-Throw Switches with Integrated TTL Decoders", Hittite Microwave, 2000.

(56)

**References Cited**

## OTHER PUBLICATIONS

- Drozdosky, et al., "Large Signal Modeling of Microwave Gallium Nitride Based HFETs", Asia Pacific Microwave Conference, 2001, pp. 248-251.
- Ayasli, "Microwave Switching with GaAs FETs", Microwave Journal, 1982, pp. 719-723.
- Eron, "Small and Large Signal Analysis of MESETs as Switches" Microwave Journal, 1992.
- "A Voltage Regulator for GaAs FETs", Microwave Journal, 1995.
- Slobodnik, et al., "Millimeter Wave GaAs Switch FET Modeling", Microwave Journal, 1989.
- Caverly, "Distortion in GaAs MESFET Switch Circuits", 1994.
- Chen, et al., "Dual-Gate GaAs FET: A Versatile Circuit Component for MMICs", Microwave Journal, Jun. 1989, pp. 125-135.
- Bullock, "Transceiver and System Design for Digital Communication", Noble, 2000.
- Cros, "CMOS Wireless Transceiver Design", Kluwer Academic, 1997.
- Hickman, "Practical RF Handbook", Newnes, 1997.
- Hagen, "Radio Frequency Electronics", Cambridge University Press, 1996.
- Kuo, et al., "Low-Voltage SOI CMOS VLSI Devices and Circuits", Wiley Interscience, XP001090589, New York, 2001, pp. 57-60, 349-354.
- Leenaerts, "Circuits Design for RF Transceivers" Kluwer Academic, 2001.
- Johnson, "Advanced High-Frequency Radio Communication", Artech House, 1997.
- Larson, "RF and Microwave Circuit Design for Wireless Communications", Artech House, 1996.
- Misra, "Radio Frequency and Microwave Communication Circuits", Wiley, 2001.
- Barker, Communications Electronics-Systems, Circuits, and Devices, 1987, Prentice-Hall.
- Carr, "Secrets of RF Circuit Design", McGraw-Hill, 1997.
- Couch, "Digital and Analog Communication Systems", 2001, Prentice-Hall.
- Couch, "Modern Telecommunication System", Prentice-Hall, 1995.
- Freeman, "Radio System Design for Telecommunications", Wiley, 1997.
- Gibson, "The Communication Handbook", CRC Press, 1997.
- Hanzo, "Adaptive Wireless Transceivers", Wiley, 2002.
- Itoh, "RF Technologies for Low Power Wireless Communications", Wiley, 2001.
- Lossee, "RF Systems, Components, and Circuits Handbook", Artech House, 1997.
- Miller, "Modern Electronic Communications", Prentice-Hall, 1999.
- Scheinberg, et al., "A Computer Simulation Model for Simulating Distortion in FET Resistors", IEEE Transactions on Computer-Aided Design of Integrated Circuits and Systems, vol. 19, No. 9, Sep. 2000, pp. 981-989.
- Streetman, et al., "Solid State Electronic Devices", Microelectronics Research Center, Dept. of Electrical and Computer Engineering, The University of Texas at Austin, Chapter 6, 2004 by Pearson Education Inc., 4 pgs.
- Tokumitsu, et al., "A Low-Voltage, High-Power T/R-Switch MMIC Using LC Resonators", IEEE Transactions on Microwave Theory and Techniques, vol. 43, No. 5, May 1995, pp. 997-1003.
- Adan, et al., "Off-State Leakage Current Mechanisms in BulkSi and SOI MOSFETs and Their Impact on CMOS ULSIs Standby Current", IEEE Transactions on Electron Devices, vol. 48, No. 9, Sep. 2001, pp. 2050-2057.
- Chan, et al., "A Novel SOI CbICMOS Compatible Device Structure for Analog and Mixed-Mode Circuits", Dept. of EECS, University of California at Berkeley, IEEE 1995, pp. 40-43.
- Street, A.M., "RF Switch Design", The Institution of Electrical Engineers, 2000, pp. 4/1-4/7.
- Adan, et al., "Linearity and Low-Noise Performance of SOI MOSFETs for RF Applications", IEEE Transactions on Electron Devices, vol. 49, No. 5, May 2002, pp. 881-888.
- Cristoloveanu, et al., "The Four-Gate Transistor", Institute of Microelectronics, Electromagnetism and Photonics, ESSDERC 2001, pp. 323-326.
- Ayasli, et al., "An X-Band 10 W Monolithic Transmit-Receive GaAs FET Switch", Raytheon Research Division, 1982 IEEE, pp. 42-46.
- Dufrene, et al., "The G4-FET: Low Voltage to High Voltage Operation and Performance", Dept. of Electrical and Computer Engineering, The University of Tennessee, IEEE 2003, pp. 55-56.
- Pucel, et al., "A Multi-Chip GaAs Monolithic Transmit/Receive Module for X-Band", Research Division, Raytheon Company, 1982 IEEE MTT-S Digest, pp. 489-492.
- Dufrene, et al., "Investigation of the Four-Gate Action in G4-FETs", IEEE Transactions on Electron Devices, vol. 51, No. 11, Nov. 2004, pp. 1931-1935.
- Ayasli, et al., "A Monolithic Single-Chip X-Band Four-Bit Phase Shifter", IEEE Transactions on Microwave Theory and Techniques, vol. MTT-30, No. 12, Dec. 1982, pp. 2201-2206.
- Akarvardar, et al., "Multi-Bias Dependence of Threshold Voltage, Subthreshold Swing, and Mobility in G4-FETs", Institute of Microelectronics, Electromagnetism, and Photonics, IEEE 2003, pp. 127-130.
- Lim, et al., "Partial SOI LDMOSFETs for High-Side Switching", Dept. of Engineering, University of Cambridge, 1999 IEEE, pp. 149-152.
- Akarvardar, et al., "Threshold Voltage Model of the SOI 4-Gate Transistor", 2004 IEEE International SOI Conference, Oct. 2004, pp. 89-90.
- Imam, et al., "A Simple Method to Determine the Floating-Body Voltage of SOI CMOS Devices", IEEE Electron Device Letters, vol. 21, No. 1, Jan. 2000, pp. 21-23.
- Allen, Thomas P., "Characterization and Modeling of Silicon-on-Insulator Field Effect Transistors", Department of Electrical Engineering and Computer Science, MIT, May 20, 1999, 80 pgs.
- Fung, et al., "Frequency Dispersion in Partially Depleted SOI MOSFET Output Resistance", Proceedings 1996 IEEE International SOI Conference, Oct. 1996, pp. 146-147.
- Chen, Suheng, "G4-FET Based Voltage Reference", Masters Theses, University of Tennessee, Knoxville, Trace: Tennessee Research and Creative Exchange, May 2004, 57 pgs.
- Zhu, et al., "Simulation of Suppression of Floating-Body Effect in Partially Depleted SOI MOSFET Using a Sil-xGex Dual Source Structure", Materials Science and Engineering B 114-115 (2004), pp. 264-268.
- Hieda, et al., Floating-Body Effect Free Concave SOI-MOSFETs (COSMOS), ULSI Research Center, Toshiba Corporation, IEEE 1991, pp. 26.2.1-26.2.4.
- Ming, et al., "A New Structure of Silicon-on-Insulator Metal-Oxide-Semiconductor Field Effect Transistor to Suppress the Floating Body Effect", Chin. Phys. Lett., vol. 20, No. 5 (2003), pp. 767-769.
- Marks, Jeffery Earl, "SOI for Frequency Synthesis in RF Integrated Circuits", Thesis submitted to North Carolina State University, 2003, 155 pgs.
- Moye, et al., "A Compact Broadband, Six-Bit MMIC Phasor with Integrated Digital Drivers+", IEEE 1990 Microwave and Millimeter-Wave Monolithic Circuits Symposium, 1988 IEEE, pp. 123-126.
- Smuk, et al., "Monolithic GaAs Multi-Throw Switches with Integrated Low-Power Decoder-Driver Logic", Hitrite Microwave Corporation, Jun. 1997, 4 pgs.
- Han, et al., "A Simple and Accurate Method for Extracting Substrate Resistance of RF MOSFETs", IEEE Electron Device Letters, vol. 23, No. 7, Jul. 2002, pp. 434-436.
- Wei, et al., "Large-Signal Model of Triple-Gate MESFET/PHEMT for Switch Applications", Alpha Industries, Inc., 1999 IEEE, pp. 745-748.
- Soyuer, et al., "RF and Microwave Building Blocks in a Standard BiCMOS Technology", IBM T.J. Watson Research Center, 1996 IEEE, pp. 89-92.
- Mizutani, et al., "Compact DC-60-GHz HJFET MMIC Switches using Ohmic Electrode-Sharing Technology", IEEE Transactions on Microwave Theory and Techniques, vol. 46, No. 11, Nov. 1998, pp. 1597-1603.

(56)

## References Cited

## OTHER PUBLICATIONS

- Ota, et al. "High Isolation and Low Insertion Loss Switch IC Using GaAs MESFETs", IEEE Transactions on Microwave Theory and Techniques, vol. 43, No. 9, Sep. 1995, pp. 2175-2177.
- Koo, Raymond, "RF Switches", Univ. Toronto, Elec. and Computer Engineering Dept. 2001, 12 pgs.
- Titus, et al., "A Silicon BICMOS Transceiver Front-End MMIC Covering 900 and 1900 MHz Applications", Hitite Microwave Corporation, IEEE 1996 Microwave and Millimeter-Wave Monolithic Circuits Symposium, pp. 73-75.
- Rossek, Sacha, "Direct Optical Control of a Microwave Phase Shifter Using GaAs Field-Effect Transistors", Communications Research Group, School of Electronic Engineering, Faculty of Technology, Middlesex University, Sep. 1998, 224 pgs.
- Schindler, et al., "DC-20 GHz N X M Passive Switches", Raytheon Co., 1998 IEEE MTT-S Digest, pp. 1001-1005.
- Houng, et al., "60-70 dB Isolation 2-19 GHz Switches", Raytheon Electromagnetic Systems Division, 1989 IEEE, GaAs IC Symposium, pp. 173-176.
- Schindler, et al., "DC-40 GHz and 20-40 GHz MMIC SPDT Switches", IEEE Transactions of Electron Devices, vol. ED-34, No. 12, Dec. 1987, pp. 2595-2602.
- Schindler, et al., "A 2-18 GHz Non-Blocking Active 2 X 2 Switch", Raytheon Company, 1989 IEEE, GaAs IC Symposium, pp. 181-183.
- Schindler, et al., "A Single Chip 2-20 GHz T/R Module" 1988 IEEE, IEEE 1990 Microwave and Millimeter-Wave Monolithic Circuits Symposium, pp. 99-102.
- Bernkopf, et al., "A High Power K/Ka-Band Monolithic T/R Switch", 1991 IEEE, IEEE 1991 Microwave and Millimeter-Wave Monolithic Circuits Symposium, pp. 15-18.
- Schindler, et al., "DC-20 GHz N X M Passive Switches", IEEE Transactions on Microwave Theory and Techniques, vol. 36, No. 12, Dec. 1988, pp. 1604-1613.
- Patel, Reema, Final Office Action received from the USPTO dated Apr. 7, 2015 for U.S. Appl. No. 14/028,357, 159 pgs.
- Mishra, et al., "High Power Broadband Amplifiers for 1-18 GHz Naval Radar" University of California, Santa Barbara, pp. 1-9, Jul. 1, 1998.
- Perraud, et al., "A Direct-Conversion CMOS Transceiver for the 802.11a/b/g WLAN Standard Utilizing a Cartesian Feedback Transmitter", IEEE Journal of Solid-State Circuits, vol. 39, No. 12, Dec. 2004, pp. 2226-2238.
- Rohde, et al., "Optic/Millimeter-Wave Converter for 60 Ghz Radio-Over-Fiber Systems", Fraunhofer-Institut für Angewandte Festkörperphysik Freiburg i. Br., Apr. 1997, pp. 1-5.
- Darabi, et al. "A Dual-Mode 802.11b/Bluetooth Radio in 0.35- $\mu$ m CMOS", IEEE Journal of Solid-State Circuits, vol. 40, No. 3, Mar. 2005, pp. 698-706.
- Schlechtweg, et al., "Multifunctional Integration Using HEMT Technology", Fraunhofer Institute for Applied Solid State Physics, (date uncertain, believed Mar. 1997).
- Chow, Charles Chiang, Office Action received from the USPTO dated Mar. 2, 2011 for related U.S. Appl. No. 11/347,671, 14 pgs.
- Kelly, Dylan, Amendment filed in the USPTO dated May 2, 2011 for related U.S. Appl. No. 11/347,671, 6 pgs.
- Nguyen, Patricia T., Office Action received from the USPTO dated Oct. 25, 2005 for related U.S. Appl. No. 10/875,405, 7 pgs.
- Burgener, et al., Amendment filed in USPTO dated Jan. 25, 2006 for related U.S. Appl. No. 10/875,405, 11 pgs.
- Nguyen, Patricia, Office Action received from USPTO dated Apr. 20, 2006 for related U.S. Appl. No. 10/875,405, 10 pgs.
- Burgener, et al., Amendment filed in USPTO dated Aug. 21, 2006 for related U.S. Appl. No. 10/875,405, 10 pgs.
- Nguyen, Patricia, Notice of Allowance received from USPTO dated Sep. 27, 2006 for related U.S. Appl. No. 10/875,405, 5 pgs.
- Burgener, et al., Comments on Examiner's Statement of Reasons for Allowance dated Dec. 26, 2006 for related U.S. Appl. No. 10/875,405, 2 pgs.
- Le, Lana N., Notice of Allowance received from the USPTO dated Sep. 26, 2005 for related U.S. Appl. No. 11/158,597, 10 pgs.
- Le, Lana, International Search Report received from USPTO dated Nov. 15, 2005 for related PCT appln. No. PCT/US2005/022407, 10 pgs.
- Le, Lana N., Notice of Allowance received from the USPTO dated Feb. 27, 2006 for related U.S. Appl. No. 11/158,597, 8 pgs.
- Dinh, Le T., International Search Report received from USPTO dated Mar. 28, 2003 for related application No. PCT/US02/32266, 2 pgs.
- Notice of Allowance received from USPTO dated May 12, 2004 for U.S. Appl. No. 10/267,531, now U.S. Pat. No. 6,804,502, 8 pgs.
- Huang, "A 0.5  $\mu$ m CMOS T/R Switch for 900-MHz Wireless Application", IEEE Journal of Solid-State Circuits, vol. 36, No. 3, Mar. 2001, pp. 486-492.
- Lauterbach, et al. "Charge Sharing Concept and New Clocking Scheme for Power Efficiency and Electromagnetic Emission Improvement of Boosted Charge Pumps", IEEE Journal of Solid-State Circuits, vol. 35, No. 5, May 2000, pp. 719-723.
- Makioka, et al., "Super Self-Aligned GaAs RF Switch IC with 0.25 dB Extremely Low Insertion Loss for Mobile Communication Systems", IEEE Transactions on Electron Devices, vol. 48, No. 8, Aug. 2001, pp. 1510-1514.
- Maxim Integrated Products, "Charge Pumps Shine in Portable Designs", published Mar. 15, 2001, pp. 1-16.
- Texas Instruments, "TPS60204, TPS60205, Regulated 3.3-V, 100-mA Low-Ripple Charge Pump Low Power DC/DC Converters", published Feb. 2001, rev. Sep. 2001, pp. 1-18.
- Nork, Sam, "New Charge Pumps Offer Low Input and Output Noise" Linear Technology Corporation, Design Notes, Design Note 243, published Nov. 2000, pp. 1-2.
- Linear Technology, "LTC1550/LTC1551L: Low Noise Charge Pump Inverters in MS8 Shrink Cell Phone Designs", published Dec. 1998, pp. 1-2.
- Lascari, Lance, "Accurate Phase Noise Prediction in PLL Synthesizers" Applied Microwave & Wireless, published May 2000, pp. 90-96.
- Tran, Pablo N., Office Action received from the USPTO dated Mar. 19, 2009 for related U.S. Appl. No. 11/501,125, 17 pgs.
- Burgener, et al., Amendment filed in the USPTO dated Jun. 19, 2009 for related U.S. Appl. No. 11/501,125, 5 pgs.
- Aquilani, Dario, Communication and Supplementary European Search Report for related European appln. No. 05763216.8, dated Nov. 27, 2009, 10 pgs.
- Tran, Pablo N., Office Action received from the USPTO dated Oct. 29, 2009 for related U.S. Appl. No. 11/501,125, 19 pgs.
- Burgener, et al., Response (in Japanese) as filed in the Japanese Patent Office for related appln. No. 2007-518298 dated Oct. 15, 2010, 45 pages, plus translation of Response as filed dated Oct. 12, 2010, 10 pages.
- Kai, Tetsuo, Translation of an Office Action received from the Japanese Patent Office dated Mar. 29, 2011 for related Japanese appln. No. 2010-232563, 4 pgs.
- Chow, Charles Chiang, Office Action received from USPTO for related U.S. Appl. No. 11/347,671 dated Aug. 19, 2008, 14 pgs.
- Kelly, Dylan, Amendment filed in the USPTO for related U.S. Appl. No. 11/347,671 dated Dec. 19, 2008, 15 pgs.
- Chow, Charles Chiang, Office Action received from USPTO for related U.S. Appl. No. 11/347,671 dated Apr. 16, 2009, 16 pgs.
- Kelly, Dylan, Response filed in the USPTO for related U.S. Appl. No. 11/347,671 dated Jun. 16, 2009, 14 pgs.
- Chow, Charles Chiang, Office Action received from the USPTO for related U.S. Appl. No. 11/347,671 dated Jul. 20, 2009, 17 pgs.
- Kelly, Dylan, Amendment filed in the USPTO for related U.S. Appl. No. 11/347,671 dated Jan. 20, 2010, 18 pgs.
- Kelly, Dylan, Amendment filed in the USPTO for related U.S. Appl. No. 11/347,671 dated Jul. 28, 2010, 6 pgs.
- Kelly, Dylan, Amendment filed in the USPTO for related U.S. Appl. No. 11/347,671 dated Dec. 20, 2010, 12 pgs.
- Chow, Charles Chiang, Office Action received from the USPTO for related U.S. Appl. No. 11/347,671 dated Mar. 2, 2011, 15 pgs.
- Chow, Charles Chiang, Advisory Action received from the USPTO for related U.S. Appl. No. 11/347,671 dated May 12, 2011, 3 pgs.
- Shifrin, Mitchell, "Monolithic FET Structures for High-Power Control Component Applications", IEEE Transactions on Microwave Theory and Techniques, vol. 37, No. 12, Dec. 1989, pp. 2134-2141.

(56)

**References Cited**

## OTHER PUBLICATIONS

Chow, Charles Chiang, Office Action received from the USPTO for related U.S. Appl. No. 11/347,671 dated Apr. 28, 2010, 20 pgs.

Chow, Charles Chiang, Office Action received from the USPTO for related U.S. Appl. No. 11/347,671, dated Aug. 20, 2010, 18 pgs.

Hoffmann, Niels, Office Action received from the EPO dated Feb. 4, 2009 for related appln. No. 06786943.8, 101 pgs.

Peregrine Semiconductor Corporation, Response filed in the EPO dated Aug. 12, 2009 for related appln. No. 06786943.8, 31 pgs.

Hoffmann, Niels, Summons to Attend Oral Proceedings Pursuant to Rule 115(1)EPC dated Jul. 22, 2011 for related appln. No. 06786943.8, 8 pgs.

Peregrine Semiconductor Corporation, Response filed in the EPO dated Oct. 24, 2011 for related appln. No. 06786943.8, 1 pg.

Benker, Guido, Decision to Refuse a European Patent Application (Art. 97(2)EPC) dated Nov. 18, 2011 or related appln. No. 06786943.8, 4 pgs.

Peregrine Semiconductor Corporation, Response filed in the EPO dated Jan. 17, 2012 for related appln. No. 06786943.8, 1 pg.

Peregrine Semiconductor Corporation, Appeal to the Decision for Refusal filed in the EPO dated Mar. 20, 2012 for related appln. No. 06786943.8, 27 pgs.

Nguyen, Tram Hoang Notice of Allowance received from the USPTO dated Nov. 17, 2011 for related U.S. Appl. No. 13/053,211, 41 pgs.

Hoffmann, Niels, International Search Report received from the EPO dated Feb. 27, 2012 for related appln. No. PCT/US2011/056942, 12 pgs.

Iijima, et al., "Boosted Voltage Scheme with Active Body-Biasing Control on PD-SOI for Ultra Low Voltage Operation", IEICE Transactions on Electronics, Institute of Electronics, Tokyo, JP, vol. E90C, No. 4, Apr. 1, 2007, pp. 666-674.

Peregrine Semiconductor Corporation, Translation of a Response filed in the Chinese Patent Office dated Nov. 30, 2009 for related appln. No. 2006800251287.3, 3 pgs.

Chinese Patent Office, Translation of an Office Action received from the Chinese Patent Office dated Nov. 2, 2011 for related appln. No. 2006800251281, 12 pgs.

Shingleton, Michael, Office Action received from the USPTO dated Oct. 7, 2008 for related U.S. Appl. No. 11/811,816, 4 pgs.

Dribinsky, et al., Response filed in the USPTO dated Jan. 7, 2009 for related U.S. Appl. No. 11/881,816, 7 pgs.

Shingleton, Michael, Office Communication received from the USPTO dated Apr. 28, 2009 for related U.S. Appl. No. 11/811,816, 3 pgs.

Dribinsky, et al., Response filed in the USPTO dated Aug. 28, 2009 for related U.S. Appl. No. 11/881,816, 7 pgs.

Shingleton, Michael, Office Action received from the USPTO dated Jan. 19, 2010 for related U.S. Appl. No. 11/811,816, 16 pgs.

Dribinsky, et al., Response filed in the USPTO dated Jul. 19, 2010 for related U.S. Appl. No. 11/881,816, 22 pgs.

Shingleton, Michael, Office Action received from the USPTO dated Oct. 14, 2010 for related U.S. Appl. No. 11/811,816, 15 pgs.

Dribinsky, et al., Response filed in the USPTO dated Jan. 14, 2011 for related U.S. Appl. No. 11/881,816, 19 pgs.

Shingleton, Michael, Advisory Action received from the USPTO dated Mar. 18, 2011 for related U.S. Appl. No. 11/811,816, 3 pgs.

Shingleton, Michael, Interview Summary received from the USPTO dated Apr. 12, 2011 for related U.S. Appl. No. 11/811,816, 2 pgs.

Shingleton, Michael, Interview Summary received from the USPTO dated Apr. 18, 2011 for related U.S. Appl. No. 11/811,816, 3 pgs.

Dribinsky, et al., General Letter filed in the USPTO dated Jun. 29, 2011 for related U.S. Appl. No. 11/881,816, 1 pg.

Shingleton, Michael, Notice of Allowance received from the USPTO dated Oct. 12, 2011 for related U.S. Appl. No. 11/811,816, 5 pgs.

Dribinsky, et al., RCE and IDS filed in the USPTO dated Mar. 26, 2012 for related U.S. Appl. No. 11/881,816, 4 pgs.

Englekirk, Robert Mark, Amendment filed in the USPTO dated Mar. 5, 2012 for related U.S. Appl. No. 13/046,560, 4 pgs.

Nguyen, Tram Hoang, Office Action received from the USPTO dated Apr. 11, 2012 for related U.S. Appl. No. 13/412,529, 6 pgs.

Peregrine Semiconductor Corporation, Response filed in the EPO dated Apr. 17, 2012 for related appln. No. EP1451890, 42 pgs.

Numata, et al., "A +2.4/0 V Controlled High Power GaAs SPDT Antenna Switch IC for GSM Application", IEEE Radio Frequency Integrated Circuits Symposium, 2002, pp. 141-144.

Tinella, et al., "A 0.7dB Insertion Loss CMOS-SOI Antenna Switch with More than 50dB Isolation over the 2.5 to 5GHz Band", Proceeding of the 28th European Solid-State Circuits Conference, 2002, pp. 483-486.

Ohnakado, et al., "A 1.4dB Insertion Loss, 5GHz Transmit/Receive Switch Utilizing Novel Depletion-Layer Extended Transistors (DETs) in 0.18um CMOS Process", Symposium on VLSI Circuits Digest of Technical Papers, 2002, pp. 162-163.

Nakayama, et al., "A 1.9 GHz Single-Chip RF Front-End GaAs MMIC with Low-Distortion Cascade FET Mixer for Personal Handy-Phone System Terminals", IEEE, 1998, pp. 101-104.

McGrath, et al., "A 1.9-GHz GaAs Chip Set for the Personal Handyphone System", IEEE Transaction on Microwave Theory and Techniques, 1995, pp. 1733-1744.

Nakayama, et al., "A 1.9GHz Single-Chip RF Front End GaAs MMIC for Personal Communications", Microwave and Millimeter-Wave Monolithic Circuits Symposium, 1996, pp. 69-72.

Nakayama, et al., "A 1.9GHz Single-Chip RF Front End GaAs MMIC with Low-Distortion Cascode FET Mixer for Personal Handy-Phone System Terminals", Radio Frequency Integrated Circuits Symposium, 1998, pp. 205-208.

Gu, et al., "A 2.3V PHEMT Power SP3T Antenna Switch IC for GSM Handsets", IEEE GaAs Digest, 2003, pp. 48-51.

Darabi, et al., "A 2.4GHz CMOS Transceiver for Bluetooth", IEEE, 2001, pp. 89-92.

Huang, et al., "A 2.4-GHz Single-Pole Double Throw T/R Switch with 0.8-dB Insertion Loss Implemented in a CMOS Process", Silicon Microwave Integrated Circuits and Systems Research, 2001, pp. 1-4.

Huang, et al., "A 2.4-GHz Single-Pole Double Throw T/R Switch with 0.8-dB Insertion Loss Implemented in a CMOS Process (slides)", Silicon Microwave Integrated Circuits and Systems Research, 2001, 4 pgs.

Yamamoto, et al., "A 2.4GHz Band 1.8V Operation Single Chip SI-CMOS T/R MMIC Front End with a Low Insertion Loss Switch", IEEE Journal of Solid-State Circuits, vol. 36, No. 8, Aug. 2001, pp. 1186-1197.

Kawakyu, et al., "A 2-V Operation Resonant Type T/R Switch with Low Distortion Characteristics for 1.9GHz PHS", IEICE Trans Electron, vol. E81-C, No. 6, Jun. 1998, pp. 862-867.

Huang, et al., "A 900-MHz T/R Switch with a 0.8-dB Insertion Loss Implemented in a 0.5-um CMOS Process", IEEE Custom Integrated Circuits Conference, 2000, pp. 341-344.

Valeri, et al., "A Composite High Voltage Device Using Low Voltage SOI MOSFET's", IEEE, 1990, pp. 169-170.

Miyatsuji, et al., "A GaAs High Power RF Single Pole Double Throw Switch IC for Digital Mobile Communication System", IEEE International Solid-State Circuits Conference, 1994, pp. 34-35.

Miyatsuji, et al., "A GaAs High Power RF Single Pole Dual Throw Switch IC for Digital Mobile Communication System", IEEE Journal of Solid-State Circuits, 1995, pp. 979-983.

Puechberty, et al., "A GaAs Power Chip Set for 3V Cellular Communications", 1994.

Yamamoto, et al., "A GaAs RF Transceiver IC for 1.9GHz Digital Mobile Communication Systems", ISSCC96, 1996, pp. 340-341, 469.

Choumei, et al., "A High Efficiency, 2V Single Supply Voltage Operation RF Front End MMIC for 1.9GHz Personal Handy Phone Systems", IEEE, 1998, pp. 73-76.

Schindler, et al., "A High Power 2-18 GHz T/R Switch", IEEE Microwave and Millimeter-Wave Monolithic Circuits Symposium, 1990, pp. 119-122.

Gu, et al., "A High Power DPDT MMIC Switch for Broadband Wireless Applications", IEEE MTT-S Digest, 2003, pp. 173-176.

Gu, et al., "A High Performance GaAs SP3T Switch for Digital Cellular Systems", IEEE MTT-S Digest, 2001, pp. 241-244.

(56)

## References Cited

## OTHER PUBLICATIONS

- Numata, et al., "A High Power Handling GSM Switch IC with New Adaptive Control Voltage Generator Circuit Scheme", IEEE Radio Frequency Integrated Circuits Symposium, 2003, pp. 233-236.
- Madihian, et al., "A High Speed Resonance Type FET Transceiver Switch for Millimeter Wave Band Wireless Networks", 26th EuMC, 1996, pp. 941-944.
- Tokumitsu, et al., "A Low Voltage High Power T/R Switch MMIC Using LC Resonators", IEEE Transactions on Microwave Theory and Techniques, 1995, pp. 997-1003.
- Colinge, et al., "A Low Voltage Low Power Microwave SOI MOSFET", IEEE International SOI Conference, 1996, pp. 128-129.
- Johnson, et al., "A Model for Leakage Control by MOS Transistor Stacking", ECE Technical Papers, 1997, pp. 1-28.
- Matsumoto, et al., "A Novel High Frequency Quasi-SOI Power MOSFET for Multi-Gigahertz Application", IEEE, 1998, pp. 945-948.
- Giugni, "A Novel Multi-Port Microwave/Millimeter-Wave Switching Circuit", Microwave Conference, 2000.
- Caverly, "A Project Oriented Undergraduate CMOS Analog Microelectronic System Design Course", IEEE, 1997, pp. 87-88.
- Harjani, et al., "A Prototype Framework for Knowledge Based Analog Circuit Synthesis", IEEE Design Automation Conference, 1987, pp. 42-49.
- DeRossi, et al., "A Routing Switch Based on a Silicon-on-Insulator Mode Mixer", IEEE Photonics Technology Letters, 1999, pp. 194-196.
- Caverly, et al., "A Silicon CMOS Monolithic RF and Microwave Switching Element", 27th European Microwave Conference, 1997, pp. 1046-1051.
- Valeri, et al., "A Silicon-on-Insulator Circuit for High Temperature, High-Voltage Applications", IEEE, 1991, pp. 60-61.
- Yamamoto, et al., "A Single-Chip GaAs RF Transceiver for 1.9GHz Digital Mobile Communication Systems", IEEE Journal of Solid-State Circuits, 1996.
- Tsutsumi, et al., "A Single Chip PHS Front End MMIC with a True Single +3 Voltage Supply", IEEE Radio Frequency Integrated Circuits Symposium, 1998, pp. 105-108.
- Wambacq, et al., "A Single Package Solution for Wireless Transceivers", IEEE, 1999, pp. 1-5.
- Eggert, et al., "A SOI-RF-CMOS Technology on High Resistivity SIMOX Substrates for Microwave Applications to 5 GHz", IEEE Transactions on Electron Devices, 1997, pp. 1981-1989.
- Szedon, et al., "Advanced Silicon Technology for Microwave Circuits", Naval Research Laboratory, 1994, pp. 1-110.
- Heller, et al., "Cascode Voltage Switch Logic: A Different CMOS Logic Family", IEEE International Solid-State Circuits Conference, 1984, pp. 16-17.
- Pylarinos, "Charge Pumps: An Overview", Proceedings of the IEEE International Symposium on Circuits and Systems, 2003, pp. 1-7.
- Doyama, "Class E Power Amplifier for Wireless Transceivers", University of Toronto, 1999, pp. 1-9.
- "CMOS Analog Switches", Harris, 1999, pp. 1-9.
- "CMOS SOI RF Switch Family", Honeywell, 2002, pp. 1-4.
- "CMOS SOI Technology", Honeywell, 2001, pp. 1-7.
- Analog Devices, "CMOS, Low Voltage RF/Video, SPST Switch", Analog Devices, inc., 1999, pp. 1-10.
- Eggert, et al., "CMOS/SIMOX-RF-Frontend for 1.7GHz", Solid State Circuits Conference, 1996.
- Yamamoto, et al., "Design and Experimental Results of a 2V-Operation Single-Chip GaAs T/R MMIC Front-End for 1.9GHz Personal Communications", IEEE, 1998, pp. 7-12.
- Savla, "Design and Simulation of a Low Power Bluetooth Transceiver", The University of Wisconsin, 2001, pp. 1-90.
- Henshaw, "Design of an RF Transceiver", IEEE Colloquium on Analog Signal Processing, 1998.
- Baker, et al., "Designing Nanosecond High Voltage Pulse Generators Using Power MOSFET's", Electronics Letters, 1994, pp. 1634-1635.
- Caverly, "Development of a CMOS Cell Library for RF Wireless and Telecommunications Applications", VLSI Symposium, 1998.
- Caverly, "Distortion Properties of Gallium Arsenide and Silicon RF and Microwave Switches", IEEE, 1997, pp. 153-156.
- Colinge, "Fully Depleted SOI CMOS for Analog Applications", IEEE Transactions on Electron Devices, 1998, pp. 1010-1016.
- Flandre, et al., "Fully Depleted SOI CMOS Technology for Low Voltage Low Power Mixed Digital/Analog/Microwave Circuits", Analog Integrated Circuits and Signal Processing, 1999, pp. 213-228.
- Yamao, "GaAs Broadband Monolithic Switches", 1986, pp. 63-71.
- Gopinath, et al., "GaAs FET RF Switches", IEEE Transactions on Electron Devices, 1985, pp. 1272-1278.
- HI-5042 thru HI-5051 Datasheet, Harris Corporation, 1999.
- Eisenberg, et al., "High Isolation 1-20GHz MMIC Switches with On-Chip Drivers", IEEE Microwave and Millimeter-Wave Monolithic Circuits Symposium, 1989, pp. 41-45.
- Shifrin et al., "High Power Control Components Using a New Monolithic FET Structure", IEEE Microwave and Millimeter-Wave Monolithic Circuits Symposium, 1988, pp. 51-56.
- Kohama, et al., "High Power DPDT Antenna Switch MMIC for Digital Cellular Systems", GaAs IC Symposium, 1995, pp. 75-78.
- Kohama, et al., "High Power DPDT Antenna Switch MMIC for Digital Cellular Systems", IEEE Journal of Solid-State Circuits, 1996, pp. 1406-1411.
- Yun, et al., "High Power-GaAs MMIC Switches with Planar Semi-Insulated Gate FETs (SIGFETs)", International Symposium on Power Semiconductor Devices & ICs, 1990, pp. 55-58.
- Caverly, "High Power Gallium Nitride Devices for Microwave and RF Control Applications", 1999, pp. 1-30.
- Caverly, "High Power Gallium Nitride Devices for Microwave and RF Control Applications", 2000, pp. 1-33.
- Masuda, et al., "High Power Heterojunction GaAs Switch IC with P-1dB of more than 38dBm for GSM Application", IEEE, 1998, pp. 229-232.
- De Boer, et al., "Highly Integrated X-Band Multi-Function MMIC with Integrated LNA and Driver Amplifier", TNO Physics and Electronics Laboratory, 2002, pp. 1-4.
- Kanda, et al., "High Performance 19GHz Band GaAs FET Switches Using LOXI (Layer Oxide Isolation)—MESFETs", IEEE, 1997, pp. 62-65.
- Uda, et al., "High-Performance GaAs Switch IC's Fabricated Using MESFET's with Two Kinds of Pinch-Off Voltages and a Symmetrical Pattern Configuration", IEEE Journal of Solid-State Circuits, vol. 29, No. 10, Oct. 1994, pp. 1262-1269.
- Uda, et al., "High Performance GaAs Switch IC's Fabricated Using MESFETs with Two Kinds of Pinch Off Voltages", IEEE GaAs IC Symposium, 1993, pp. 247-250.
- Armijos, "High Speed DMOS FET Analog Switches and Switch Arrays", Temic Semiconductors 1994, pp. 1-10.
- Katzin, et al., "High Speed 100+ W RF Switches Using GaAs MMICs", IEEE Transactions on Microwave Theory and Techniques, 1992, pp. 1989-1996.
- Honeywell, "Honeywell SPDT Absorptive RF Switch", Honeywell, 2002, pp. 1-6.
- Honeywell, "Honeywell SPDT Reflective RF Switch", Honeywell Advance Information, 2001, pp. 1-3.
- Larson, "Integrated Circuit Technology Options for RFIC's—Present Status and Future Directions", IEEE Journal of Solid-State Circuits, 1998, pp. 387-399.
- Burghartz, "Integrated RF and Microwave Components in BiCMOS Technology", IEEE Transactions on Electron Devices, 1996, pp. 1559-1570.
- Kelly, "Integrated Ultra CMIS Designs in GSM Front End", Wireless Design Magazine, 2004, pp. 18-22.
- Bonkowski, et al., "Integrator of Triple Band GSM Antenna Switch Module Using SOI CMOS", IEEE Radio Frequency Integrated Circuits Symposium, 2004, pp. 511-514.
- Marenk, et al., "Layout Optimization of Cascode RF SOI Transistors", IEEE International SOI Conference, 2001, pp. 105-106.
- Suematsu, et al., "L-Band Internally Matched Si-MMIC Front End", IEEE, 1996, pp. 2375-2378.
- Adan, et al., "Linearity and Low Noise Performance of SOIMOSFETs for RF Applications", IEEE International SOI Conference, 2000, pp. 30-31.

(56)

**References Cited**

## OTHER PUBLICATIONS

- Rodgers, et al., "Silicon UTSi CMOS RFIC for CDMA Wireless Communications Systems", Peregrine Semiconductor Corporation, 1999 IEEE MTT-S Digest.
- Megahed, et al., "Low Cost UTSi Technology for RF Wireless Applications", Peregrine Semiconductor Corporation, 1998 IEEE MTT-S Digest.
- Johnson, et al., "Advanced Thin-Film Silicon-on-Sapphire Technology: Microwave Circuit Applications", IEEE Transactions on Electron Devices, vol. 45, No. 5, May 1998, pp. 1047-1054.
- Mark L. Burgener, "CMOS SOS Switches Offer Useful Features, High Integration", CMOS SOS Switches, Microwaves & RF, Aug. 2001, pp. 107-118.
- Notice of Allowance and Fee(s) Due from the USPTO, May 12, 2004, U.S. Appl. No. 10/267,531, 8 pgs.
- Burgener, et al., Comments on Examiner's Statement of Reasons for Allowance filed in PTO on Aug. 12, 2004 for U.S. Appl. No. 10/267,531, 2 pgs.
- Office Action from USPTO, Jun. 3, 2005, U.S. Appl. No. 10/922,135, 8 pgs.
- Burgener, et al., Amendment filed in PTO on Dec. 5, 2005 for U.S. Appl. No. 10/922,135, 7 pgs.
- Miyajima, Ikumi, Notice of Reasons for Refusal from the Japanese Patent Office dated Feb. 13, 2006 for Appln. No. 2003-535287, 3 pgs.
- Office Action from USPTO, Jan. 17, 2006, U.S. Appl. No. 10/922,135, 8 pgs.
- Burgener, et al., Response filed in PTO on May 16, 2006 for U.S. Appl. No. 10/922,135, 4 pgs.
- Notice of Allowance from USPTO, Jun. 2, 2006 for U.S. Appl. No. 10/922,135, 5 pgs.
- Van Der Peet, H., Communication Pursuant to Article 94(3) EPC received from the EPO in related appln. No. 02 800 982.7-2220 dated Jun. 19, 2008, 3 pgs.
- Office Action from USPTO dated Nov. 15, 2007 for related U.S. Appl. No. 11/582,206, 9 pages.
- Burgener, et al., Amendment filed in USPTO dated May 15, 2008 for related U.S. Appl. No. 11/582,206, 11 pages.
- Notice of Allowance from USPTO dated Jul. 15, 2008 for related U.S. Appl. No. 11/582,206, 7 pages.
- Notice of Allowance received from the USPTO dated Dec. 19, 2008 for related U.S. Appl. No. 11/127,520, 7 pgs.
- Orndorff, et al., "CMOS/SOS/LSI Switching Regulator Control Device", Solid-State Circuits Conf., Digest of Technical Papers, Feb. 1978 IEEE International, vol. XXI, pp. 234-235.
- Luu, An T., Office Action received from USPTO for related U.S. Appl. No. 11/351,342, dated Oct. 30, 2008, 11 pages.
- Caverly, Robert H., et al., "A Silicon CMOS Monolithic RF and Microwave Switching Element", 1997 European Microwave Conference, Jerusalem, Sep. 1997, 4 pgs.
- Kelly, Dylan, et al., Response to Office action mailed to the USPTO for related U.S. Appl. No. 11/351,342, dated Jan. 30, 2009, 11 pages.
- Luu, An T., Final Office Action received from USPTO, dated Apr. 8, 2009, for related U.S. Appl. No. 11/351,342, 14 pgs.
- Kelly, Dylan, et al., Proposed Amendment After Final filed in the USPTO dated Jun. 8, 2009 for related U.S. Appl. No. 11/351,342, 11 pgs.
- Luu, An T., Notice of Allowance received from USPTO, dated Jul. 2, 2009, for related U.S. Appl. No. 11/351,342, 5 pgs.
- Van Der Peet, H., Communication pursuant to Article 94(3) EPC for related application No. 02 800 982.7-2220 dated Aug. 6, 2009, 2 pgs.
- Office Action received from the USPTO dated Sep. 16, 2009 for related U.S. Appl. No. 11/347,014, 26 pages.
- Weman, Eva, Communication under Rule 71(3) EPC and Annex Form 2004 received from the European Patent Office for related appln. No. 02800982.7 ated Nov. 27, 2009, 68 pgs.
- Aquilani, Dario, Communication and Supplementary European Search Report for related European appln. No. 05763216, dated Nov. 27, 2009, 10 pgs.
- Kelly, Dylan, et al., Response and Terminal Disclaimers filed in the USPTO for related U.S. Appl. No. 11/347,014, dated Mar. 16, 2010, 7 pages.
- Aquilani, Dario, Communication Pursuant to Article 94(3) EPC received from the EPO for related appln. No. 05763216.8, dated Mar. 22, 2010, 7 pages.
- Burgener, et al., Amendment as filed in the USPTO dated Apr. 29, 2010 for related U.S. Appl. No. 11/501,125, 9 pgs.
- Tran, Pablo N., Notice of Allowance received from the USPTO for related U.S. Appl. No. 11/501,125, dated Jun. 10, 2010, 11 pages.
- Notice of Allowance received from the USPTO for related U.S. Appl. No. 11/347,014, dated Apr. 29, 2010, 12 pages.
- Chow, Charles Chiang, Office Action received from the USPTO for related U.S. Appl. No. 11/347,671, dated Apr. 28, 2010, 20 pages.
- Kai, Tetsuo, an English translation of an Office Action received from the Japanese Patent Office for related appln. No. 2007-518298 dated Jul. 20, 2010, 5 pgs.
- Chow, Charles Chang, Office Action received from the USPTO for related U.S. Appl. No. 11/347,671, dated Aug. 20, 2010, 18 pgs.
- Notice of Allowance received from the USPTO for related U.S. Appl. No. 12/315,395, dated Aug. 11, 2010, 26 pgs.
- Supplemental Notice of Allowance received from the USPTO for related U.S. Appl. No. 12/315,395, dated Oct. 29, 2010, 10 pgs.
- Kelly, et al., Comments on Examiner's Statement of Reasons for Allowance filed in the USPTO for related U.S. Appl. No. 11/347,014, dated Jul. 29, 2010, 2 pgs.
- Raab, et al., "Power Amplifiers and Transmitters for RF and Microwave", IEEE Transactions on Microwave Theory and Techniques, vol. 50, No. 3, pp. 814-826, Mar. 2002, USA.
- Ueda, et al., "A 5GHz-Band On-Chip Matching CMOS MMIC Front-End", 11th GAAS Symposium—Munich 2003, pp. 101-104, Germany.
- Nelson Pass, Pass Labs, "Cascode Amp Design", Audio Electronics, pp. 1-4, Mar. 1978.
- Lester F. Eastman, P.L., "High Power, Broadband, Linear, Solid State Amplifier", 16th Quarterly Rep. under MURI Contract No. N00014-96-1-1223 for period Jun. 1, 2000-Aug. 31, 2000, Sep. 2000.
- Jeon, et al., "A New "Active" Predistorter with High Gain Using Cascode-FET Structures", IEEE Radio Frequency Integrated Circuits Symposium, 2002, pp. 253-256.
- Hsu, et al., "Comparison of Conventional and Thermal-Stable Cascode (TSC) AlGaAs/GaAs HBTs for Microwave Power Applications", Journal of Solid-State Electronics, V. 43, Sep. 1999, 2 pgs.
- Kim, et al., "High-Performance V-Band Cascode HEMT Mixer and Downconverter Module", IEEE Transactions on Microwave Theory and Techniques, vol. 51, No. 3, Mar. 2003, pp. 805-810.
- Kelly, Dylan, Notice of Appeal filed in USPTO dated Jun. 2, 2011 for related U.S. Appl. No. 11/347,671, 6 pgs.
- Peregrine Semiconductor Corporation, Response (in Japanese), dated Aug. 14, 2006, for related Japanese application No. 2003-535287, 32 pgs.
- Miyajima, Ikumi, translation of Notice of Reasons for Refusal, dated Oct. 5, 2006 for related Japanese application No. 2003-535287, 4 pgs.
- Peregrine Semiconductor Corporation, Response filed in the EPO, dated Dec. 23, 2008 for related application No. 02 800 982.7-2220, 22 pgs.
- Peregrine Semiconductor Corporation, Response filed in the EPO, dated Oct. 7, 2009 for related application No. 02 800 982.7-2220, 23 pgs.
- Tran, Pablo N., Notice of Allowance received from the USPTO dated May 19, 2011 for related U.S. Appl. No. 11/501,125, 11 pgs.
- Chow, Charles Chiang, Notice of Allowance received from the USPTO dated Aug. 16, 2011 for related U.S. Appl. No. 11/347,671, 12 pgs.
- Tran, Pablo N., Notice of Allowance received from the USPTO dated Oct. 6, 2011 for related U.S. Appl. No. 11/501,125, 11 pgs.
- Unterberger, Michael, Extended European Search Report received from the EPO dated Sep. 30, 2011 for related appln. No. 10011669.8-2220, 9 pgs.
- Weman, Eva, Communication of a notice of opposition received from the EPO dated Nov. 8, 2011 for related appln. No. 02800982.7-2220, 33 pgs.

(56)

**References Cited**

## OTHER PUBLICATIONS

- Caverly, Robert H., "Linear and Nonlinear Characteristics of the Silicon CMOS Monolithic 50- $\Omega$  Microwave and RF Control Element", IEEE Journal of Solid-State Circuits, vol. 34, No. 1, Jan. 1999, pp. 124-126.
- Philips Semiconductors, Product Specificate, IC17 Data Handbook, Nov. 7, 1997, pp. 1-14.
- Iyama, Yoshitada, et al., "L-Bank SPDT Switch Using SI-MOSFET", IEICE Trans. Electronic, vol. E-79-C, No. 5, May 1996, pp. 636-643.
- Yamamoto, Kazuya, et al., "A 2.2-V Operating, 2.4-GHz Single-Chip GaAs MMIC Transceiver for Wireless Applications", IEEE Journal of Solid-State Circuits, vol. 34, No. 4, Apr. 1999, pp. 502-512.
- Patel, Reema, Office Action received from the USPTO dated Dec. 5, 2011 for related U.S. Appl. No. 13/046,560, 13 pgs.
- Trans, Pablo N., Office Action received from the USPTO dated Feb. 3, 2012 for related U.S. Appl. No. 12/903,848, 46 pgs.
- Unterberger, M., Summons to Attend Oral Proceedings pursuant to Rule 115(1) EPC received from the EPO dated Oct. 17, 2013 for appln. No. 02800982.7, 15 pgs.
- Shingleton, Michael, Office Action received from the USPTO dated Oct. 23, 2013 for U.S. Appl. No. 11/881,816, 25 pgs.
- Funakoshi, Ryo, Office Action and translation received from the JPO dated Oct. 29, 2013 for appln. No. 2013-006353, 15 pgs.
- Morena, Enrico, Communication Pursuant to Article 94(3) EPC received from the EPO dated Dec. 18, 2013 for appln. No. 06814836.0, 5 pgs.
- Stuber, et al., Amendment filed in the USPTO dated Dec. 20, 2013 for U.S. Appl. No. 13/028,144, 25 pgs.
- Brindle, et al., Amendment After Final filed in the USPTO dated Dec. 27, 2013 for U.S. Appl. No. 13/277,108, 8 pgs.
- Peregrine Semiconductor Corporation, Response filed in the EPO dated Jan. 9, 2014 for appln. No. 02800982.7, 21 pgs.
- Nguyen, Niki Hoang, Notice of Allowance received from the USPTO dated Jan. 10, 2014 for U.S. Appl. No. 13/277,108, 24 pgs.
- European Patent Office, Brief Communication received from the EPO dated Jan. 16, 2014 for appln. No. 02800982.7, 7 pgs.
- Schussler, Andrea, Report received from foreign filing associate regarding outcome of opposition conclusion, dated Feb. 25, 2014 for appln. No. 02800982.7, 13 pgs.
- Unterberger, Michael, Communication pursuant to Article 101(1) and Rule 81(2) to (3) EPC received from the EPO dated Mar. 3, 2014 for appln. No. 02800982.7, 3 pgs.
- Tanada, Kazuya, Translation of an Office Action received from the JPO dated Mar. 11, 2014 for appln. No. 2013-003388, 4 pgs.
- Nguyen, Niki Hoang, Office Action received from the USPTO dated Apr. 2, 2014 for U.S. Appl. No. 13/850,251, 9 pgs.
- Unterberger, Michael, Communication pursuant to Article 94(3) EPC received from the EPO dated Apr. 9, 2014 for appln. No. 10011669.8, 5 pgs.
- Weman, Eva, Provision of the minutes in accordance with Rule 124(4) EPC received from the EPO dated Apr. 10, 2014 for appln. No. 02800982.7, 9 pgs.
- Wang, Chi-Chang, et al., "Efficiency Improvement in Charge Pump Circuits", IEEE Journal of Solid-State Circuits, vol. 32, No. 6, Jun. 1997, pp. 852-860.
- Hiramoto, Toshiro, et al., "Low Power and Low Voltage MOSFETs with Variable Threshold Voltage Controlled by Back-Bias", IEICE Trans. Electron, vol. E83-C, No. 2, Feb. 2000, pp. 161-169.
- Su, Pin, et al., "On the Body-Source Built-In Potential Lowering of SOI MOSFETs", IEEE Electron Device Letters, vol. 24, No. 2, Feb. 2003, pp. 90-92.
- Yang, Min, "Sub-100nm Vertical MOSFET's with Si—x—y GexCy Source/Drains", a dissertation presented to the faculty of Princeton University, Jun. 2000, 272 pgs.
- Ytterdal, T., et al., "MOSFET Device Physics and Operation", Device Modeling for Analog and RF CMOS Circuit Design, 2003 John Wiley & Sons, Ltd., 46 pgs.
- Sudhama, et al., "Compact Modeling and Circuit Impact of a Novel Frequency Dependence of Capacitance in RF MOSFETs", Nano Science and Technology Institute, Technical Proceedings of the 2001 Int'l Conference of Modeling and Simulation of Microsystems, 2001.
- Casu, et al., "Comparative Analysis of PD-SOI Active Body-Biasing Circuits", IEEE Int'l SOI Conference, Oct. 2000, pp. 94-95.
- Cho, et al., "Comparative Assessment of Adaptive Body-Bias SOI Pass-Transistor Logic", Fourth Int'l Symposium on Quality Electronic Design, Mar. 2003, pp. 55-60.
- Chan, et al., "Comparative Study of Fully Depleted and Body-Grounded Non Fully Depleted SOI MOSFET's for High Performance Analog and Mixed Signal Circuits", IEEE Transactions on Electron Devices, vol. 42, No. 11, Nov. 1995, pp. 1975-1981.
- Tseng, et al., "Comprehensive Study on AC Characteristics in SOI MOSFETs for Analog Applications", 1998 Symposium on VLSI Technology Digest of Technical Papers, Jun. 1998.
- Pellella, et al., "Control of Off-State Current in Scaled PD/SOI CMOS Digital Circuits", Proceedings IEEE Int'l SOI Conference, Oct. 1998, pp. 147-148.
- Assaderaghi, "DTMOS: Its Derivatives and Variations, and Their Potential Applications", The 12th Int'l Conference on Microelectronics, Nov. 2000, pp. 9-10.
- Lindert, et al., "Dynamic Threshold Pass-Transistor Logic for Improved Delay at Lower Power Supply Voltages", IEEE Journal of Solid-State Circuits, vol. 34, No. 1, Jan. 1999, pp. 85-89.
- Drake, et al., "Dynamic-Threshold Logic for Low Power VLSI Design", www.research.ibm.com/acas, 2001.
- Wei, et al., "Effect of Floating-Body Charge on SOI MOSFET Design", IEEE Transaction on Electron Devices, vol. 45, No. 2, Feb. 1998.
- Duyet, et al., "Effects of Body Reverse Pulse Bias on Geometric Component of Charge Pumping Current in FD SOI MOSFETs", Proceedings IEEE Int'l SOI Conference, Oct. 1998, pp. 79-80.
- Krishnan, "Efficacy of Body Ties Under Dynamic Switching Conditions in Partially Depleted SOI CMOS Technology", Proceedings IEEE Int'l SOI Conference, Oct. 1997, pp. 140-141.
- Lu, et al., "Floating Body Effects in Partially Depleted SOI CMOS Circuits", ISPLED, Aug. 1996, pp. 1-6.
- Ueda, et al., "Floating Body Effects on Propagation Delay in SOI CMOS LSIs", IEEE SOI Conference, Oct. 1996, pp. 142-143.
- Matsumoto, et al., "Fully Depleted 30-V-Class Thin Film SOI Power MOSFET", IEDM 95-979, 1995, pp. 38.6.1-38.6.4.
- Assaderaghi, et al., "History Dependence of Non-Fully Depleted (NFD) Digital SOI Circuits", 1996 Symposium on VLSI Technology Digest of Technical Papers 13.1, 1996, pp. 122-123.
- Damiano, et al., "Integrated Dynamic Body Contact for H Gate PD SOI MOSFETs for High Performance/Low Power", IEEE SOI Conference, Oct. 2004, pp. 115-116.
- Tat, International Search Report and Written Opinion received from USRO dated Jul. 3, 2008 for related appln. No. PCT/US06/36240.
- Raully, et al., "Investigation of Single and Double Gate SOI MOSFETs in Accumulation Mode for Enhanced Performances and Reduced Technological Drawbacks", Proceedings 30th European Solid-State Device Research Conference, Sep. 2000, pp. 540-543.
- Morishita, et al., "Leakage Mechanism Due to Floating Body and Countermeasure on Dynamic Retention Mode of SOI-DRAM", 1995 Symposium on VLSI Technology Digest of Technical Papers, Apr. 1995, pp. 141-142.
- Keys, "Low Distortion Mixers or RF Communications", Ph.D. Thesis, University of California-Berkeley, 1995.
- Chen, et al., "Low Power, Multi-Gigabit DRAM Cell Design Issues Using SOI Technologies", [http://bwrc.eecs.berkeley.edu/people/grad\\_students/chenff/reports](http://bwrc.eecs.berkeley.edu/people/grad_students/chenff/reports), May 1999.
- Pellella, et al., "Low-Voltage Transient Bipolar Effect Induced by Dynamic Floating-Body Charging in Scaled PD/SOI MOSFET's", IEEE Electron Device Letters, vol. 17, No. 5, May 1996.
- Wei, "Measurement and Modeling of Transient Effects in Partially Depleted SOI MOSFETs", M.S. Thesis, MIT, Jul. 1996.
- Shoucair, "Modeling, Decoupling and Suppression of MOSFET Distortion Components", IEEE Proceeding Circuit Devices Systems, vol. 146, No. 1, Feb. 1999.
- Tat, Notice of Allowance received from USPTO dated Sep. 16, 2010 for related U.S. Appl. No. 11/520,912.

(56)

## References Cited

## OTHER PUBLICATIONS

- Tat, Office Action received from USPTO dated Dec. 10, 2009 for related U.S. Appl. No. 11/520,912.
- Shingleton, Office Action received from USPTO dated Jan. 19, 2010 for related U.S. Appl. No. 11/881,816.
- Tat, Office Action received from USPTO dated Jul. 8, 2009 for related U.S. Appl. No. 11/520,912.
- Tat, Office Action received from USPTO dated Sep. 15, 2008 for related U.S. Appl. No. 11/520,912.
- Shahidi, et al., "Partially Depleted SOI Technology for Digital Logic", IEEE Int'l Solid-State Circuits Conference, 1999, pp. 426-427.
- Stuber, et al., Photocopy of an amendment that was filed with the USPTO dated Mar. 16, 2009 for related U.S. Appl. No. 11/520,912.
- Stuber, et al., Photocopy of an amendment that was filed with the USPTO dated Sep. 8, 2009 for related U.S. Appl. No. 11/520,912.
- Fuse, et al., "A 0.5V 200MHz 1-Stage 32b ALU Using a Body Bias Controlled SOI Pass-Gate Logic", IEEE Int'l Solid-State Circuits Conference, Feb. 1997.
- Douseki, et al., "A 0.5-V MTCMOS/SIMOX Logic Gate", IEEE Journal of Solid-State Circuits, vol. 32, No. 10, Oct. 1997.
- Douseki, et al., "A 0.5v SIMOX-MTCMOS Circuit with 200ps Logic Gate", IEEE Int'l Solid-State Circuits Conference, 1996, pp. 84-85, 423.
- Shimomura, et al., "A 1-V 46-ns 16-mb SOI-DRAM with Body Control Technique", IEEE Journal of Solid-State Circuits, vol. 32, No. 11, Nov. 1997, pp. 1712-1720.
- Ueda, et al., "A CAD Compatible SOI/CMOS Gate Array Having Body Fixed Partially Depleted Transistors", IEEE Int'l Solid-State Circuits Conference, Feb. 8, 1997, pp. 288-289.
- Eschenbach, Communication from the EPO dated Feb. 4, 2009 for related appln. No. 06786943.8, 101 pgs.
- Kuang, et al., "A Dynamic Body Discharge Technique for SOI Circuit Applications", IEEE Int'l SOI Conference, Oct. 1999, pp. 77-78.
- Assaderaghi, et al., "A Dynamic Threshold Voltage MOSFET (DTMOS) for Ultra-Low Voltage Operation", Int'l Electron Devices Meeting, Dec. 1994, pp. 809-812.
- Kuang, et al., "A Floating-Body Charge Monitoring Technique for Partially Depleted SOI Technology", Int'l Journal of Electronics, vol. 91, No. 11, Nov. 2004, pp. 625-637.
- Gil, et al., "A High Speed and Low Power SOI Inverter Using Active Body-Bias", Proceedings Int'l Symposium on Low Power Electronics and Design, Aug. 1998, pp. 59-63.
- Gil, et al., "A High Speed and Low Power SOI Inverter Using Active Body-Bias", Solid-State Electronics, vol. 43, 1999, pp. 791-799.
- Kuang, et al., "A High-Performance Body-Charge-Modulated SOI Sense Amplifier", IEEE Int'l SOI Conference, Oct. 2000, pp. 100-101.
- Madhian, et al., "CMOS RF ICs for 900MHz-2.4GHz Band Wireless Communication Networks", IEEE Radio Frequency Integrated Circuits Symposium, 1999, pp. 13-16.
- Chung, et al., "A New SOI Inverter for Low Power Applications", IEEE SOI Conference, Oct. 1996, pp. 20-21.
- Chung, et al., "A New SOI Inverter Using Dynamic Threshold for Low-Power Applications", IEEE Electron Device Letters, vol. 18, No. 6, Jun. 1997, pp. 248-250.
- Chung, et al., "A New SOI MOSFET Structure with Junction Type Body Contact", Int'l Electron Device Meeting (IEDM) Technical Digest, 1999, pp. 59-62.
- Terauchi, et al., "A Novel 4T SRAM Cell Using "Self-Body-Biased" SOI MOSFET Structure Operating at 0.5 Volt", IEEE Int'l SOI Conference, Oct. 2000, pp. 108-109.
- Wang, et al., "A Novel Low-Voltage Silicon-On-Insulator (SOI) CMOS Complementary Pass-Transistor Logic (CPL) Circuit Using Asymmetrical Dynamic Threshold Pass-Transistor (ADTPT) Technique", Proceedings of the 43rd IEEE Midwest Symposium on Circuits and Systems, Aug. 2000, pp. 694-697.
- Das, et al., "A Novel Sub-1 V High Speed Circuit Design Technique in Partially Depleted SOI-CMOS Technology with Ultra Low Leakage Power", Proceedings of the 28th European Solid-State Circuits Conference, Sep. 2002, pp. 24-26.
- Das, et al., "A Novel Sub-1 V High Speed Circuit Design Technique in Partially Depleted SOI-CMOS Technology with Ultra Low Leakage Power", Proceedings of the 28th European Solid-State Circuits Conference, Sep. 2002, pp. 267-270.
- Kanda, et al., "A Si RF Switch MMIC for the Cellular Frequency Band Using SOI-CMOS Technology", Institute of Electronics, Information and Communication Engineers Technical Report, vol. 100, No. 152, Jun. 2000, pp. 79-83.
- Tseng, et al., "Characterization of Floating Body and Body-Grounded Thin Film Silicon-on-Insulator MOSFETs for Analog Circuit Applications", Ph.D. Thesis, UCLA, 1999, pgs. All.
- Nakatani, "A Wide Dynamic Range Switched-LNA in SiGe BICMOS", IEEE Radio Frequency Integrated Circuits Symposium, 2001, pp. 223-226.
- Tseng, et al., "AC Floating-Body Effects and the Resultant Analog Circuit Issues in Submicron Floating body and Body-Grounded SOI MOSFET's", IEEE Transactions on Electron Devices, vol. 46, No. 8, Aug. 1999, pgs. All.
- Tseng, et al., "AC Floating-Body Effects in Submicron Fully Depleted (FD) SOI nMOSFET's and the Impact on Analog Applications", IEEE Electron Devices, vol. 19, No. 9, Sep. 1998, pp. 351-353.
- Wada, et al., "Active Body-Bias SOI-CMOS Driver Circuits", Symposium on VLSI Circuits Digest of Technical Papers, 1997, pp. 29-30.
- Stuber, et al., Amendment filed in the USPTO dated Jun. 10, 2010 for related U.S. Appl. No. 11/520,912, 28 pgs.
- Saccamango, et al., "An SOI Floating Body Charge Monitor Technique", IEEE Int'l SOI Conference, Oct. 2000, pp. 88-89.
- Koh, et al., "Body-Contacted SOI MOSFET Structure with Fully Bulk CMOS Compatible Layout and Process", IEEE Electron Device Letters, vol. 18, No. 3, Mar. 1997, pp. 102-104.
- Dunga, "Analysis of Floating Body Effects in Thin Film SOI MOSFET's Using the GIDL Current Technique", Proceedings of the 8th Int'l Symposium on Physical and Failure Analysis of Integrated Circuits, 2001, pp. 254-257.
- Gautier, et al., "Body Charge Related Transient Effects in Floating Body SOI nMOSFETs", IEDM Tech. Digest, 1995, pp. 623-626.
- Koh, et al., "Body-Contracted SOI MOSFET Structure and its Application to DRAM", IEEE Transactions on Electron Devices, vol. 45, No. 5, May 1998, pp. 1063-1070.
- Brindle, et al., Response filed in the EPO for related appln. No. 06814836.0-1235 dated Oct. 12, 2010.
- Matloubian, "Smart Body Contact for SOI MOSFETs", 1989 IEEE SOS/SOI Technology Conference, Oct. 1999, pp. 128-129.
- Chuang, et al., "SOI for Digital CMOS VLSI Design: Design Consideration and Advances", Proceedings of the IEEE, vol. 86, No. 4, Apr. 1998, pp. 689-720.
- Kuge, et al., "SOI-DRAM Circuit Technologies for Low Power High Speed Multigiga Scale Memories", IEEE Journal of Solid-State Circuits, vol. 31, No. 4, Apr. 1996, pp. 586-591.
- Morena, Supplementary European Search Report dated Feb. 17, 2010 relating to appln. No. 06814836.0.
- Duyet, et al., "Suppression of Geometric Component of Charge Pumping Current in Thin Film Silicon on Insulator Metal-Oxide-Semiconductor Field-Effect Transistors", Japanese Journal of Applied Physics, vol. 37, Jul. 1998, pp. L855-858.
- Casu, et al., "Synthesis of Low-Leakage PD-SOI Circuits with Body Biasing", Int'l Symposium on Low Power Electronics and Design, Aug. 2001, pp. 287-290.
- Wang, et al., "Threshold Voltage Instability at Low Temperatures in Partially Depleted Thin Film SOI MOSFET's", 1990 IEEE SOS/SOI Technology Conference, Oct. 1990, pp. 91-92.
- Shimomura, et al., "TP4.3: A 1V 46ns 16Mb SOI-DRAM with Body Control Technique", 1997 IEEE Int'l Solid-State Circuits Conference, Feb. 1997.
- Assaderaghi, et al., "Transient Pass-Transistor Leakage Current in SOI MOSFET's", IEEE Electron Device Letters, vol. 18, No. 6, Jun. 1997, pp. 241-243.

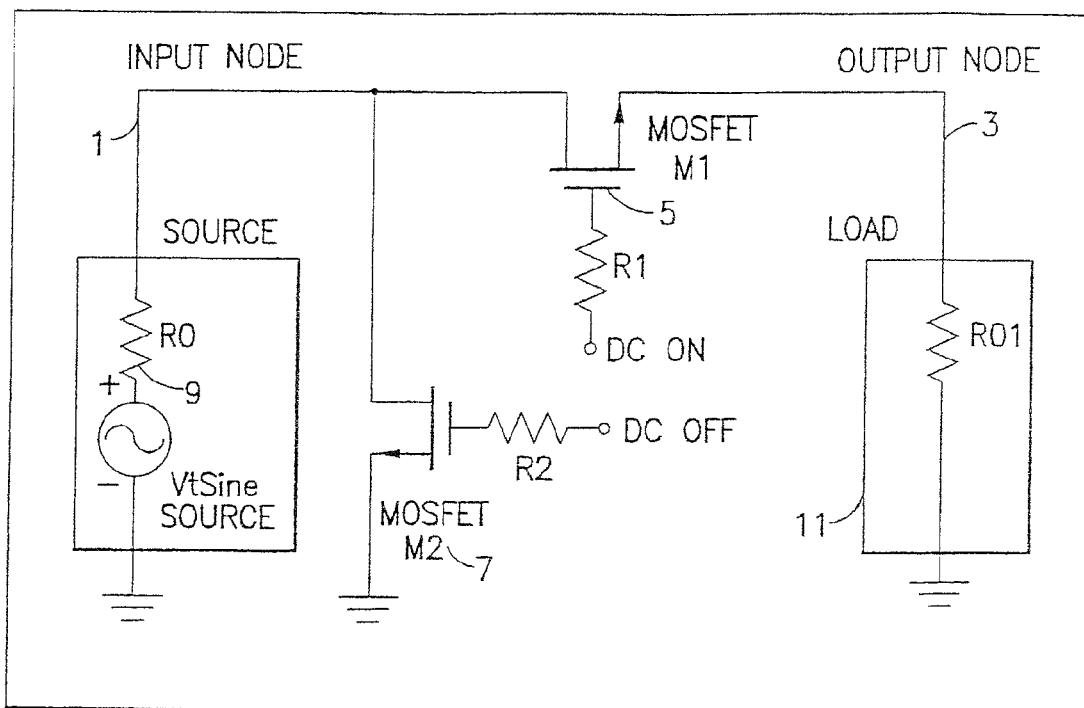
(56)

**References Cited**

## OTHER PUBLICATIONS

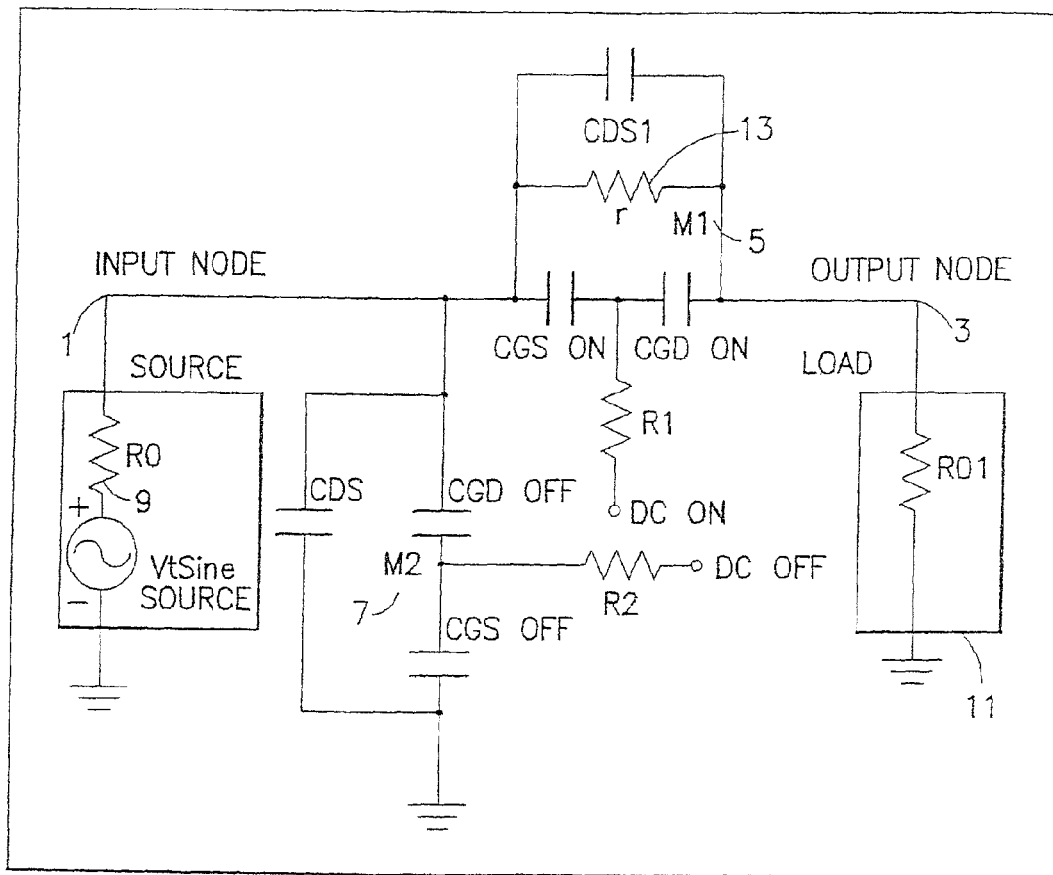
- Mashiko, et al., "Ultra-Low Power Operation of Partially-Depleted SOI/CMOS Integrated Circuits", *IEICE Transactions on Electronic Voltage*, No. 11, Nov. 2000, pp. 1697-1704.
- Das, et al., "Ultra-Low-Leakage Power Strategies for Sub-1 V VLSI: Novel Circuit Styles and Design Methodologies for Partially Depleted Silicon-on-Insulator (PD-SOI) CMOS Technology", *Proceedings of the 16th Int'l Conference on VLSI Design*, 2003.
- Pelloie, et al., "WP 25.2: SOI Technology Performance and Modeling", 1999 IEEE Int'l Solid-State Circuits Conference, Feb. 1999.
- Goldman, et al., "0.15 $\mu$ m SOI DRAM Technology Incorporating Sub-Volt Dynamic Threshold Devices for Embedded Mixed-Signal & RF Circuits", 2001 IEEE SOI Conference, Oct. 2001, pp. 97-98.
- Hirota, et al., "0.5V 320MHz 8b Multiplexer/Demultiplexer Chips Based on a Gate Array with Regular-Structured DTMOS/SOP", *ISSCC*, Feb. 1998, pp. 12.2-1-12.2-11.
- Fuse, et al., "0.5V SOI CMOS Pass-Gate Logic", 1996 IEEE Int'l Solid-State Circuits Conference, Feb. 1996, pp. 88-89, 424.
- "An Ultra-Thin Silicon Technology that Provides Integration Solutions on Standard CMOS", *Peregrine Semiconductor*, 1998.
- Caverly, "Distortion in Microwave Control Devices", 1997.
- Masuda, et al., "RF Current Evaluation of ICs by MP-10L", *NEC Research & Development*, vol. 40-41, 1999, pp. 253-258.
- "Miniature Dual Control SP4T Switches for Low Cost Multiplexing", *Hittite Microwave*, 1995.
- Uda, "Miniaturization and High Isolation of a GaAs SPDT Switch IC Mounted in Plastic Package", 1996.
- Marshall, et al., "SOI Design: Analog, Memory, and Digital Techniques", *Kluwer Academic Publishers*, 2002.
- Bernstein, et al., "SOI Circuit Design Concepts", *Springer Science + Business Media*, 2000.
- Brinkman, et al., "Respondents' Notice of Prior Art, Investigation No. 337-TA-848, dated Aug. 31, 2012, 59 pgs.
- Minoli, "Telecommunications Technology Handbook", *Artech House*, 2003.
- Morreale, "The CRC Handbook of Modern Telecommunication", *CRC Press*, 2001.
- Sayre, "Complete Wireless Design", *McGraw-Hill*, 2001.
- Schaper, "Communications, Computations, Control, and Signal Processing", *Kluwer Academic*, 1997.
- Shafi, "Wireless Communications in the 21st Century", *Wiley*, 2002.
- Willert-Porata, M., *Advances in Microwave and Radio Frequency Processing*, 8th International Conference on Microwave and High-Frequency Heating, Oct. 2009.
- Pozar, "Microwave and RF Design of Wireless Systems", *Wiley*, 2001.
- Maas, "The RF and Microwave Circuit Design Cookbook", *Artech House*, 1998.
- Smith, "Modern Communication Systems", *McGraw-Hill*, 1998.
- Van Der Puije, "Telecommunication Circuit Design", *Wiley*, 2002.
- Razavi, "RF Microelectronics", *Prentice-Hall*, 1998.
- Van Der Puije, "Telecommunication Circuit Design", *Wiley*, 1992.
- Weisman, "The Essential Guide to RF and Wireless", *Prentice-Hall*, 2000.
- Wetzel, "Silicon-on-Sapphire Technology for Microwave Power Application", *University of California, San Diego*, 2001.
- Johnson, "Silicon-on-Sapphire Technology for Microwave Circuit Applications", *Dissertation, UCSD*, 1997, pp. 1-184.
- Englekirk, Robert Mark, *Response After Final Office Action* filed in the USPTO dated Jun. 8, 2015 for U.S. Appl. No. 14/028,357, 3 pgs.
- Patel, Reema, *Notice of Allowance* received from the USPTO dated Jun. 25, 2015 for U.S. Appl. No. 14/028,357, 12 pgs.
- Stuber, et al., *Response/Amendment and Terminal Disclaimers* filed in the USPTO dated Jul. 27, 2015 for U.S. Appl. No. 13/948,094, 26 pgs.
- Aquilani, Dario, *Extended Search Report* received from the EPO dated Jun. 11, 2015 for appln. No. 14182150.4, 9 pgs.
- Tran, Pablo, *Notice of Allowance* received from the USPTO dated Oct. 26, 2012 for related U.S. Appl. No. 12/903,848, 14 pgs.
- Stuber, et al., *Supplemental Amendment* filed in the USPTO dated Nov. 8, 2012 for related U.S. Appl. No. 13/028,144, 17 pgs.
- Patel, Reema, *Notice of Allowance* received from the USPTO dated Dec. 3, 2012 for related U.S. Appl. No. 13/046,560, 9 pgs.
- Tran, Pablo, *Office Action* received from the USPTO dated Dec. 28, 2012 for related U.S. Appl. No. 13/412,463, 6 pgs.
- Aquilani, Dario, *Communication pursuant to Article 94(3) EPC* dated Jan. 21, 2013 for related appln. No. 05763216.8, 4 pgs.
- Peregrine Semiconductor Corporation, *Reply* filed in the EPO dated Jul. 29, 2013 or related appln. No. 05763216.8, 17 pgs.
- Dang, Hung Q., *Notice of Allowance* received from the USPTO dated Jan. 25, 2013 for related U.S. Appl. No. 12/735,954, 42 pgs.
- Brosa, Anna-Maria, *European Search Report* received from the EPO dated Feb. 1, 2013 for related appln. No. 12194187.6, 10 pgs.
- Tran, Pablo, *Notice of Allowance* received from the USPTO dated Feb. 15, 2013 for related U.S. Appl. No. 12/903,848, 26 pgs.
- Patel, Reema, *Notice of Allowance* received from the USPTO dated Mar. 15, 2013 for related U.S. Appl. No. 13/046,560, 10 pgs.
- Tran, Pablo, *Notice of Allowance* received from the USPTO dated May 16, 2013 for related U.S. Appl. No. 12/903,848, 101 pgs.
- Burgener, et al., *Amendment* filed in the USPTO dated May 20, 2013 for related U.S. Appl. No. 13/412,463, 6 pgs.
- Peregrine Semiconductor Corporation, *Response* filed in the EPO dated May 23, 2013 for related appln. No. 09174085.2, 16 pgs.
- Tran, Pablo N., *Notice of Allowance* received from the USPTO dated Jun. 6, 2013 for related U.S. Appl. No. 13/412,463, 142 pgs.
- Englekirk, Robert, Part B—Fee(s) Transmittal and Comments on Examiner's Statement of Reasons for Allowance filed in the USPTO dated Jun. 17, 2013 for related U.S. Appl. No. 13/046,560, 4 pgs.
- Burgener, et al., *First Preliminary Amendment* filed in the USPTO dated Apr. 27, 2012 for U.S. Appl. No. 12/980,161, 21 pgs.
- Office Action* received from the USPTO dated Feb. 19, 2013 for U.S. Appl. No. 12/980,161, 97 pgs.
- Notice of Allowance* received from the USPTO dated Sep. 30, 2013 for U.S. Appl. No. 12/980,161, 8 pgs.
- Burgener, et al., *Amendment* filed in the USPTO dated Aug. 19, 2013 for U.S. Appl. No. 12/980,161, 20 pgs.
- Ezzeddine, et al., "The High Voltage/High Power FET (HiVPI)", 2003 IEEE Radio Frequency Integrated Circuits Symposium, pp. 215-218.
- Shingleton, Michael, *Office Action* received from the USPTO dated Apr. 10, 2015 for U.S. Appl. No. 14/257,808, 8 pgs.
- Peregrine Semiconductor Corporation, *Response* filed in the EPO dated Apr. 29, 2015 for appln. No. 14182150.4, 7 pgs.
- Nguyen, Niki Hoang, *Notice of Allowance* received from the USPTO dated Apr. 22, 2015 for U.S. Appl. No. 13/850,251, 22 pgs.

\* cited by examiner



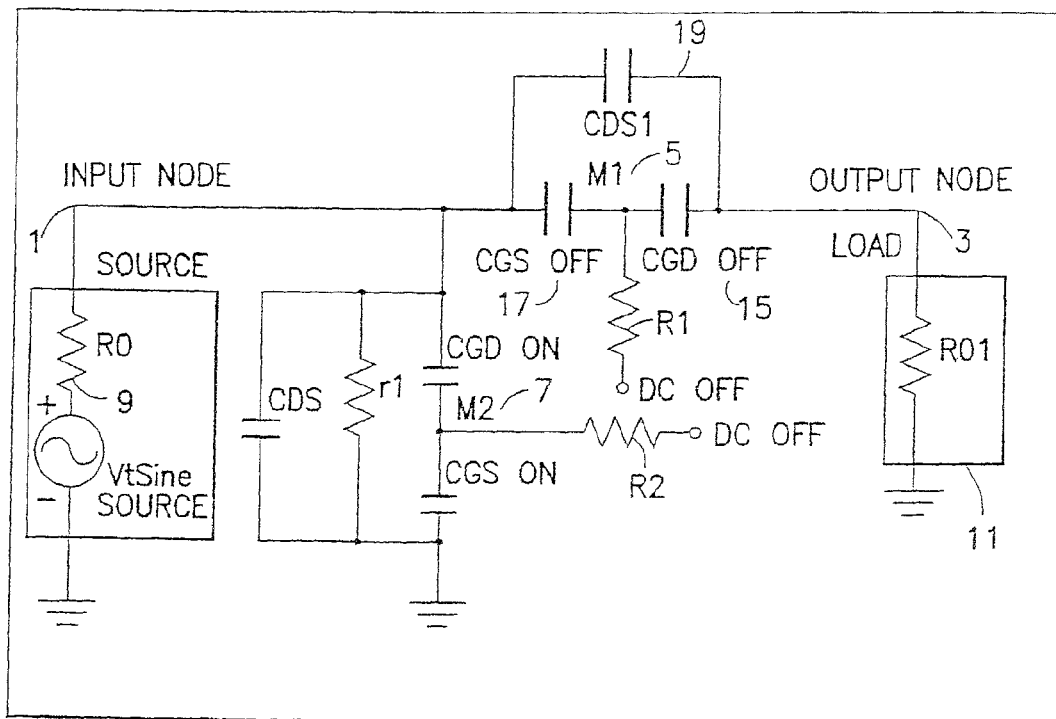
10

FIG. 1a



10

FIG. 1b



10

FIG.1c

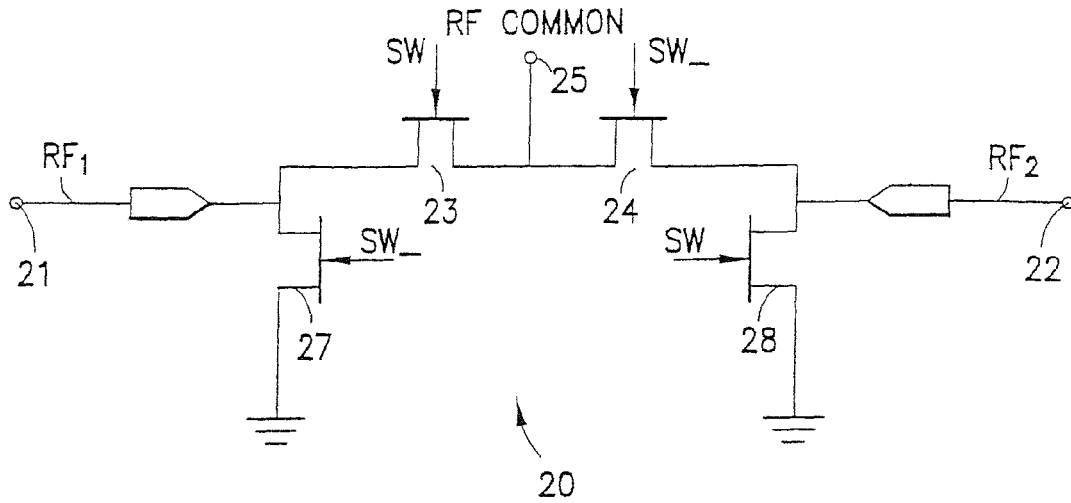


FIG. 2

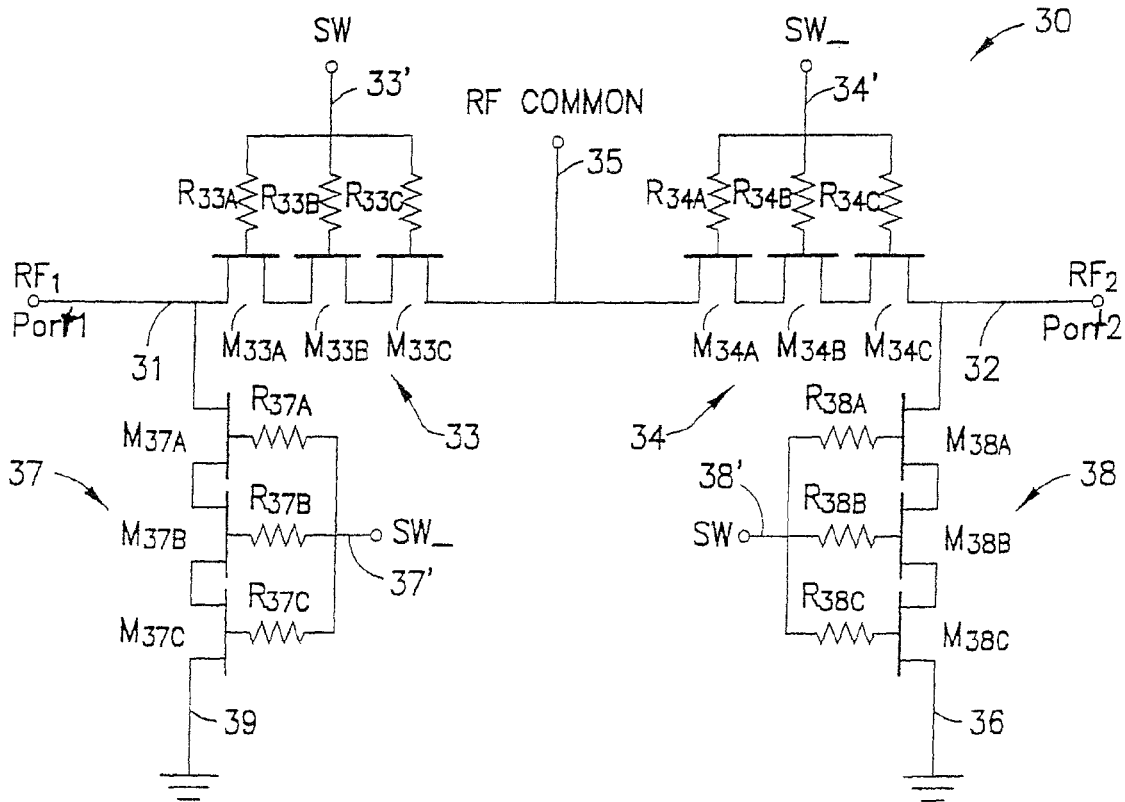


FIG. 3

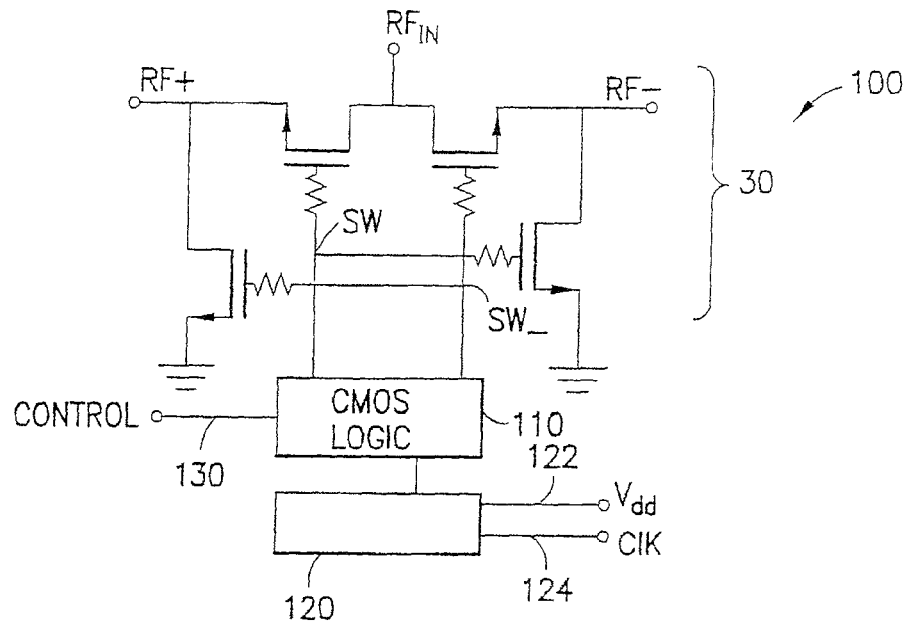


FIG. 4

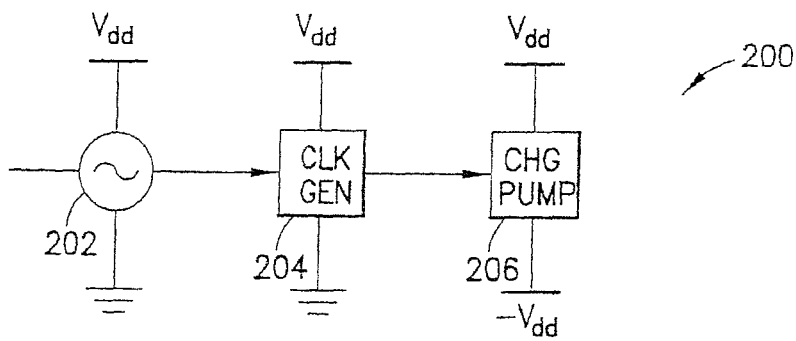


FIG. 5a

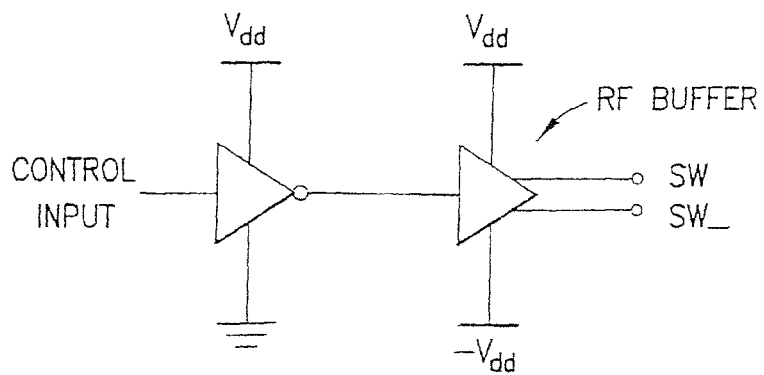


FIG. 8b

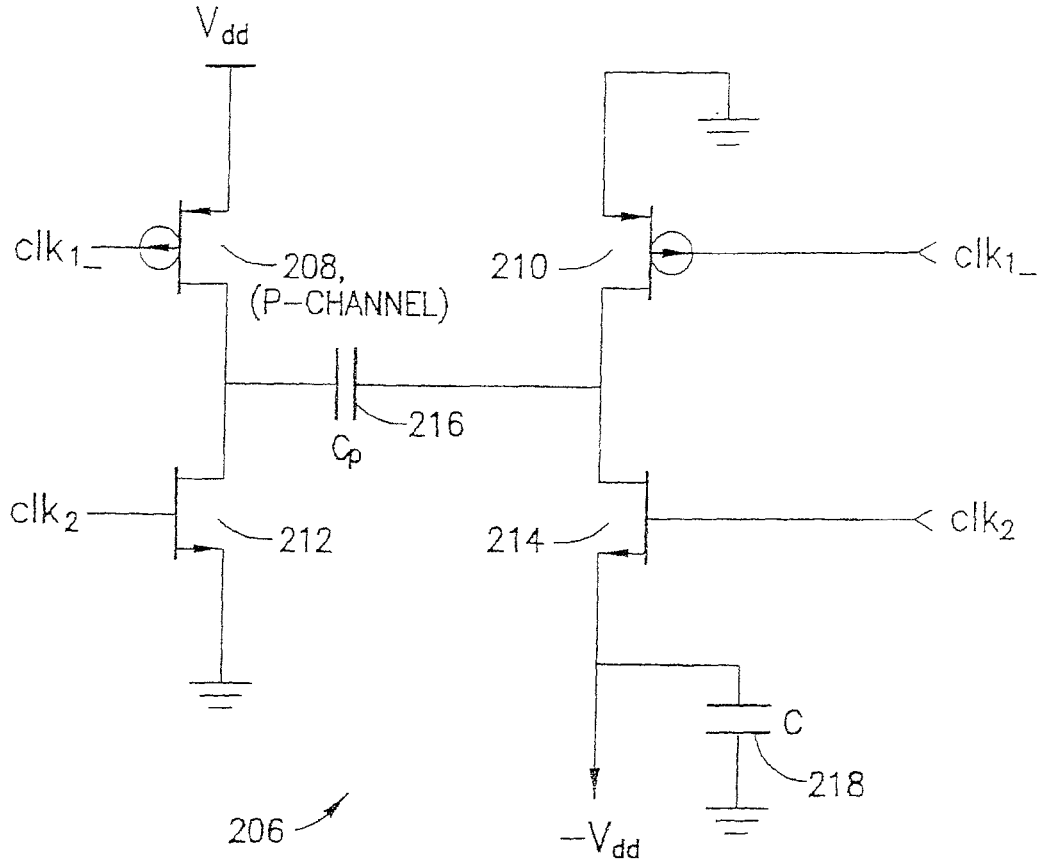


FIG.5b

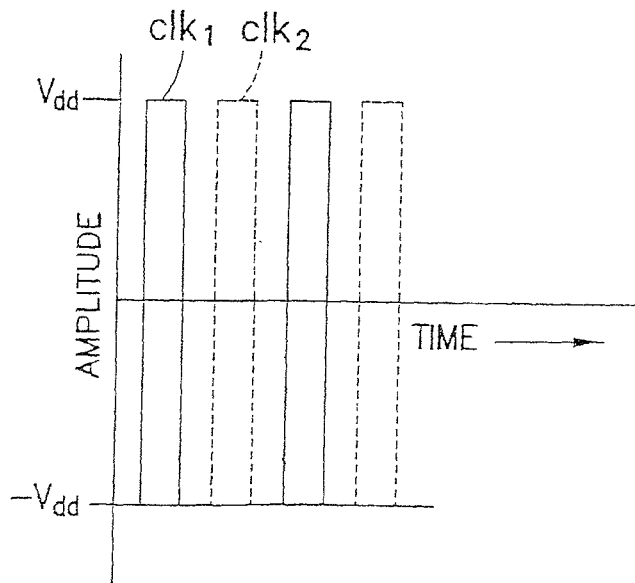


FIG.5c

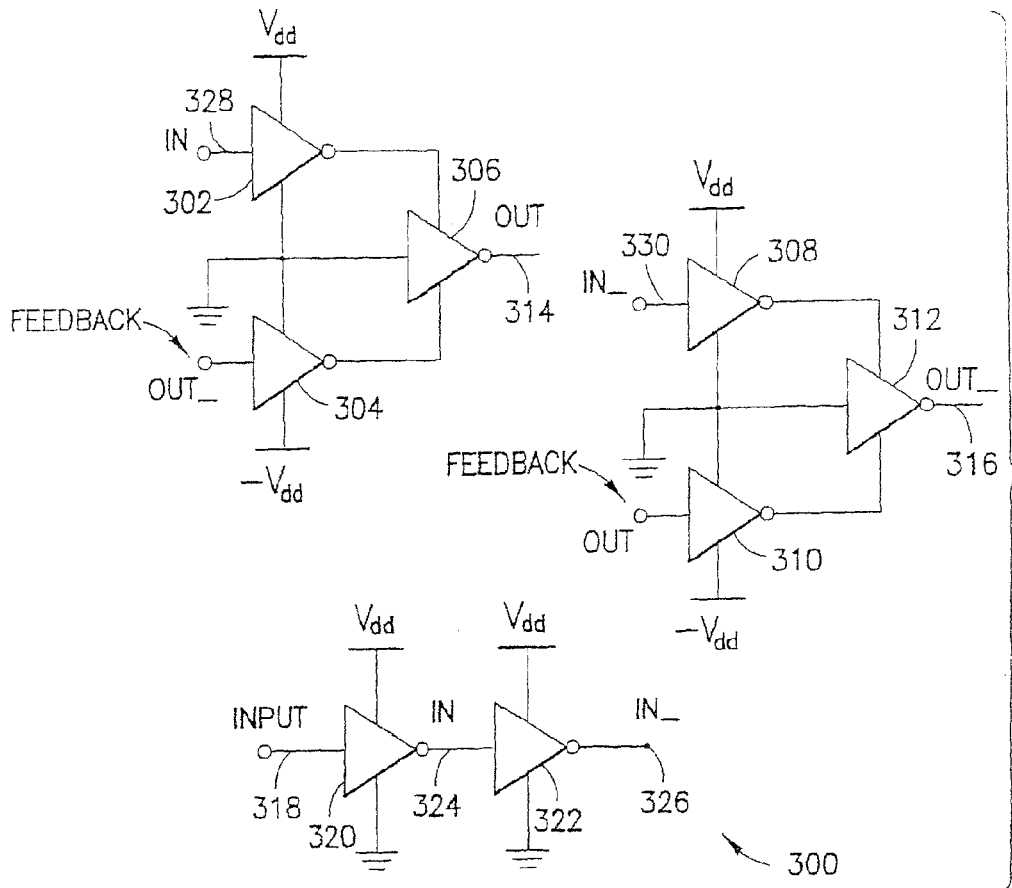


FIG.6a

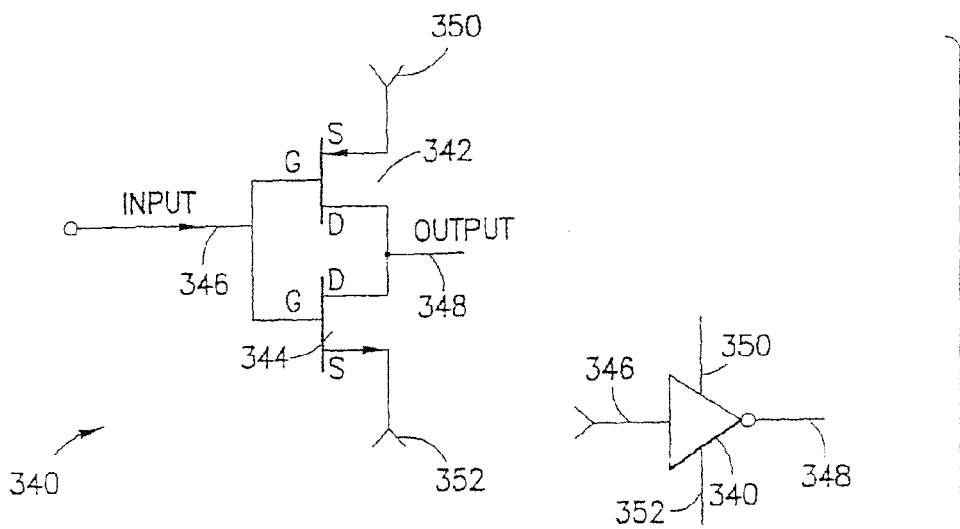


FIG.6b

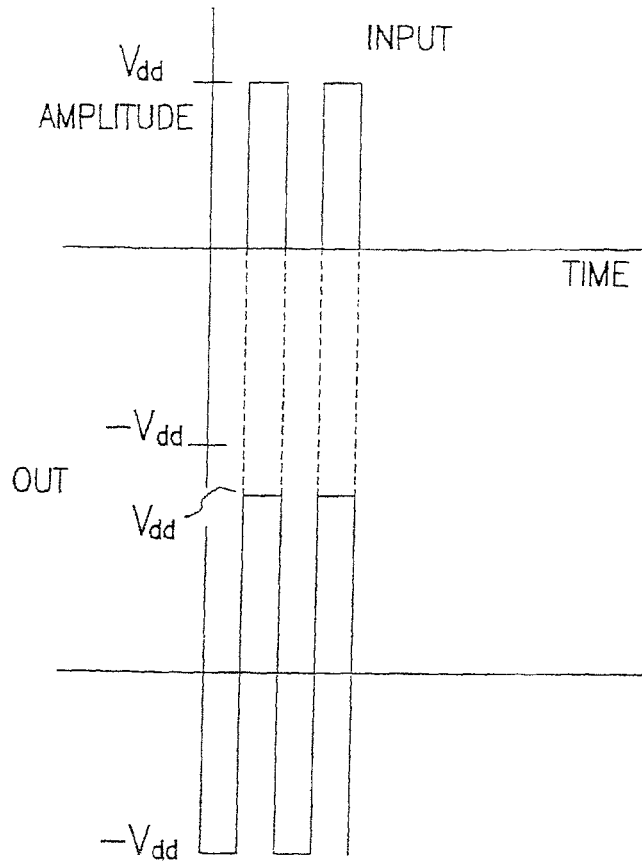


FIG.7a

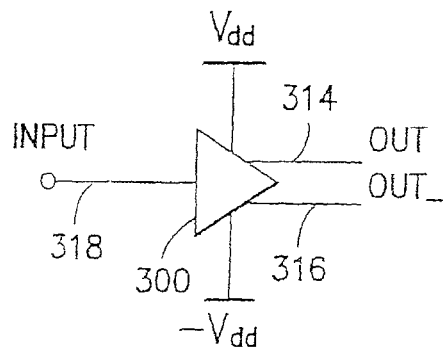


FIG.7b

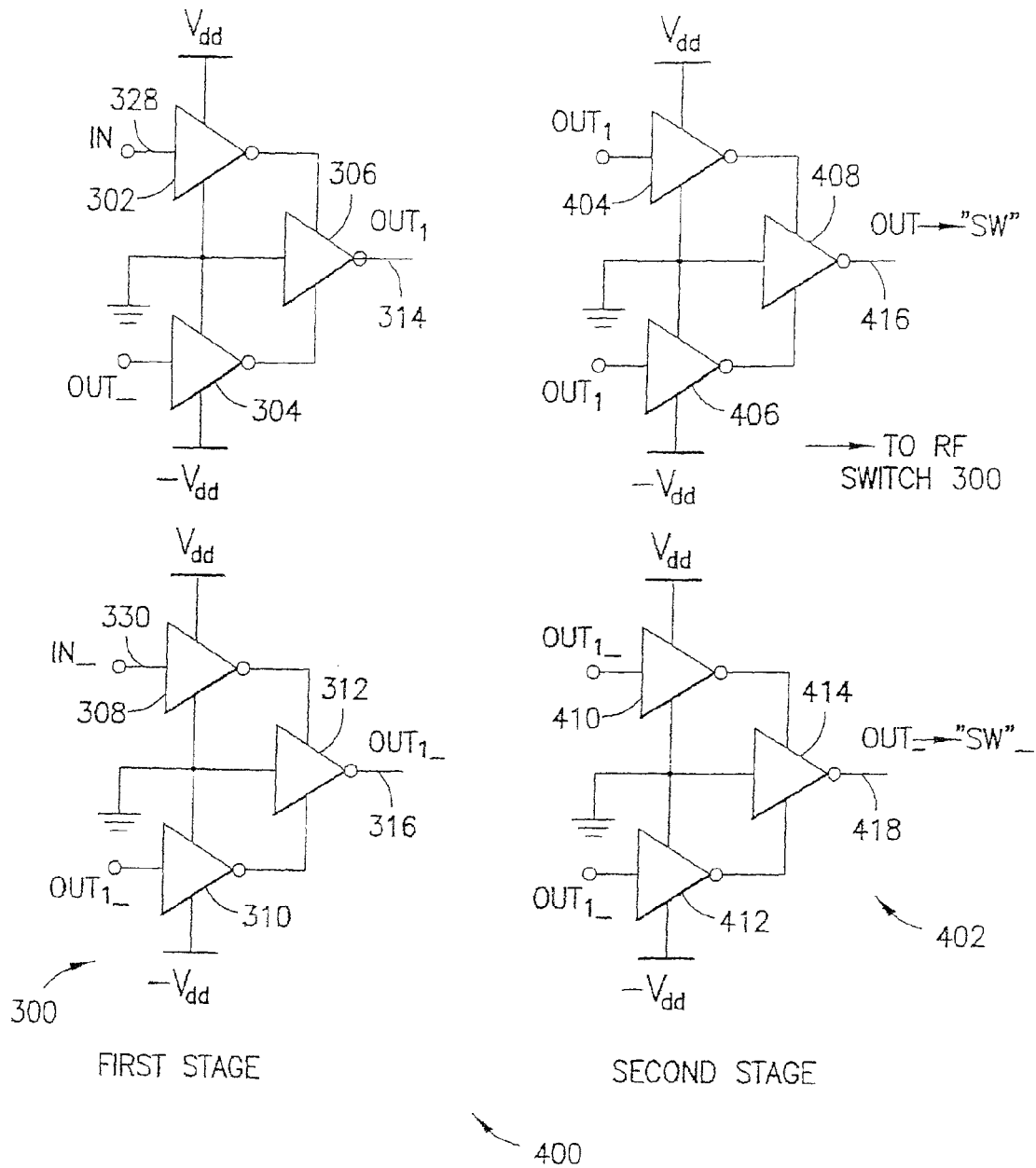


FIG. 8a

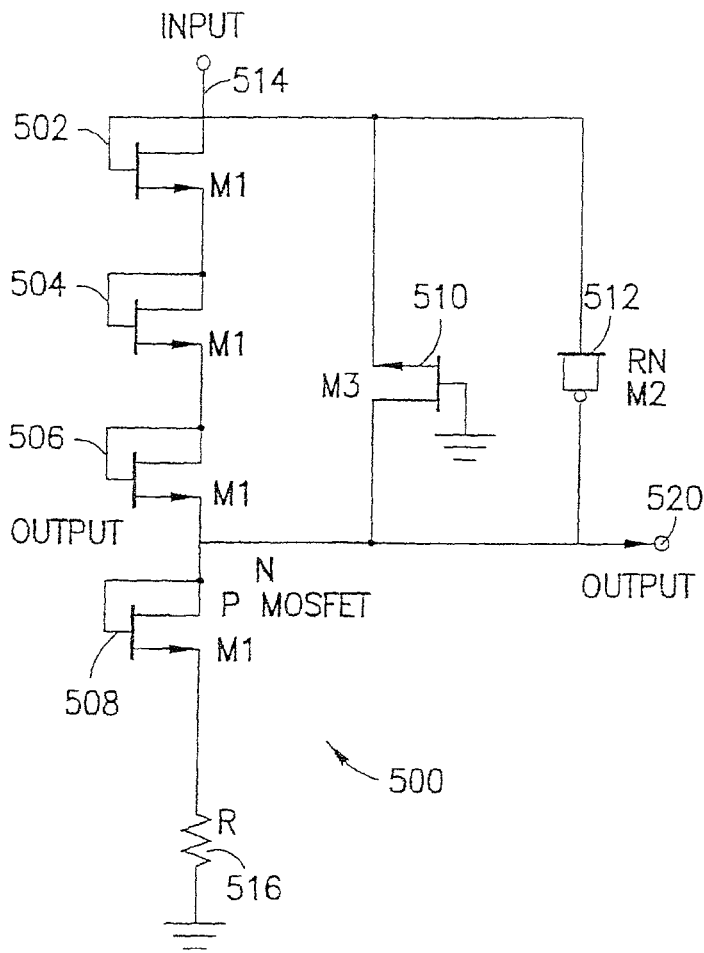


FIG. 9a

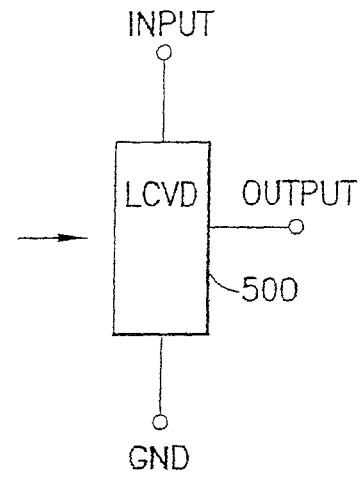


FIG. 9b

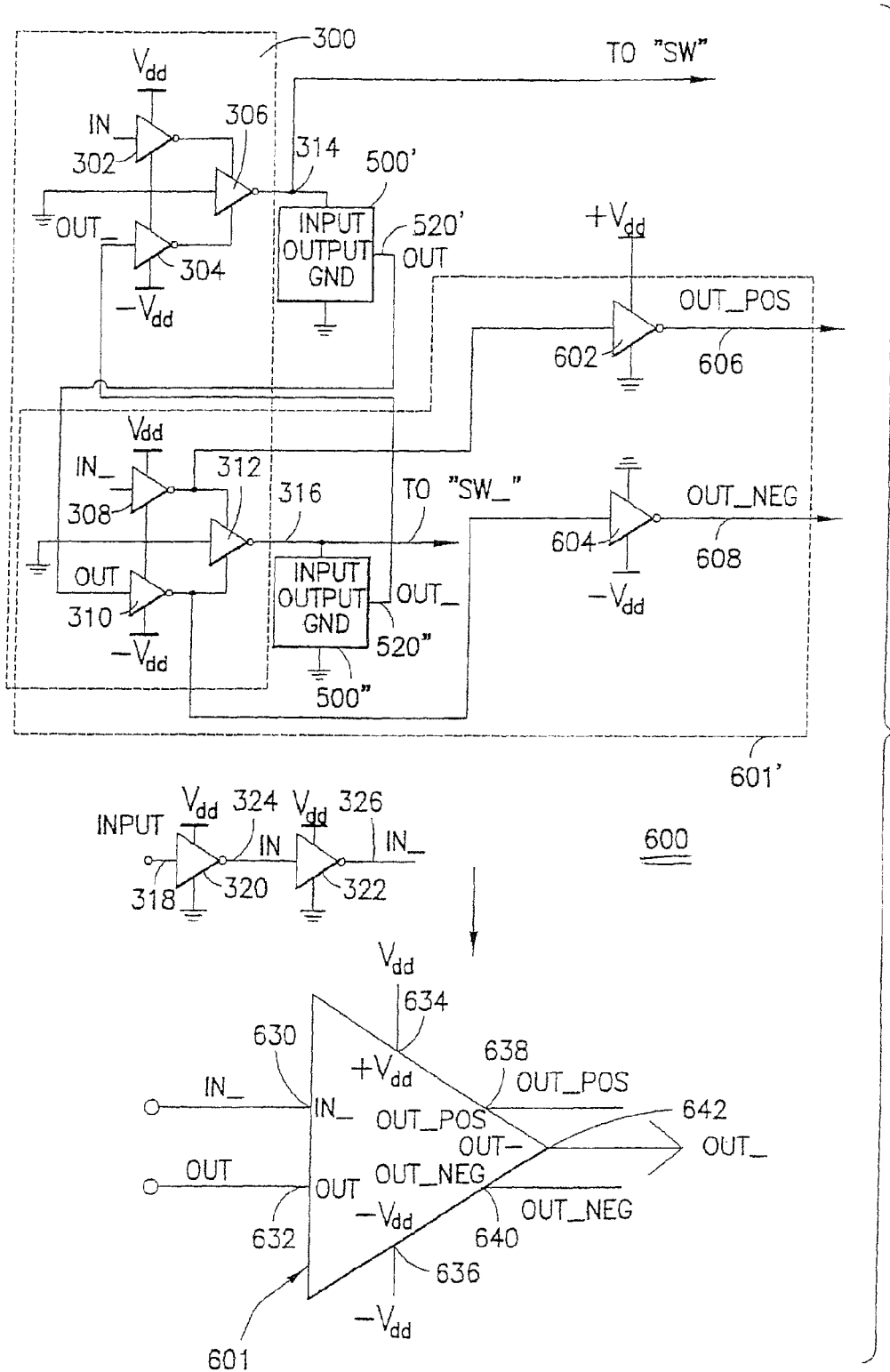


FIG.10

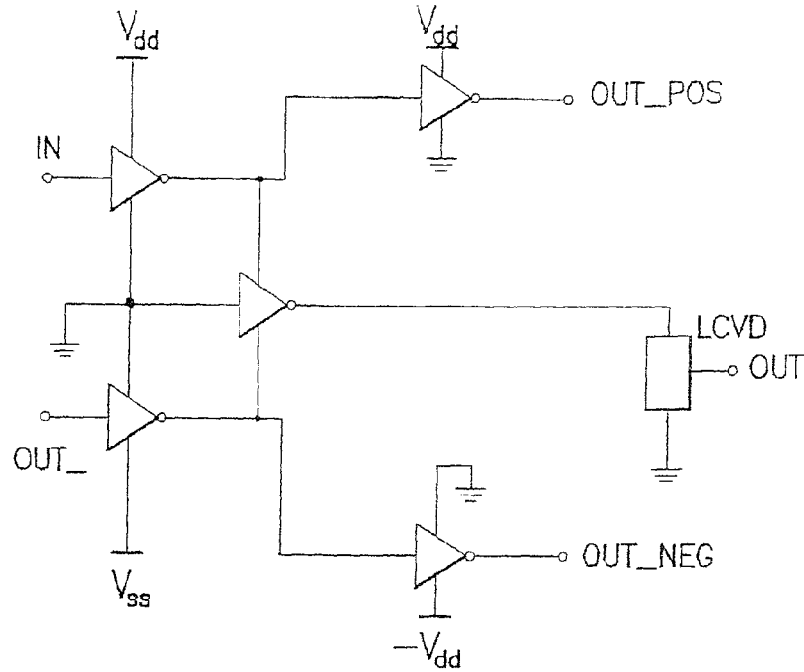


FIG. 11A

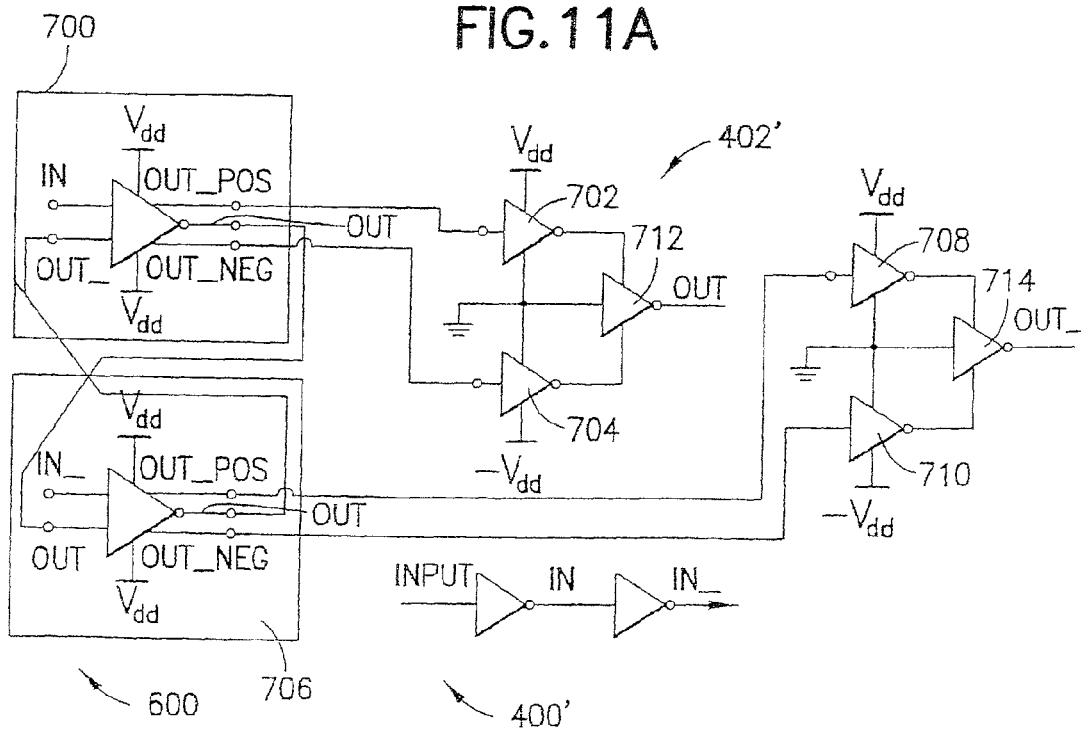


FIG. 11B

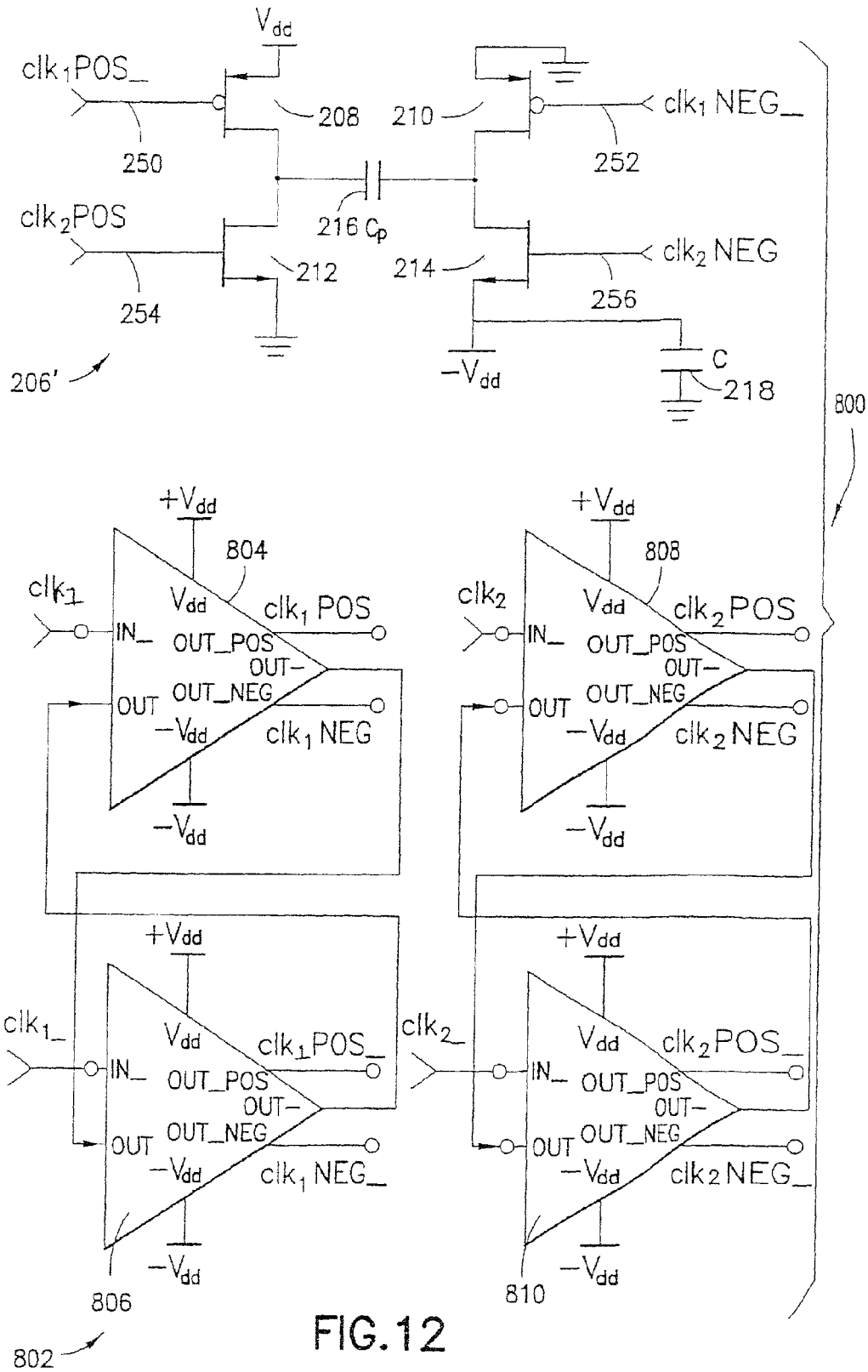


FIG. 12

1

## SWITCH CIRCUIT AND METHOD OF SWITCHING RADIO FREQUENCY SIGNALS

### CROSS-REFERENCE TO RELATED APPLICATIONS—CLAIMS OF PRIORITY

This is a continuation of application Ser. No. 12/980,161, filed Dec. 28, 2010, which is a continuation of application Ser. No. 12/315,395, filed Dec. 1, 2008, which issued Dec. 28, 2010 as U.S. Pat. No. 7,860,499, which is a continuation of application Ser. No. 11/582,206, filed Oct. 16, 2006, now U.S. Pat. No. 7,460,852 issued Dec. 2, 2008, which is a continuation of application Ser. No. 10/922,135, filed Aug. 18, 2004, now U.S. Pat. No. 7,123,898 issued Oct. 17, 2006, which is a continuation of application Ser. No. 10/267,531, filed Oct. 8, 2002, now U.S. Pat. No. 6,804,502 issued Oct. 12, 2004, which claims the benefit under 35 USC 119(e) of U.S. Provisional Application No. 60/328,353, filed Oct. 10, 2001, and each of these pending applications and issued patents are hereby incorporated by reference herein in their entirety.

### BACKGROUND

#### 1. Field

The present disclosure relates to switches, and particularly to a switch circuit and method of switching radio frequency (RF) signals within an integrated circuit. In one embodiment, the switch circuit comprises CMOS devices implemented on a silicon-on-insulator (SOI) substrate, for use in RF applications such as wireless communications, satellites, and cable television.

#### 2. Description of Related Art

As is well known, radio frequency (RF) switches are important building blocks in many wireless communication systems. RF switches are found in many different communications devices such as cellular telephones, wireless pagers, wireless infrastructure equipment, satellite communications equipment, and cable television equipment. As is well known, the performance of RF switches is controlled by three primary operating performance parameters: insertion loss, switch isolation, and the “1 dB compression point.” These three performance parameters are tightly coupled, and any one parameter can be emphasized in the design of RF switch components at the expense of others. A fourth performance parameter that is occasionally considered in the design of RF switches is commonly referred to as the switching time or switching speed (defined as the time required to turn one side of a switch on and turn the other side off). Other characteristics that are important in RF switch design include case and degree (or level) of integration of the RF switch, complexity, yield, return loss and cost of manufacture.

These RF switch performance parameters can be more readily described with reference to a prior art RF switch design shown in the simplified circuit schematics of FIGS. 1a-1c. FIG. 1a shows a simplified circuit diagram of a prior art single pole, single throw (SPST) RF switch 10. The prior art SPST switch 10 includes a switching transistor M1 5 and a shunting transistor M2 7. Referring now to FIG. 1a, depending upon the state of the control voltages of the two MOSFET transistors M1 5 and M2 7 (i.e., depending upon the DC bias applied to the gate inputs of the MOSFET switching and shunting transistors, M1 and M2, respectively), RF signals are either routed from an RF input node 1 to an RF output node 3, or shunted to ground through the shunting transistor M2 7. Actual values of the DC bias voltages depend upon the polarity and thresholds of the MOSFET transistors M1 5 and

2

M2 7. Resistor R0 9, in series with the RF source signal, isolates the bias from the source signal and is essential for optimal switch performance. FIG. 1b shows the “on” state of the RF switch 10 of FIG. 1a (i.e., FIG. 1b shows the equivalent small-signal values of the transistors M1 and M2 when the RF switch 10 is “on”, with switching transistor M1 5 on, and shunting transistor M2 7 off). FIG. 1c shows the “off” state of the switch 10 of FIG. 1a (i.e., FIG. 1c shows the equivalent small-signal values of the transistors M1 and M2 when the RF switch 10 is “off”, with switching transistor M1 5 off, and shunting transistor M2 7 on).

As shown in FIG. 1b, when the RF switch 10 is on, the switching transistor M1 5 is primarily resistive while the shunting transistor M2 7 is primarily capacitive. The “insertion loss” of the RF switch 10 is determined from the difference between the maximum available power at the input node 1 and the power that is delivered to a load 11 at the output node 3. At low frequencies, any power lost is due to the finite on resistance “r” 13 of the switching transistor M1 5 when the switch 10 is on (see FIG. 1b). The on resistance r 13 (FIG. 1b) typically is much less than the source resistor R0 9. The insertion loss, “IL”, can therefore be characterized in accordance with Equation 1 shown below:

$$IL \text{ is approximately equal to: } 10r/R0 \ln(10)=0.087r \text{ (in dB).} \quad \text{Equation 1:}$$

Thus, at low frequencies, a 3-Ω value for r results in approximately 0.25 dB insertion loss.

Because insertion loss depends greatly upon the on resistances of the RF switch transmitters, lowering the transistor on resistances and reducing the parasitic substrate resistances can achieve improvements in insertion loss.

In general, the input-to-output isolation (or more simply, the switch isolation) of an RF switch is determined by measuring the amount of power that “bleeds” from the input port into the output port when the transistor connecting the two ports is off. The isolation characteristic measures how well the RF switch turns off (i.e., how well the switch blocks the input signal from the output). More specifically, and referring now to the “off” state of the RF switch 10 of FIG. 1c, the switching transistor M1 5 off state acts to block the input 1 from the output 3. The shunting transistor M2 7 also serves to increase the input-to-output isolation of the switch 10.

When turned off (i.e., when the RF switch 10 and the switching transistor M1 5 are turned off), M1 5 is primarily capacitive with “feedthrough” (i.e., passing of the RF input signal from the input node 1 to the output node 3) of the input signal determined by the series/parallel values of the capacitors CGD off 15 (Gate-to-Drain Capacitance when the switching transistor M1 is turned off), CGS off 17 (Gate-to-Source Capacitance when the switching transistor M1 is turned off), and CDS1 19 (Drain-to-Source capacitance when the transistor M1 is turned off). Feedthrough of the input signal is undesirable and is directly related to the input-to-output isolation of the RF switch 10. The shunting transistor M2 7 is used to reduce the magnitude of the feedthrough and thereby increase the isolation characteristic of the RF switch.

The shunting transistor M2 7 of FIG. 1c is turned on when the switching transistor M1 5 is turned off. In this condition, the shunting transistor M2 7 acts primarily as a resistor having a value of r. By design, the value of r is much less than the characteristic impedance of the RF source. Consequently, r greatly reduces the voltage at the input of the switching transistor M1 5. When the value of r is much less than the source resistance R0 9 and the feedthrough capacitive resistance of the shunting transistor M2 7, isolation is easily calculated.

Switch isolation for the off state of the RF switch **10** is determined as the difference between the maximum available power at the input to the power at the output.

In addition to RF switch insertion loss and isolation, another important RF switch performance characteristic is the ability to handle large input power when the switch is turned on to ensure that insertion loss is not a function of power at a fixed frequency. Many applications require that the switch does not distort power transmitted through a “switched-on” switch. For example, if two closely spaced tones are concurrently passed through an RF switch, nonlinearities in the switch can produce inter-modulation (IM) and can thereby create a false tone in adjacent channels. If these adjacent channels are reserved, for instance, for information signals, power in these false tones must be maintained as small as possible. The switch compression, or “1 dB compression point” (“P1 dB”), is indicative of the switch’s ability to handle power. The P1 dB is defined as the input power at which the insertion loss has increased by 1 dB from its low-power value. Or stated in another way, the 1 dB compression point is a measure of the amount of power that can be input to the RF switch at the input port before the output power deviates from a linear relationship with the input power by 1 dB.

Switch compression occurs in one of two ways. To understand how switch compression occurs, operation of the MOSFET transistors shown in the RF switch **10** of FIGS. **1a-1c** are described. As is well known in the transistor design arts, MOSFETs require a gate-to-source bias that exceeds a threshold voltage,  $V_i$ , to turn on. Similarly, the gate-to-source bias must be less than  $V_i$  for the switch to be off.  $V_i$  is positive for “type-N” MOSFETs and negative for “type-P” MOSFETs. Type-N MOSFETs were chosen for the RF switch **10** of FIGS. **1a-1c**. The source of a type-N MOSFET is the node with the lowest potential.

Referring again to FIG. **1c**, if a transient voltage on the shunting transistor **M2 7** results in turning on the shunting transistor **M2 7** during part of an input signal cycle, input power will be routed to ground and lost to the output. This loss of power increases for increased input power (i.e., input signals of increased power), and thereby causes a first type of compression. The 1 dB compression point in the RF switch **10** is determined by the signal swing on the input at which point the turned-off shunting transistor **M2 7** is unable to remain off. Eventually, a negative swing of the input falls below the potential of the **M2** gate, as well as below ground (thus becoming the source). When this difference becomes equal to  $V_i$ , the transistor **M2 7** begins to turn on and compression begins. This first type of compression is caused by the phenomenon of the turning on of a normally off gate in the shunt leg of the RF switch. Once the shunting transistor **M2 7** turns on, power at the output node **3** no longer follows power at the switch input in a linear manner. A second type of RF switch compression occurs when the source and drain of the shunting transistor **M2 7** break down at excessive voltages. For submicron silicon-on-insulator (SOI) devices, this voltage may be approximately only +1 VDC above the supply voltage. At breakdown, the shunt device begins to heavily conduct current thereby reducing the power available at the output.

FIG. **2** shows a simplified schematic of a prior art single pole double throw (SPDT) RF switch **20**. As shown in FIG. **2**, the prior art RF switch **20** minimally includes four MOSFET transistors **23**, **24**, **27** and **28**. The transistors **23** and **24** act as “pass” or “switching” transistors (similar to the switching MOSFET transistor **M1 5** of FIGS. **1a-1c**), and are configured to alternatively couple their associated and respective RF input nodes to a common RF node **25**. For example, when

enabled (or switched “on”), the switching transistor **23** couples a first RF input signal “RF<sub>1</sub>”, input to a first RF input node **21**, to the RF common node **25**. Similarly, when enabled, the switching transistor **24** couples a second RF input signal “RF<sub>2</sub>”, input to a second RF input node **22**, to the RF common node **25**. The shunting transistors, **27** and **28**, when enabled, act to alternatively shunt their associated and respective RF input nodes to ground when their associated RF input nodes are uncoupled from the RF common node **25** (i.e., when the switching transistor (**23** or **24**) connected to the associated input node is turned off).

As shown in FIG. **2**, two control voltages are used to control the operation of the prior art RF switch. The control voltages, labeled “SW”, and its inverse “SW<sub>-</sub>”, control the operation of the transistors **23**, **24**, **27** and **28**. The control voltages are arranged to alternatively enable (turn on) and disable (turn off) selective transistor pairs. For example, as shown in FIG. **2**, when SW is on (in some embodiments this is determined by the control voltage SW being set to a logical “high” voltage level, e.g., “+V<sub>dd</sub>”), the switching transistor **23** is enabled, and its associated shunting transistor **28** is also enabled. However, because the inverse of SW, SW<sub>-</sub>, controls the operation of the second switching transistor **24**, and its associated shunting transistor **27**, and the control signal SW<sub>-</sub> is off during the time period that SW is on (in some embodiments this is determined by SW<sub>-</sub> being set to a -V<sub>dd</sub> value), those two transistors are disabled, or turned off, during this same time period. In this state (SW “on” and SW<sub>-</sub> “off”), the RF<sub>1</sub> input signal is coupled to the RF common port **25** (through the enabled switching transistor **23**). Because the second switching transistor **24** is turned off, the RF<sub>2</sub> input signal is blocked from the RF common port **25**. Moreover, the RF<sub>2</sub> input signal is further isolated from the RF common port **25** because it is shunted to ground through the enabled shunting transistor **28**. As those skilled in the transistor designs arts shall easily recognize, the RF<sub>2</sub> signal is coupled to the RF common port **25** (and the RF<sub>1</sub> signal is blocked and shunted to ground) in a similar manner when the SW control signal is “off” (and SW<sub>-</sub> is “on”).

With varying performance results, RF switches, such as the SPDT RF switch **20** of FIG. **2**, have heretofore been implemented in different component technologies, including bulk complementary-metal-oxide-semiconductor (CMOS) and gallium-arsenide (GaAs) technologies. In fact, most high performance high-frequency switches use GaAs technology. The prior art RF switch implementations attempt to improve the RF switch performance characteristics described above, however, they do so with mixed results and with varying degrees of integrated circuit complexity and yields. For example, bulk CMOS RF switches disadvantageously exhibit high insertion loss, low compression, and poor linearity performance characteristics. In contrast, due to the semi-insulating nature of GaAs material, parasitic substrate resistances can be greatly reduced thereby reducing RF switch insertion loss. Similarly, the semi-insulating GaAs substrate improves switch isolation.

Although GaAs RF switch implementations offer improved performance characteristics, the technology has several disadvantages. For example, GaAs technology exhibits relatively low yields of properly functioning integrated circuits. GaAs RF switches tend to be relatively expensive to design and manufacture. In addition, although GaAs switches exhibit improved insertion loss characteristics as described above, they may have low frequency limitations due to slow states present in the GaAs substrate. The technology also does not lend itself to high levels of integration, which requires that digital control circuitry associated with the RF switch be

implemented “off chip” from the switch. The low power control circuitry associated with the switch has proven difficult to integrate. This is disadvantageous as it both increases the overall system cost or manufacture, size and complexity, as well as reducing system throughput speeds.

It is therefore desirable to provide an RF switch and method for switching RF signals having improved performance characteristics. Specifically, it is desirable to provide an RF switch having improved insertion loss, isolation, and compression. It is desirable that such an RF switch be easily designed and manufactured, relatively inexpensive to manufacture, lend itself to high levels of integration, with low-to-high frequency application. Power control circuitry should be easily integrated on-chip together with the switch functions. Such integration has been heretofore difficult to achieve using Si and GaAs substrates. The present teachings provide such an RF switch and method for switching RF signals.

#### SUMMARY

A novel RF switch circuit and method for switching RF signals is described. The RF switch circuit may be used in wireless applications, and may be fabricated in a silicon-on-insulator technology. In one embodiment the RF switch is fabricated on an Ultra-Thin-Silicon (“UTSi”) substrate. In one embodiment the RF switch includes: an input for receiving an RF signal; a first switching transistor grouping connected to the input to receive the RF signal and connected to an RF common port, wherein the first switching transistor is controlled by a switching voltage (SW); a second switching transistor grouping connected to the first switching transistor grouping and the RF common port, wherein the second switching transistor is controlled by a switching voltage SW<sub>-</sub>, and wherein SW<sub>-</sub> is the inverse of SW so that when the first switching transistor grouping is on, the second switching transistor grouping is off. The switching transistor groupings, when enabled, alternatively connect their respective RF input signals to the RF common port. In this embodiment the RF switch also includes shunting transistor groupings coupled to the switching transistor groupings and also controlled by the switching voltages SW and SW<sub>-</sub>. The shunting transistor groupings, when enabled, act to alternatively shunt their associated RF input nodes to ground thereby improving RF switch isolation.

The switching and shunting transistor groupings comprise one or more MOSFET transistors connected together in a “stacked” or serial configuration. Within each transistor grouping, the gates of the stacked transistors are commonly controlled by a switching voltage (SW or SW<sub>-</sub>) that is coupled to each transistor gate through respective gate resistors. The stacking of transistor grouping devices and gate resistors increases the compression point of the switch. The RC time constant formed by the gate resistors and the gate capacitance of the MOSFETs is designed to be much longer than the period of the RF signal, causing the RF voltage to be shared equally across the series connected devices. This configuration increases the 1 dB compression point of the RF switch.

A fully integrated RF switch is described that includes digital switch control logic and a negative power supply voltage generator circuit integrated together with the inventive RF switch. In one embodiment, the fully integrated RF switch provides several functions not present in prior art RF switches. For example, in one embodiment, the fully integrated RF switch includes a built-in oscillator that provides clocking input signals to a charge pump circuit, an integrated charge pump circuit that generates the negative power supply

voltages required by the other RF switch circuits, CMOS logic circuitry that generates control signals to control the RF switch transistors, level-shifting and low current voltage divider circuits that provide increased reliability of the switch devices, and an RF buffer circuit that isolates RF signal energy from the charge pump and digital control logic circuits. Several embodiments of the charge pump, level shifting, voltage divider, and RF buffer circuits are described. The inventive RF switch provides improvements in insertion loss, switch isolation, and switch compression. In addition, owing to the higher levels of integration made available by the present inventive RF switch, RF system design and fabrication costs are reduced and reliability is increased using the present method and apparatus.

#### BRIEF DESCRIPTION OF THE DRAWINGS

FIG. 1a is a simplified electrical schematic of a prior art single pole, single throw (SPST) RF switch used to demonstrate performance characteristics of the RF switch.

FIG. 1b is a simplified electrical schematic of the SPST RF switch of FIG. 1a showing the dominant characteristics of the switch when the switch is turned “on” allowing the RF signal to pass from an input node to an output node.

FIG. 1c shows the equivalent small-signal electrical characteristics of the RF switch of FIGS. 1a and 1b when the RF switch is turned “off” thereby blocking the RF signal from the output node.

FIG. 2 is a simplified electrical schematic of a prior art single pole double throw (SPDT) RF switch.

FIG. 3 is an electrical schematic of an RF switch according to one embodiment of the present method and apparatus.

FIG. 4 is a simplified block diagram of an exemplary fully integrated RF switch made in accordance with the present method and apparatus.

FIG. 5a is a simplified block diagram of one exemplary embodiment of the negative voltage generator shown in the simplified block diagram of FIG. 4; FIG. 5b is an electrical schematic of a first embodiment of a charge pump circuit that is used to generate a negative supply voltage to the RF switch of FIG. 4.

FIG. 5c is a plot of voltage amplitude versus time showing the voltage amplitude of two non-overlapping clock signals used to control the charge pump circuit of FIG. 5b varying over time.

FIG. 6a is an electrical schematic of a first embodiment of an inventive level shifting circuit; FIG. 6b is an electrical schematic of one embodiment of the inverters used to implement the level shifter shown in FIG. 6a.

FIG. 7a is a voltage amplitude versus time plot of a digital input signal and corresponding output signal generated by the inventive level shifter of FIG. 6a; FIG. 7b is a simplified logic symbol for the inventive level shifter of FIG. 6a.

FIG. 8a is an electrical schematic of one embodiment of a two-stage level shifter and RF buffer circuit including a first stage level shifter and a second stage RF buffer circuit; FIG. 8b is a simplified block diagram of the digital control input and interface to the RF buffer circuit of FIG. 8a.

FIG. 9a is an electrical schematic of one embodiment of a low current voltage divider (LCVD) circuit made in accordance with the present RF switch method and apparatus; FIG. 9b is a simplified logic symbol used to represent the voltage divider of FIG. 9a.

FIG. 10 is an electrical schematic of a second embodiment of a level shifting circuit using the low current voltage divider circuit of FIG. 9a in combination with the level shifting circuit of FIG. 6a.

FIGS. 11a and 11b are electrical schematics showing an alternative embodiment of the two-stage level shifter and RF buffer circuit of FIG. 8a.

FIG. 12 is an electrical schematic of a modified charge pump using the level shifting circuit of FIG. 10.

Like reference numbers and designations in the various drawings indicate like elements.

#### DETAILED DESCRIPTION

Throughout this description, the preferred embodiment and examples shown should be considered as exemplars, rather than as limitations on the present method and apparatus.

##### The Inventive RF Switch

The present method and apparatus is a novel RF switch design and method for switching RF circuits. A first exemplary embodiment of the present inventive RF switch 30 is shown in FIG. 3. As shown in FIG. 3, in one embodiment, the inventive RF switch 30 includes four clusters or “groupings” of MOSFET transistors, identified in FIG. 3 as transistor groupings 33, 34, 37 and 38. Two transistor groupings comprise “pass” or “switching” transistor groupings 33 and 34, and two transistor groupings comprise shunting transistor groupings 37 and 38. Each transistor grouping includes one or more MOSFET transistors arranged in a serial configuration. For example, in the embodiment shown in FIG. 3, the switching grouping 33 includes three switching transistors,  $M_{33A}$ ,  $M_{33B}$ , and  $M_{33C}$ . Similarly, the switching grouping 34 includes three switching transistors,  $M_{34A}$ ,  $M_{34B}$ , and  $M_{34C}$ . The shunting grouping 37 includes three transistors  $M_{37A}$ ,  $M_{37B}$ , and  $M_{37C}$ . Similarly, the shunting grouping 38 includes three transistors,  $M_{38A}$ ,  $M_{38B}$ , and  $M_{38C}$ . Although the transistor groupings 33, 34, 37 and 38 are shown in FIG. 3 as comprising three MOSFET transistors, those skilled in the RF switch design arts shall recognize that alternative grouping configurations can be used without departing from the scope or spirit of the present method and apparatus. For example, as described below in more detail, any convenient number of transistors can be used to implement the groupings shown in FIG. 3 without departing from the scope of the present method and apparatus.

In one embodiment of the present inventive RF switch, the MOSFET transistors (e.g., the transistors  $M_{37A}$ ,  $M_{37B}$ , and  $M_{37C}$ ) are implemented using a fully insulating substrate silicon-on-insulator (SOI) technology. More specifically, and as described in more detail hereinbelow, the MOSFET transistors of the inventive RF switch are implemented using “Ultra-Thin-Silicon (UTSi)” (also referred to herein as “ultrathin silicon-on-sapphire”) technology. In accordance with UTSi manufacturing methods, the transistors used to implement the inventive RF switch are formed in an extremely thin layer of silicon in an insulating sapphire wafer. The fully insulating sapphire substrate enhances the performance characteristics of the inventive RF switch by reducing the deleterious substrate coupling effects associated with non-insulating and partially insulating substrates. For example, improvements in insertion loss are realized by lowering the transistor on resistances and by reducing parasitic substrate resistances. In addition, switch isolation is improved using the fully insulating substrates provided by UTSi technology. Owing to the fully insulating nature of silicon-on-sapphire technology, the parasitic capacitance between the nodes of the RF switch 30 is greatly reduced as compared with bulk CMOS and other traditional integrated circuit manufacturing technologies. Consequently, the inven-

tive RF switch exhibits improved switch isolation as compared with the prior art RF switch designs.

As shown in FIG. 3, similar to the switch described above with reference to FIG. 2, the transistor groupings are controlled by two control signals, SW, and its inverse, SW<sub>-</sub>. The control signals are coupled to the gates of their respective transistors through associated and respective gate resistors. For example, the control signal SW controls the operation of the three transistors in the switching transistor grouping 33 ( $M_{33A}$ ,  $M_{33B}$ , and  $M_{33C}$ ) through three associated and respective gate resistors ( $R_{33A}$ ,  $R_{33B}$ , and  $R_{33C}$ , respectively). The control signal SW is input to an input node 33' to control the switching transistor grouping 33. SW is also input to an input node 38' to control the shunting transistor grouping 38. Similarly, the inverse of SW, SW<sub>-</sub>, controls the switching transistor grouping 34 via an input node 34'. SW<sub>-</sub> is also input to an input node 37' to control the shunting transistor grouping 37.

In one embodiment, the transistor grouping resistors comprise approximately 30 K ohm resistors, although alternative resistance values can be used without departing from the spirit or scope of the present method and apparatus. In addition, in some embodiments of the present method and apparatus, the gate resistors comprise any resistive element having a relatively high resistance value. For example, reversed-biased diodes may be used to implement the gate resistors in one embodiment. As described in more detail below, the gate resistors help to increase the effective breakdown voltage across the series connected transistors.

The control signals function to control the enabling and disabling of the transistor groupings 33, 34, 37 and 38, and the RF switch 30 generally functions to pass and block RF signals in a manner that is similar to the control of the analogous transistors of the switch of FIG. 2. More specifically, the switching transistor groupings 33 and 34 act as pass or switching transistors, and are configured to alternatively couple their associated and respective RF input nodes to a common RF node 35. For example, when enabled, the switching transistor grouping 33 couples a first RF input signal “RF<sub>1</sub>”, input to a first RF input node 31, to the RF common node 35. Similarly, when enabled, the switching transistor grouping 34 couples a second RF input signal “RF<sub>2</sub>”, input to a second RF input node 32, to the RF common node 35. The shunting transistor groupings, 37 and 38, when enabled, act to alternatively shunt their associated and respective RF input nodes to ground when their associated RF input nodes are uncoupled from the RF common node 35 (i.e., when the switching transistor grouping (33 or 34) that is connected to the associated input node is turned off).

The control voltages are connected to alternatively enable and disable selective pairs of transistor groupings. For example, as shown in FIG. 3, when SW is on (in some embodiments this is determined when the control voltage SW is set to a logical “high” voltage level), the switching transistor grouping 33 is enabled (i.e. all of the transistors in the grouping 33 are turned on), and its associated shunting transistor grouping 38 is also enabled (i.e., all of the transistors in the grouping 38 are turned on). However, similar to the operation of the switch of FIG. 2, because the inverse of SW, SW<sub>-</sub>, controls the operation of the second switching transistor grouping 34, and its associated shunting transistor grouping 37, these two transistor groupings are disabled (i.e., all of the transistors in the groupings 34, 37 are turned off) during this time period. Therefore, with SW on, the RF<sub>1</sub> input signal is coupled to the RF common port 35. The RF<sub>2</sub> input signal is blocked from the RF common port 35 because the switching transistor grouping 34 is off. The RF<sub>2</sub> input signal is further isolated from the RF common port 35 because it is shunted to ground through the enabled shunting transistor grouping 38.

As those skilled in the RF switch design arts shall recognize, the RF<sub>2</sub> signal is coupled to the RF common port **35** (and the RF<sub>1</sub> signal is blocked and shunted to ground) in a similar manner when the SW control signal is off (and the SW<sub>-</sub> control signal is on).

One purpose of the stacking of MOSFET transistors and using gate resistors as shown in the inventive RF switch **30** of FIG. **3** is to increase the breakdown voltage across the series connected transistors. The RC time constant formed by the gate resistor and the gate capacitance of the MOSFETs is designed to be much longer than the period of the RF signal. Thus, very little RF energy is dissipated through the gate resistor. This arrangement effectively causes the RF voltage to be shared equally across the series connected transistors. The net effect is that the breakdown voltage across the series connected devices is increased to n times the breakdown voltage of an individual FET, where n is the number of transistors connected in series. This configuration increases the 1 dB compression point of the inventive RF switch **30**.

To achieve improved switch performance, the RC time constant must be sized so that it is large with respect to the period of the RF signal. This largely places a constraint on the minimum value of R that can be used to implement the gate transistors. As noted above, in one embodiment of the present method and apparatus, a typical value of R is 30 k-ohms, although other resistance values can be used without departing from the scope of the present method and apparatus. Because a MOSFET gate input draws no DC current, there is no change in the biasing of the devices due to IR drops across this resistance.

Advantageously, the present inventive RF switch **30** can accommodate input signals of increased power levels. Owing to the serial arrangement of the MOSFET transistors that comprise the transistor groupings (**33**, **34**, **37** and **38**), increased power signals can be presented at the RF input nodes (i.e., at the input nodes **31** and **32**) without detrimentally affecting switch operation. Those skilled in the transistor design arts shall recognize that greater input power levels can be accommodated by increasing the number of transistors per transistor grouping, or by varying the physical configuration of the transistors. For example, in one embodiment, the transistors are approximately 0.5×2,100 micro-meters in dimension. However, alternative configurations can be used without departing from the scope or spirit of the present method and apparatus.

#### Silicon-on-Insulator (SOI) Technologies

As noted above in the description of the RF switch of FIG. **3**, SOI technology is attractive in implementing RF switches due to the fully insulating nature of the insulator substrate. As is well known, SOI has been used in the implementation of high performance microelectronic devices, primarily in applications requiring radiation hardness and high speed operation. SOI technologies include, for example, SIMOX, bonded wafers having a thin silicon layer bonded to an insulating layer, and silicon-on-sapphire. In order to achieve the desired switch performance characteristics described above, in one embodiment, the inventive RF switch is fabricated on a sapphire substrate.

Fabrication of devices on an insulating substrate requires that an effective method for forming silicon CMOS devices on the insulating substrate be used. The advantages of using a composite substrate comprising a monocrystalline semiconductor layer, such as silicon, epitaxially deposited on a supporting insulating substrate, such as sapphire, are well-recognized, and can be realized by employing as the substrate an insulating material, such as sapphire (Al<sub>2</sub>O<sub>3</sub>), spinel, or other

known highly insulating materials, and providing that the conduction path of any inter-device leakage current must pass through the substrate.

An "ideal" silicon-on-insulator wafer can be defined to include a completely monocrystalline, defect-free silicon layer of sufficient thickness to accommodate the fabrication of active devices therein. The silicon layer would be adjacent to an insulating substrate and would have a minimum of crystal lattice discontinuities at the silicon-insulator interface. Early attempts to fabricate this "ideal" silicon-on-insulator wafer were frustrated by a number of significant problems, which can be summarized as (1) substantial incursion of contaminants into the epitaxially deposited silicon layer, especially the p-dopant aluminum, as a consequence of the high temperatures used in the initial epitaxial silicon deposition and the subsequent annealing of the silicon layer to reduce defects therein; and (2) poor crystalline quality of the epitaxial silicon layers when the problematic high temperatures were avoided or worked around through various implanting, annealing, and/or re-growth schemes.

It has been found that the high quality silicon films suitable for demanding device applications can be fabricated on sapphire substrates by a method that involves epitaxial deposition of a silicon layer on a sapphire substrate, low temperature ion implant to form a buried amorphous region in the silicon layer, and annealing the composite at temperatures below about 950° C.

Examples of and methods for making such silicon-on-sapphire devices are described in U.S. Pat. No. 5,416,043 ("Minimum charge FET fabricated on an ultrathin silicon on sapphire wafer"); U.S. Pat. No. 5,492,857 ("High-frequency wireless communication system on a single ultrathin silicon on sapphire chip"); U.S. Pat. No. 5,572,040 ("High-frequency wireless communication system on a single ultrathin silicon on sapphire chip"); U.S. Pat. No. 5,596,205 ("High-frequency wireless communication system on a single ultrathin silicon on sapphire chip"); U.S. Pat. No. 5,600,169 ("Minimum charge FET fabricated on an ultrathin silicon on sapphire wafer"); U.S. Pat. No. 5,663,570 ("High-frequency wireless communication system on a single ultrathin silicon on sapphire chip"); U.S. Pat. No. 5,861,336 ("High-frequency wireless communication system on a single ultrathin silicon on sapphire chip"); U.S. Pat. No. 5,863,823 ("Self-aligned edge control in silicon on insulator"); U.S. Pat. No. 5,883,396 ("High-frequency wireless communication system on a single ultrathin silicon on sapphire chip"); U.S. Pat. No. 5,895,957 ("Minimum charge FET fabricated on an ultrathin silicon on sapphire wafer"); U.S. Pat. No. 5,920,233 ("Phase locked loop including a sampling circuit for reducing spurious side bands"); U.S. Pat. No. 5,930,638 ("Method of making a low parasitic resistor on ultrathin silicon on insulator"); U.S. Pat. No. 5,973,363 ("CMOS circuitry with shortened P-channel length on ultrathin silicon on insulator"); U.S. Pat. No. 5,973,382 ("Capacitor on ultrathin semiconductor on insulator"); and U.S. Pat. No. 6,057,555 ("High-frequency wireless communication system on a single ultrathin silicon on sapphire chip"). All of these referenced patents are incorporated herein in their entirety for their teachings on ultrathin silicon-on-sapphire integrated circuit design and fabrication.

Using the methods described in the patents referenced above, electronic devices can be formed in an extremely thin layer of silicon on an insulating synthetic sapphire wafer. The thickness of the silicon layer is typically less than 150 nm. Such an "ultrathin" silicon layer maximizes the advantages of the insulating sapphire substrate and allows the integration of multiple functions on a single integrated circuit. Traditional transistor isolation wells required for thick silicon are unne-

essary, simplifying transistor processing and increasing circuit density. To distinguish these above-referenced methods and devices from earlier thick-silicon embodiments, they are herein referred to collectively as “ultrathin silicon-on-sapphire.”

In some preferred embodiments of the method and apparatus, the MOS transistors are formed in ultrathin silicon-on-sapphire wafers by the methods disclosed in U.S. Pat. Nos. 5,416,043; 5,492,857; 5,572,040; 5,596,205; 5,600,169; 5,663,570; 5,861,336; 5,863,823; 5,883,396; 5,895,957; 5,920,233; 5,930,638; 5,973,363; 5,973,382; and 6,057,555. However, other known methods of fabricating ultrathin silicon-on-sapphire integrated circuits can be used without departing from the spirit or scope of the present method and apparatus.

As described and claimed in these patents, high quality silicon films suitable for demanding device applications can be fabricated on insulating substrates by a method that involves epitaxial deposition of a silicon layer on an insulating substrate, low temperature ion implantation to form a buried amorphous region in the silicon layer, and annealing the composite at temperatures below about 950° C. Any processing of the silicon layer which subjects it to temperatures in excess of approximately 950° C. is performed in an oxidizing ambient environment. The thin silicon films in which the transistors are formed typically have an areal density of electrically active states in regions not intentionally doped which is less than approximately  $5 \times 10^{11} \text{ cm}^{-2}$ .

As noted above, UTSi substrates are especially desirable for RF applications because the fully insulating substrate reduces the detrimental effects of substrate coupling associated with traditional substrates (i.e., substrates that are not fully insulating). Consequently, in one embodiment, the RF switch **30** of FIG. **3** is fabricated on an UTSi substrate.

#### RF Switch Design Tradeoffs

Several design parameters and tradeoffs should be considered in designing and implementing the inventive RF switch **30** described above with reference to FIG. **3**. The inventive RF switch can be tailored to meet or exceed desired system design requirements and RF switch performance objectives. The design tradeoffs and considerations that impact the inventive RF switch design are now described.

As described above with reference to FIG. **3**, the RF switch **30** is implemented using MOSFET transistors, which may be “N-type” or “P-type”. However, N channel transistors are preferred for RF switches implemented in CMOS technology. N channel transistors are preferred because, for a given transistor size, the “on” resistance of an N channel transistor is much lower than for a P channel transistor due to the higher mobility in silicon of electrons versus holes. The control voltages are selected to insure that the on resistance of the “on” transistor is reduced. The control voltages are also selected to insure that the “off” transistor remains off when disabled.

As is well known in the transistor design arts, in an N channel MOS transistor, the “on” resistance is inversely proportional to the difference between the voltage applied at the transistor gate and the voltage applied at the transistor source. This voltage is commonly referred to as the “Vgs” (gate-to-source voltage). It is readily observed that as the magnitude of the RF signal (Vs) increases at the input port (e.g., at the first RF input node **31** of FIG. **3**), and hence at the RF common port **35**, the Vgs of the on transistors decrease (e.g., the Vgs of the transistor **M33<sub>A</sub>** in the switching transistor grouping **33** decreases as the magnitude of the RF **1** signal increases). This argues for making the gate control voltage (e.g., SW at the

input node **33'**) as positive as possible. Unfortunately, reliability concerns limit the extent to which the gate control voltage can be made positive.

A similar concern exists for the “off” transistors. It is important to note that for typical RF switch applications, the RF input signals (e.g., the RF **1** input signal) generally swing about a zero reference voltage. The off transistors (e.g., the transistors in the shunting transistor grouping **37**) must remain disabled or turned off during both the positive and negative voltage excursions of the RF input signal. This argues for making the gate control voltage of the off transistors (e.g., the SW<sub>-</sub> control voltage signal) as negative as possible. Again, reliability concerns limit the extent to which this gate control voltage can be made negative.

For a CMOS switch, the design of the off transistor also limits the 1 dB compression point of the switch. As is well known in the transistor design arts, MOS transistors have a fundamental breakdown voltage between their source and drain. When the potential across the device exceeds this breakdown voltage, a high current flows between source and drain even when a gate potential exists that is attempting to keep the transistor in an off state. Improvements in switch compression can be achieved by increasing the breakdown voltage of the transistors. One method of fabricating a MOS transistor with a high breakdown voltage is to increase the length of the gate. Unfortunately, an increase in gate length also disadvantageously increases the channel resistance of the device thereby increasing the insertion loss of the device. The channel resistance can be decreased by making the device wider, however, this also decreases the switch isolation. Hence, tradeoffs exist in MOS switch designs.

As described above with reference to the inventive RF switch **30** of FIG. **3**, the transistors are stacked in a series configuration to improve the switch 1 dB compression point. The relatively high value gate resistors, in combination with the stacking configuration of the transistors in the transistor groupings, increase the effective breakdown voltage across the series connected transistors. The switch elements are designed and fabricated such that the RC time constant (determined by the resistance values of the gate resistors and the gate capacitance of the MOSFETs) is much longer than the period of the RF signal processed by the RF switch **30**. As noted above, the net effect of the stacking configuration and the relatively high resistance gate resistors is to increase the breakdown voltage across the series connected transistors by a factor of n times the breakdown voltage of an individual transistor (where n equals the number of transistors connected in series in a transistor grouping).

An additional design consideration concerns the “body tie” used in traditional bulk CMOS transistors. As is well known in the transistor design arts, the body tie electrically couples the device either to the well or to the substrate. The well-substrate junction must remain reversed biased at all times. The source-to-body and drain-to-body junctions must remain reversed biased at all times. In general, for bulk CMOS designs, the well (for N-well technology) is tied to the most positive potential that will be applied to the circuit. The substrate (for P-well technology) is tied to the most negative potential that will be applied to the circuit. Because the RF input signal swings symmetrically above and below ground, bulk CMOS switch designs exhibit poor insertion loss, isolation, and 1 dB compression point performance. For these reasons, and those described above, the present RF switch **30** is preferably implemented on an insulating substrate.

Implementing the inventive RF switch on an insulating substrate provides several advantages such as improved switch isolation and reduced insertion loss. Further advan-

tages are achieved by implementing the inventive RF switch using UTSi technology. For example, as compared with the prior art RF switch implementations in GaAs, improvements in integrated circuit yields, reduced fabrication costs, and increased levels of integration are achieved using UTSi. As is well known in the integrated circuit design arts, GaAs does not lend itself to high levels of integration. Thus, the digital control circuitry and other circuitry associated with the operation and function of the RF switch (such as a negative voltage power supply generator, level shifting, low current voltage divider and RF buffer circuits) must often be implemented off-chip (i.e., these functions are not easily integrated with the RF switch). This leads to increased costs and reduced performance of the prior art RF switch implementations.

In contrast, in accordance with the present RF switch method and apparatus, using UTSi technology, the circuitry necessary for the proper operation and functioning of the RF switch can be integrated together on the same integrated circuit as the switch itself. For example, and as described below in more detail, by implementing the RF switch in UTSi technology, the RF switch can be integrated in the same integrated circuit with a negative voltage generator and the CMOS control logic circuitry required to control the operation of the RF switch. The complexity of the RF switch is also reduced owing to the reduction in control lines required to control the operation of the switch. Advantageously, the RF switch control logic can be implemented using low voltage CMOS transistors. In addition, even for high power RF switch implementations, a single, relatively low power external power supply can be used to power the present inventive RF switch. This feature is advantageous as compared to the prior art GaAs implementations that require use of a relatively high power external power supply and power generation circuitry necessary to generate both positive and negative power supplies. For example, in the exemplary embodiments described below with reference to FIGS. 4-12, the present inventive RF switch requires only a single 3 V external power supply. The prior art switch designs typically require at least a 6 volt external power supply, and external voltage generation circuitry to generate both positive and negative power supplies.

FIG. 4 shows a simplified block diagram of an exemplary fully integrated RF switch **100** made in accordance with the present method and apparatus. As shown in FIG. 4, the fully integrated RF switch **100** includes the inventive RF switch **30** described above in FIG. 3 (shown in a simplified schematic representation in FIG. 4), CMOS control logic **110**, and a negative voltage generator circuit **120** (implemented in one embodiment using a “charge pump” circuit). A control signal **130** is input to the CMOS logic block **110**. In one embodiment, the control signal **130** ranges from 0 volts to +Vdd, however those skilled in the digital logic design arts shall recognize that other logic levels can be used without departing from the scope or spirit of the present method and apparatus. For the reasons provided above, in one exemplary embodiment, the fully integrated RF switch **100** is fabricated on UTSi substrates, although other insulating substrate technologies can be used.

As described in more detail below, the fully integrated RF switch **100** includes several functions and features not present in the prior art RF switch of FIG. 2. For example, in addition to the inventive RF switch **30** (which makes use of the novel transistor stacking and gate transistor configuration described above with reference to FIG. 3), the fully integrated RF switch **100** integrates the negative voltage generator and RF switch control functions together on the same integrated circuit as the inventive RF switch. As described below in more detail,

the fully integrated RF switch **100** includes a built-in oscillator that provides clocking input signals to a charge pump circuit, an integrated charge pump circuit that generates the negative power supply voltages required by the other RF switch circuits, CMOS logic circuitry that generates the control signals that control the RF switch transistors, a level-shifting circuit that provides increased reliability by reducing the gate-to-drain, gate-to-source, and drain-to-source voltages of the switch transistors, and an RF buffer circuit that isolates RF signal energy from the charge pump and digital control logic circuits. Each of these circuits is described below in more detail with reference to their associated figures.

#### Negative Voltage Generator—Charge Pump—A First Embodiment

As shown in FIG. 4, one embodiment of the fully integrated RF switch **100** includes a negative voltage generator or charge pump **120**. The negative voltage generator **120** generates the negative power supply voltage (specified hereafter as “-Vdd”) required by other circuits of the fully integrated RF switch **100**. Two sets of inputs are provided to the negative voltage generator **120**: a positive DC power supply voltage signal (Vdd) **122**; and a clocking input (shown in the figure as a single input signal, “Clk”) **124**. Although the clocking input **124** is shown as a single input signal in FIG. 4, as described below with reference to FIG. 5b, in some embodiments of the present inventive RF switch, the clocking input **124** may comprise two or more clock input signals.

In addition, in the embodiment shown in FIG. 4, the positive supply voltage that is input to the negative voltage generator circuit **120** comprises a 3 VDC power supply. However, other power supply levels may be used without departing from the scope or spirit of the present method and apparatus. For example, if desired, a 3.5 VDC, 5 VDC or any other convenient positive DC power supply can be input to the negative voltage generator circuit **120** of FIG. 4. The positive power supply signal is typically generated by an external low voltage power supply.

In one embodiment of the present method and apparatus, the negative voltage generator **120** of FIG. 4 is implemented using a charge pump circuit. FIG. 5a shows a simplified block diagram of one exemplary embodiment **200** of the negative voltage generator **120** of FIG. 4. As shown in the simplified block diagram of FIG. 5a, the negative voltage generator includes an oscillator **202**, a clock generator circuit **204**, and an inventive charge pump circuit **206**. The oscillator **202** output is input to the clock generator circuit **204**. The output of the clock generator circuit **204** is input to the charge pump circuit **206**. The negative voltage generator **120** provides the negative power supply voltage used by the other circuits of the fully integrated RF switch **100**.

Many prior art RF switches disadvantageously require that the negative power supply voltages be generated by circuitry that is external to the RF switch circuitry. Other RF switch implementations use a coupling approach necessary to shift the DC value of the RF input signal to the midpoint of the applied bias voltage. This approach generally requires that relatively high bias voltages be applied because of the effective halving of the FET gate drive due to this level shifting. If the bias voltages are not increased, this produces a negative effect on the switch insertion loss because the gate drive is thereby reduced and the FET channel resistances are increased.

To address these problems, one embodiment of the fully integrated RF switch **100** uses the inventive charge pump circuit **206** shown in detail in FIG. 5b. As shown in FIG. 5b, a first embodiment of the charge pump circuit **206** includes

15

two P-channel MOSFET transistors, **208** and **210**, connected in series with two N-channel MOSFET transistors **212** and **214**. The left leg of the charge pump circuit **206** (comprising the first P-channel transistor **208** connected in series with the first N-channel transistor **212**) is coupled to the right leg of the charge pump circuit (comprising the second P-channel transistor **210** connected in series with the second N-channel transistor **214**) using a first capacitor **Cp 216**. The source of the second P-channel transistor **214** is coupled to a second capacitor, an output capacitor, **C 218**, as shown. Two non-overlapping clock control signals, “Clk1” and “Clk2”, are used to control the operation of the transistors **208**, **210**, **212** and **214**. For example, as shown in FIG. **5b**, the inverse of “Clk1”, “Clk1<sub>̄</sub>”, control the gates of the P-channel transistors **208**, **210**. The other non-overlapping clock control signal, “Clk2”, controls the gate of the N-channel transistors **212**, **214**, as shown.

The charge pump **206** generates a negative power supply voltage ( $-V_{dd}$ ) by alternately charging and discharging the two capacitors (**Cp 216** and the output capacitor **C 218**) using the non-overlapping clock input signals **Clk1** and **Clk2** to drive the transistor gates. The negative power supply voltage,  $-V_{dd}$ , is generated from the charge that is stored on the capacitor **C 218**. In one embodiment, a pulse shift circuit (not shown) is used to generate a pulse train that drives the charge pump (i.e., the pulse train is input as the clock input signals **Clk1** and **Clk2**). As the pulse train is applied to the charge pump **206**, the capacitor **Cp 216** is applied the positive power supply **V<sub>dd</sub>** and then discharged across the output capacitor **C 218** in an opposite direction to produce the negative power supply voltage  $-V_{dd}$ . No transistor in the charge pump must standoff more than **V<sub>dd</sub>** across any source/drain nodes, hence greatly increasing the reliability of the charge pump **206**.

In one embodiment of the inventive charge pump circuit **206**, the output **C 218** has a capacitance of approximately 200 pF, and **Cp 216** has a capacitance of approximately 50 pF. Those skilled in the charge pump design arts shall recognize that other capacitance values can be used without departing from the scope or spirit of the present method and apparatus.

In one embodiment, as shown in the simplified block diagram of FIG. **5a**, the two non-overlapping clock signals are derived from an oscillator signal generated by an internal oscillator **202**. As shown in FIG. **5a**, the oscillator **202** inputs an oscillation signal to a clock generator circuit **204**, which in turn, generates the two non-overlapping clock signals (in any convenient well known manner) that control the charge pump transistor gates. In one embodiment of the present inventive fully integrated RF switch **100**, the oscillator **202** comprises a relatively low frequency (on the order of a few MHz) oscillator. In this embodiment, the oscillator comprises a simple relaxation oscillator. However, as those skilled in the integrated circuit arts shall recognize, other types of oscillators can be used to practice the present method and apparatus without departing from its spirit or scope.

FIG. **5c** shows the voltage amplitude of the two non-overlapping clock signals, **Clk1** and **Clk2**, varying over time. As shown in FIG. **5c**, the two non-overlapping clock signals vary in voltage amplitude from  $-V_{dd}$  to  $+V_{dd}$ . In one embodiment, the clock signals vary from  $-3$  VDC to  $+3$  VDC. This arrangement improves the efficiency of the charge pump **206**.

The charge pump transistors, **208**, **210**, **212** and **214** advantageously comprise single-threshold N-channel (**212**, **214**) and P-channel (**208**, **210**) devices. Previous charge pump circuits require use of multi-threshold level devices. These previous implementations are therefore more complex in design and cost than the inventive charge pump circuit **206** of FIG. **5b**. In one embodiment of the present charge pump **206**,

16

the P-channel transistors **208**, **210** have widths of approximately 20 micro-meters, and lengths of approximately 0.8 micro-meters. The N-channel transistors **212**, **214** have widths of approximately 8 micro-meters, and lengths of approximately 0.8 micro-meters. Those skilled in the integrated circuit design arts shall recognize that other transistor dimensions can be used without departing from the scope or spirit of the present method and apparatus. The inventive charge pump circuit **206** is very efficient and performs well despite temperature and process variations.

#### Level Shifting Circuitry

Because the charge pump circuitry effectively doubles the power supply voltages that are applied to the circuit, careful attention must be paid to any potential reliability issues associated with these higher voltages. In order to implement the charge pump in a manner that increases the reliability of the transistors, level shifting circuitry is used to limit the gate-to-source, gate-to-drain, and drain-to-source voltages on the transistors to acceptable levels.

An inventive level shifting circuit **300** made in accordance with the present method and apparatus is shown in FIG. **6a**. The level shifting circuit **300** is used to convert or shift typical or “normal” digital input signals (digital signals typically range from ground (GND) to  $+V_{dd}$ ) such that they range from  $-V_{dd}$  to  $+V_{dd}$ . The reliability of the fully integrated RF switch transistors is thereby increased. In one embodiment of the present method and apparatus, the control signals are shifted to  $-3$  VDC to  $+3$  VDC, although those skilled in the RF switch control arts shall recognize that other level shifting voltage ranges can be used without departing from the spirit or scope of the present method and apparatus.

As shown in FIG. **6a**, the inventive level shifting circuit **300**, hereinafter referred to as the level shifter **300**, comprises a plurality of inverters coupled in a feedback configuration. More specifically, in the embodiment shown in FIG. **6a**, the level shifter **300** includes two groups of inverters used to generate first and second shifted output signals, “out” on a first output node **314**, and its inverse “out<sub>̄</sub>” on a second output node **316**. The first group of inverters comprises inverters **302**, **304** and **306**. A second group of inverters comprises inverters **308**, **310** and **312**. A typical or “normal” digital input signal (i.e., a digital input signal that ranges from GND to  $+V_{dd}$ ) is input to the level shifter **300** at an input node **318** of a first inverter **320**. The first inverter **320** generates a first input signal “in” (on an output node **324**) which is input to a second inverter **322**. The second inverter **322** generates a second input signal “in<sub>̄</sub>”, the inverse of the first input signal “in”, on an output node **326**. Therefore, the first and second inverters, **320**, **322**, generate the signals that are input to the two groups of inverters described above. For example, the first input signal “in” is coupled to the input **328** of the inverter **302**. Similarly, the second input signal “in<sub>̄</sub>” is coupled to the input **330** of the inverter **308**.

The output of the first group of inverters, “out”, is generated by a first output inverter **306**, and is provided on a first output node **314**. The output of the second group of inverters, “out<sub>̄</sub>”, is generated by a second output inverter **312**, and is provided on a second output node **316**. The two level shifter outputs, “out” and “out<sub>̄</sub>”, are input to other circuits of the fully integrated RF switch **100** of FIG. **4**. For example, in one embodiment, the first output, “out”, is coupled to the gates of the devices of the switching transistor grouping **33** and the shunting transistor grouping **38** (i.e., the “out” signal on the first output node **314** of FIG. **6a** is coupled to the “SW” control input signal of FIG. **3**, at the input nodes **33'** and **38'**, and thereby controls the operation of the switching transistor grouping **33** and the shunting transistor grouping **38** as

described above with reference to FIG. 3). Similarly, in this embodiment, the second level shifter output, “out\_”, is coupled to the “SW\_” control input signal of FIG. 3 (at the input nodes 34' and 37') and thereby controls the switching transistor grouping 34 and the shunting transistor grouping 37 as described above.

The level shifter 300 of FIG. 6a shifts the DC level of an input signal (i.e., the input signal provided on the input node 318) while leaving the frequency response of the input signal unchanged. The level shifter 300 takes full advantage of the floating technology offered by the silicon-on-insulator substrate implementation of the fully integrated RF switch 100. The inverters of the level shifter 300 operate on a differential basis, i.e., the level shifter shifts the digital input signals based upon the difference between two voltage signals. More specifically, as long as the difference between the power supply signals provided to the inverters (such as, for example, the output inverters 306 and 312) is on the order of Vdd, the level shifter 300 reliably functions to shift the input signals to a range between -Vdd to +Vdd. In one embodiment, Vdd is equal to 3 VDC. In this embodiment, the transistors comprising the inverters of the level shifter 300 (e.g., the output inverters 306 and 312) never have greater than 3 VDC applied across their source/drain nodes. This increases the reliability of the transistor devices.

Referring again to FIG. 6a, the level shifter uses a feedback approach to shift the digital input signals to voltage levels ranging from -Vdd to +Vdd. Specifically, the output of the second group of inverters (308, 310, 312) on the second output node 316 (i.e., the “out\_” signal) is provided as feedback to an input of the first group of inverters at the input of the inverter 304. Similarly, the output of the first group of inverters (302, 304, 306) on the first output node 314 (i.e., the “out” output signal) is provided as input to the second group of inverters, specifically, is provided as input to the inverter 310.

When the digital input signal on the input node 318 reaches a logical “high” state (i.e., in some embodiments, when the input signal transitions from GND to +Vdd), the “in” signal (at the node 324) and the “in\_” signal (at the node 326) go to ground (e.g., 0 VDC) and Vdd (e.g. 3 VDC), respectively. The “out” signal at the first output node 314 is driven to +Vdd. At the same time, the “out\_” signal at the second output node 316 is driven towards -Vdd. The feedback (of “out\_” fed back to the input of the inverter 304 and “out” fed forward to the input of the inverter 310) configuration ensures the rapid change in state of the level shifter 300. The level shifter 300 works similarly when the input signal transitions from a logic high to a logic low state (i.e., transitions from +Vdd to GND). When the digital input signal on the input node 318 reaches a logic “low” state, the “in” signal (at the node 324) and the “in\_” signal (at the node 326) go to Vdd (e.g., 3 VDC), and ground, respectively. The “out” signal at the first output node 314 is driven to -Vdd. At the same time, the “out\_” signal at the second output node 316 is driven towards +Vdd. The feedback again ensures the rapid change in state of the level shifter 300. The grounding contribution ensures that the level shifter inverters never see more than a full Vdd voltage drop across the source/drain nodes of the MOSFET transistors of the inverters.

FIG. 6b shows one embodiment of the inverters (e.g., the inverters 302, 304, and 306) used to implement the level shifter 300 of FIG. 6a. As shown in FIG. 6b, the inverter 340 includes two MOSFET devices, a P-channel transistor 342 and an N-channel transistor 344. The devices are connected in series as shown, having their gates coupled together and controlled by an input signal provided at an input node 346.

The source of the P-channel transistor 342 is coupled to a first power supply voltage signal at node 350, while the source of the N-channel transistor 344 is coupled to a second power supply voltage signal at a node 352. The device drains are coupled together as shown to produce an output of the inverter at an output node 348. In one embodiment of the present inventive inverter 340, the P-channel transistor 342 has a width of 5 micro-meters and a length of 0.8 micro-meters. In this embodiment, the N-channel transistor has a width of 2 micro-meters and a length of 0.8 micro-meters. Those skilled in the transistor design arts shall recognize that other physical dimensions can be used for the transistors of the inverter 340 without departing from the scope or spirit of the present method and apparatus. A logical representation of the inverter 340 is also shown as symbol 360 in FIG. 6b.

Thus, using the present inventive level shifter 300, digital input signals that initially range from GND to +Vdd are shifted to range from -Vdd to +Vdd. FIG. 7a shows a voltage amplitude versus time plot of the digital input signal and the corresponding output signal that is generated by the inventive level shifter 300 of FIG. 6a. As shown in FIG. 7a, the digital input signal ranges from ground, or 0 VDC to Vdd. The output of the inventive level shifter 300 ranges from -Vdd to +Vdd. In one embodiment of the present inventive RF switch, the input signal ranges from 0 VDC to +3 VDC, and the output of the level shifter 300 ranges from -3 VDC to +3 VDC. Other values of power supply voltages can be used without departing from the scope or spirit of the present method and apparatus. For example, in one embodiment, the input signal can range from 0 to +3.5 VDC, or from 0 to 4 VDC. In this embodiment, the level shifter shifts the signal to range from -3.5 (or -4) VDC, to +3.5 (or +4) VDC.

FIG. 7b shows a simplified logic symbol for the inventive level shifter 300 of FIG. 6a. This logic symbol is used in subsequent figures. As shown in FIG. 7b, the digital input signal is provided on the input node 318 (the same input node 318 described above with reference to FIG. 6a). The level shifter 300 provides two shifted outputs, “out” and its inverse “out\_”, and these are provided on output nodes 314 and 316, respectively (the same output nodes 314, 316 described above with reference to FIG. 6a).

#### RF Buffer Circuit

FIG. 8a is an electrical schematic of a two-stage level shifter and RF buffer circuit 400. FIG. 8b is a simplified block diagram of the digital control input and interface to the RF buffer circuit 400. The two-stage level shifter and RF buffer circuit 400 of FIG. 8a comprises a first stage level shifter 300 and a second stage RF buffer circuit 402. The first stage level shifter 300 is identical to that described above with reference to FIGS. 6a, 6b, 7a and 7b, and is therefore not described in more detail here. As described above, the level shifter stage 300 shifts the logic levels of the digital control signals to range from -Vdd and +Vdd. The second stage of the circuit 400 comprises the RF buffer circuit 402. The RF buffer circuit 402 acts as a driver stage only (i.e., no level shifting is performed by the RF buffer circuit).

The RF buffer electrically isolates the digital control signals (such as those generated by the CMOS logic block 110 of FIG. 4) from the RF switch 30 described above with reference to FIG. 3. The RF buffer 402 functions to inhibit drooping of the control voltages (SW, SW\_, which are also referred to herein and shown in FIG. 8a as the control signals “out” and “out\_”, respectively) that control the enabling and disabling of the transistors in the RF switch 30. As described below in more detail, the RF buffer 402 also functions to prevent coupling of large power RF signals to the negative power supply (i.e., -Vdd) that is generated by the charge pump circuit 206

described above with reference to FIGS. 5a-5c. More specifically, the RF buffer 402 prevents large power RF signals extant in the RF switch 30 from RF-coupling to, and thereby draining current from, the negative power supply generated by the charge pump 206 (FIG. 5b).

When very large power RF input signals are input to the inventive RF switch 30, coupling of the RF signals to the digital logic signals can occur unless an RF buffer circuit is used to isolate the digital logic signals from the RF switch. The RF coupling can and usually will detrimentally affect the RF transistor control signals (SW and SW<sub>-</sub>). For example, when RF input signals on the order of approximately 30 dBm are input to a 1 watt RF switch 30, RF coupling can cause voltage swings of several tenths of a volt on the digital control lines. This is due to the feedback of RF signals from the RF switch through to the digital control circuitry. This RF coupling effect can adversely affect the enabling and disabling of the RF transistor groupings and hence the proper operation of the RF switch 30. The buffer circuit 402 of FIG. 8a prevents the undesirable RF coupling effect.

As shown in FIG. 8a, the inventive buffer circuit 402 is very similar in configuration to the level shifter 300 described above and shown as the first stage of the two-stage circuit 400. Similar to the level shifter 300, the RF buffer 402 comprises two groups of inverters, a first group of inverters (404, 406 and 408) and a second group of inverters (410, 412, and 414). The output of the first group of inverters (404, 406, and 408), generated by the first output inverter 408, is labeled "out" in the figure and is provided at a first output node 416. The output of the second group of inverters (410, 412, and 414), generated by the second output inverter 414, is labeled "out<sub>-</sub>", and is provided at a second output node 418. The output signal "out<sub>-</sub>" is the inverse of the output signal "out".

Importantly, although the first stage level shifter 300 uses feedback to perform the level shifting function (as described above with reference to FIG. 6a), the RF buffer circuit 402 does not feedback its output signals to the input. Consequently, the digital input signals input to the first stage (i.e., the control input signals that are input to the level shifter 300 at the nodes 328 and 330) are isolated from the output signals that are used to control the RF switch transistors (i.e., the control output signals "out" and its inverse signal "out<sub>-</sub>" at the output nodes 416 and 418, respectively, and coupled to the SW and SW<sub>-</sub> control signal lines, respectively).

More specifically, and referring again to FIG. 8a, the level shifter 300 inputs the digital control signals "in" and its inverse signal "in<sub>-</sub>" at the nodes 328, 330 respectively (as described in more detail above with reference to FIG. 6a). The first output of the level shifter 300, "out1", at the output node 314, is fed back to the input of the inverter 310 as shown. Similarly, the second output of the level shifter 300, "out1<sub>-</sub>", at the output node 316, is fed back to the input of the inverter 304. As described above, because of this feedback topology, RF coupling occurs (i.e., the level shifter output signals have RF signals superimposed thereon) if the output signals of the level shifter are used to directly control the RF switch transistors (i.e., in the absence of the buffer circuit 402). Therefore the inventive RF buffer circuit 402 is used without feedback of the output signals to isolate the input signals (i.e., the digital input signals "in" and "in<sub>-</sub>" from the RF signals present in the RF switch. As shown in FIG. 8a, the first output signal "out1" of the level shifter 300 is input to the inverters 404, 406 of the RF buffer circuit. Similarly, the second output signal "out1<sub>-</sub>" of the level shifter 300 is input to the inverters 410, 412 of the buffer circuit. The two control outputs of the RF buffer circuit 402 ("out" and "out<sub>-</sub>") control the enabling and disabling of the transistors of the RF switch and are not

provided as feedback to the level shifter. Hence, improved isolation between the RF switch and the digital logic circuitry is achieved.

In one embodiment, the inverters used to implement the two-stage level shifter and RF buffer circuit 400 comprise the inverter 340 described above with reference to FIG. 6b. However, those skilled in the inverter design arts shall recognize that alternative inverter designs can be used in implementing the two-stage circuit 400 without departing from the scope or spirit of the present method and apparatus. In one embodiment, the transistors used to implement the first stage level shifter 300 are physically smaller than those used to implement the second stage RF buffer circuit 402. Larger dimension transistors are used in the RF buffer circuit 402 to achieve an efficient amplification of the control signals. For example, in one embodiment, the transistors used to implement the RF buffer are three times wider than those used to implement the level shifter 300, resulting in an amplification of approximately three times the current. Those skilled in the transistor design arts shall recognize that other convenient transistor dimensions can be used to achieve any desired amplification of the digital control signals.

Voltage Divider for Use in an Alternative Level Shifting Circuit

FIG. 9a is an electrical schematic of one embodiment of a low current voltage divider ("LCVD") circuit 500 that is used in the feedback path of one embodiment of the level shifter 300 described above with reference to FIG. 6a. FIG. 9b shows a simplified logic symbol that is used to represent the voltage divider 500 of FIG. 9a. The voltage divider 500 is used in one embodiment to address potential gate oxide reliability issues related to excessive voltage swings across the gate oxides of the feedback inverter transistors. As described above with reference to the level shifter 300, although the source-to-drain voltages of the various MOSFETs used to implement the level shifter are never applied voltages greater than V<sub>dd</sub>, because the outputs of the level shifter (i.e., the output signals "out" and "out<sub>-</sub>" can swing as much as 2\*V<sub>dd</sub> (i.e., from -V<sub>dd</sub> to +V<sub>dd</sub>), the gate oxides of the feedback inverters 304 and 310 can have applied voltages of 2\*V<sub>dd</sub>. These feedback voltage levels can be applied across the gate oxides of the feedback inverters 304, 310, and can result in gate oxide reliability problems.

The gate oxide reliability issues can be averted by ensuring that the maximum voltage applied across the gate oxide of the feedback inverters 304, 310 is lowered to approximately V<sub>dd</sub> (as contrasted with gate oxide voltages of 2\*V<sub>dd</sub>). Therefore, in one embodiment of the present inventive fully integrated RF switch, the voltage divider of FIG. 9a limits the voltages applied to the gates of the level shifter feedback inverters 304, 310. In this embodiment, instead of directly feeding back the level shifter outputs to their respective feedback inverters as shown in the level shifter of FIG. 6a (i.e., the outputs "out" and "out<sub>-</sub>", at the output nodes 314, 316, respectively), the level shifter output signals are first conditioned by the voltage divider 500 of FIG. 9a before being fed back to the feedback inverters. As described below in more detail, the voltage divider 500 ensures that the voltages applied to the gate oxides of the feedback inverters 304, 310 do not exceed more than approximately V<sub>dd</sub> plus a small voltage drop (the voltage drop being a function of the number of transistors used to implement the voltage divider 500 and a transistor threshold voltage). In one embodiment V<sub>dd</sub> is 3 VDC, and the voltage drop is 0.9 VDC. In this embodiment, the voltage divider 500 ensures that the gate oxides are never applied voltages exceeding approximately 3.9 VDC (i.e., the feedback inverters are applied voltages that range from -3 VDC to 0.9 VDC).

Referring now to FIG. 9a, the voltage divider 500 includes a plurality of MOSFET devices (502, 504, 506 and 508) coupled together in a serial configuration (i.e., stacked on top of each other in a source to drain arrangement as shown). In one embodiment, the gate and drain of the MOSFETs 502, 504, 506 and 508 are coupled together to implement stacked diodes. The diode-implementing MOSFETs, hereafter referred to as “diode devices”, are stacked in series as shown. The voltage divider 500 also includes a MOSFET M3 510 and an output MOSFET M2 512. The function of these two transistors is described in more detail below.

The diode devices are used to divide the voltage of an input signal provided to the voltage divider 500 at an input node 514. As shown in FIG. 9a, the signal that is divided by the voltage divider 500 is provided as input to the drain (and connected gate) of the first device 502. Once the input signal exceeds a positive voltage level of  $(n \cdot V_{thn})$ , where “n” is the number of diode devices used to implement the voltage divider 500, and  $V_{thn}$  is the threshold voltage of the device (i.e., the “diode-drop” from the drain to the source of the device), the diode devices (502, 504, 506, and 508) begin to conduct current heavily. In the embodiment shown in FIG. 9a,  $n=4$ , and  $V_{thn}=0.7$  volts, although alternative values for “n” and  $V_{thn}$  can be used without departing from the scope or spirit of the present method and apparatus. For example, in other embodiments, the input signal provided to the divider can be limited to any desired voltage level by varying the number of diode devices used to implement the voltage divider 500 (i.e., by varying the value of “n”). In the embodiment shown in FIG. 9a, once the input voltage exceeds a voltage level of  $(4 \cdot 0.7)$ , or 2.8 volts, the stacked diode devices begin conducting heavily.

A ballast resistor, R 516, is connected to the source of the output diode device 508 as shown. Once the diode devices turn on fully, the ballast resistor R 516 drops any additional input voltage that exceeds the value of  $n \cdot V_{thn}$ . In the embodiment shown in FIG. 9a, the ballast resistor R 516 drops any additional input voltage exceeding the value of  $(input\ voltage - (4 \cdot V_{thn}))$ . The output of the voltage divider 500 is tapped from the connected gate-drain of the output diode device 508. The voltage-divided output signal is provided on an output node 520. Due to the diode voltage drops of the diode devices 502, 504, 506, (i.e.,  $3 \cdot V_{thn}$ ), and the voltage dropped across the ballast resistor R 516, the output at the output node 520 is guaranteed to never exceed approximately  $(input\ voltage - (3 \cdot V_{thn}))$ . For  $V_{thn}$  approximately 0.7 volts, and a maximum input voltage of approximately 3 volts, the output node 520 will never exceed  $(3\ VDC - (3 \cdot 0.7\ VDC))$ , or 0.9 VDC. Thus, in the embodiment shown in FIG. 9a, for an input voltage ranging between -3 VDC to +3 VDC, the voltage divider 500 limits the output of the output node 520 to a range of -3 VDC to 0.9 VDC.

The output MOSFET M2 512 is configured as a capacitor and is used to assist in accelerating the switching time of the voltage divider 500. The MOSFET M3 510 assures that the output node 520 swings to the potential of the input signal at the input node 514 when the input goes to a negative potential. This is accomplished by the device M3 510 turning on when the input signal goes to a negative potential. Thus, when the input signal goes to a  $-V_{dd}$  potential (e.g., -3 VDC), the output signal at the output node 520 also goes to  $-V_{dd}$ . The output device 508 is reversed biased during negative voltage swings of the input signal assuring that no DC current is drained from the negative power supply during the negative voltage swings of the input signal. When the voltage divider output is approximately -3 VDC, the voltage divider 500 draws no current. This is important because a current at -3

VDC discharges the charge pump circuit described above with reference to FIG. 5b. When the voltage divider output is approximately 0.9 volts, the current that is drawn is very small if the ballast resistor R 516 is selected to be relatively large. However, because the current in this case occurs between a positive voltage (0.9 volts) and ground, no additional charge pump current is delivered due to the operation of the voltage divider 500 of FIG. 9a.

In one embodiment, the ballast resistor R 516 has a value of 100 k-ohms. In one embodiment all of the devices of the voltage divider 500 have the same length. For example, in one embodiment, all of the devices have a length of 0.8 micrometers. In one embodiment, all of the diode devices (502, 504, 506, and 508) have identical physical dimensions. In one embodiment, the diode devices each have a width of 2 micrometers, the device M3 510 has the same width of 2 micrometers, and the output MOSFET M2 512 has a width of 14 micrometers. Those skilled in the integrated circuit design arts shall recognize that other values and alternative configurations for the devices shown in FIG. 9a can be used without departing from the scope or spirit of the present method and apparatus. For example, those skilled in the electrical circuit design arts shall recognize that other voltage divider output levels can easily be accommodated by varying the number “n” of diode elements, varying the values of  $V_{thn}$ , or by tapping the output node 520 at a different point in the stack of diode devices (e.g., by tapping the output from the drain of diode device 506, or 504, instead of from the drain of device 508 as shown).

#### Modified Level Shifter Using the Voltage Divider

By reducing the voltages that are applied to the gate oxides of the RF switch transistors, the voltage divider 500 of FIGS. 9a and 9b advantageously can be used to increase the reliability of the transistors in both the level shifter 300 and the charge pump circuit described above. For example, FIG. 10 shows a modified level shifter 600 using the voltage divider 500 of FIG. 9a in combination with the level shifter 300 of FIG. 6a. As shown in FIG. 10, the output (at output node 314) of the inverter 306 of the level shifter 300 is applied to an input of a first voltage divider 500'. Similarly, the output (at the output node 316) of the inverter 312 of the level shifter 300 is applied to an input of a second voltage divider 500". The outputs of the voltage dividers are fed back to the input of the feedback inverters 304, 310 as shown in FIG. 10. Specifically, and referring to FIG. 10, the output of the first voltage divider, “out\_”, on the output node 520' is fed back to the input of the feedback inverter 310. Similarly, the output of the second voltage divider, “out\_”, on the output node 520" is fed back to the input of the feedback inverter 304. As described above with reference to FIG. 9a, the level shifters 500' and 500" reduce the feedback voltages to ranges of  $-V_{dd}$  to approximately +0.9 VDC. This reduced voltage swing on the feedback paths does not alter the function of the level shifter 600.

Note that the RF switch control signals, “SW” and “SW\_”, can be tapped from the level shifter outputs prior to their input to the voltage dividers 500' and 500", and provided as input to the inventive RF switch 30 of FIG. 3. For example, as shown in FIG. 10, the output of inverter 306 at the output node 314 can be tapped and used to generate the switch control signal “SW”. Similarly, the output of the inverter 312 at the output node 316 can be tapped and used to generate the switch control signal “SW\_”. In one embodiment, as described above with reference to the two-stage level shifter and RF buffer circuit 400 of FIG. 8a, the control signals tapped from the nodes 314, 316 are first buffered before being coupled to the RF switch transistors. The switch control signals, SW and SW\_, are allowed to have a full-rail voltage swing which does not create gate oxide reliability problems in the RF switch.

More specifically, the switch control signals range from  $-V_{dd}$  to  $+V_{dd}$  (i.e., the voltage levels of the switch control signals are not limited by the voltage dividers). The full voltage swings of the switch control signals do not raise gate oxide reliability issues with respect to the RF switch MOSFETs because the sources of the RF switch MOSFETs are grounded. The switch input signals are therefore relative to ground in the RF switch MOSFETs. Consequently, the MOSFETs are applied either a positive  $V_{dd}$  voltage relative to ground across the gate oxides, or a negative  $V_{dd}$  voltage relative to ground across the gate oxides.

FIG. 10 also shows a simplified symbolic representation 601 of a section of the modified level shifter 600. The symbol 601 represents the portion indicated by the dashed region 601' of FIG. 10. As shown in FIG. 10, the symbolic modified level shifter 601 includes a first input "in\_" 630 corresponding to the input node 326 ("in\_"). The symbolic level shifter 601 also includes a second input "out" 632 corresponding to the input to the feedback inverter 310. Note that this signal is also derived from the output 520' of the first voltage divider 500'. A positive power supply voltage is input at a  $+V_{dd}$  input 634. A negative power supply voltage is input at a  $-V_{dd}$  input 636. The modified level shifter 601 has three output signals, "out\_pos" (at output 638), "out\_neg" (at output 640), and "out" (at output 642). These outputs correspond to the output nodes 606, 608, and 520' described above. For ease of understanding, the symbolic representation of the level shifter 601 is used in the figures described below.

The potential gate oxide reliability problems associated with the level shifter 300 described above with reference to FIG. 6a are averted using the voltage dividers 500' and 500" in the feedback paths of the modified level shifter 600. In addition, the voltage dividers 500' and 500" can also function to reduce potential gate oxide reliability problems associated with the charge pump circuit. As shown in FIG. 10, the outputs of the inverters 308 and 310 are tapped from the level shifter 300 and provided as input to two output inverters to produce two output signals, "out\_pos" and "out\_neg." More specifically, the output of the inverter 308 is provided as input to a first output inverter 602. Similarly, the output of the feedback inverter 310 is provided as input to a second output inverter 604.

By coupling the output inverters 602, 604 in this manner, the modified level shifter 600 output signals never exceed  $V_{dd}$  (or  $-V_{dd}$ ). More specifically, the first output inverter 602 generates an output signal, "out\_pos", at a first output node 606, that ranges from GND (i.e., 0VDC) to  $+V_{dd}$ . The second output inverter 604 generates a second output signal, "out\_neg", at a second output node 608, which ranges from  $-V_{dd}$  to GND. When the input signal "in\_" goes to GND, the output signal "out\_pos" also goes to GND. The output signal "out\_neg" transfers from GND to  $-V_{dd}$ . When the input signal "in\_" goes positive to  $+V_{dd}$ , "out\_pos" also goes to  $V_{dd}$ , and "out\_neg" transfers from  $-V_{dd}$  to GND. Thus, using the present modified level shifter 600, the "out\_pos" output signal ranges from GND to  $+V_{dd}$ , while the "out\_neg" output signal ranges from  $-V_{dd}$  to GND. As described below in more detail, the two output signals, "out\_pos" and "out\_neg", are used to address potential gate oxide reliability problems in a modified charge pump circuit. As described now with reference to FIGS. 11a and 11b, these output signals can also be used to address potential gate oxide reliability problems in the RF buffer circuit.

#### Modified Level Shifter and RF Buffer Circuit

The two-stage level shifter and RF buffer 400 described above with reference to FIG. 8a can experience voltage swings at the RF buffer inverter inputs of approximately

$2*V_{dd}$ . As already described, this level of voltage swing may present gate oxide reliability problems and detrimentally affect the function of the RF buffer transistors.

FIGS. 11a and 11b show an alternative embodiment 400' of the two-stage level shifter and RF buffer circuit 400 described above with reference to FIG. 8a. The alternative embodiment of the RF buffer shown in FIG. 11b uses the voltage divider circuit described above to assure that voltages on the gate oxides of the RF buffer never exceed greater than 0.9 volts above  $V_{dd}$ . As shown in FIG. 11b, the alternative two-stage level shifter and RF buffer circuit 400' includes a first stage level shifter circuit 600 coupled to a second stage RF buffer circuit 402'. In this embodiment of the level shifter and RF buffer circuit 400', the modified level shifter outputs, "out\_pos" and "out\_neg", described above with reference to FIG. 10, are used as input to the RF buffer inverters to generate the RF buffer output signals "out" and "out\_". For example, as shown in FIG. 11b, the "out\_pos" and "out\_neg" output signals generated by a first modified level shifter 700 are input to two RF buffer inverters, 702, 704, respectively. Similarly, the "out\_pos" and "out\_neg" output signals generated by a second modified level shifter 706 are input to two RF buffer inverters, 708, 710, respectively. In accordance with the alternative embodiment 400' shown in FIGS. 11a and 11b, when an input signal "in" is a logical high signal, the "out\_pos" output goes to  $V_{dd}$  while the "out\_neg" goes to GND. Thus, when the input signal "in" is a logical high value, the output of the inverter 702 goes to GND, and the output of the inverter 704 goes to  $-V_{dd}$ . Therefore, when the input signal "in" is high, the output of the inverter 712 ("out") goes to  $-V_{dd}$ . When the input signal "in" is low, the opposite outputs are produced.

The RF buffer inverters 702, 704 are used to control the power supply voltages of a first RF output inverter 712. Similarly, the RF buffer inverters 708, 710 are used to control the power supply voltages of a second RF output inverter 714. In this embodiment, the RF buffer output signals, "out" and "out\_", are used to control the RF switch (i.e., output signal "out" acts as control voltage "SW", while "out\_" acts as control voltage "SW\_").

#### Modified Charge Pump—An Alternative Embodiment

As noted above, the two output signals "out\_pos" and "out\_neg" generated by the modified level shifter 600 of FIG. 10 can be used in an alternative embodiment of the charge pump circuit to reduce or eliminate potential gate oxide reliability problems associated with excessive voltages applied to the charge pump. As described above with reference to FIGS. 5b and 5c, the clock signals used to control the gates of the charge pump transistors (i.e., the P-channel transistors 208, 210, and the N-channel transistors 212, 214) have voltage swings of  $2*V_{dd}$ . For example, as shown in FIG. 5c, the charge pump clock signals, "Clk1" and "Clk2", range from the negative power supply voltage  $-V_{dd}$  to the positive power supply voltage  $+V_{dd}$ . Similar to the gate oxide reliability issues described above with reference to the RF buffer and level shifter circuits, this full-rail voltage swing may present oxide reliability problems in the charge pump circuit. Therefore, a modified charge pump circuit is shown in FIG. 12 which reduces or eliminates potential gate oxide reliability problems by limiting the voltages applied to gate oxides to range from  $-V_{dd}$  to 0.9 volts.

FIG. 12 shows a modified charge pump 800 that uses the modified level shifter 600 described above with reference to FIG. 10. As shown in FIG. 12, the modified charge pump 800 comprises a charge pump circuit 206' and an inventive charge pump clock generation circuit 802. The charge pump clock

generation circuit **802** generates the clock control signals used by the charge pump circuit **206'**. The charge pump circuit **206'** is very similar in design to the charge pump **206** described above with reference to FIG. **5b**. For example, the charge pump **206'** includes a pair of P-channel transistors **208**, **210**, and a pair of N-channel transistors **212**, **214**, in addition to a pass capacitor **Cp 216** and an output capacitor **C 218**. In one embodiment of the charge pump circuit **206'**, the output capacitor **C 218** has a capacitance on the order of a few hundred pF, and the capacitor **Cp 216** has a capacitance of approximately 50 pF. Those skilled in the charge pump design arts shall recognize that other capacitance values can be used without departing from the scope or spirit of the present method and apparatus.

The charge pump **206'** functions very similarly to the charge pump **206** described above with reference to FIG. **5a**, and therefore its operation is not described in detail again here. The charge pump **206'** shown in FIG. **12** differs from the charge pump **206** in that the control signals used to control the charge pump **206'** transistor gates (i.e., the gates of the transistors **208**, **210**, **212**, and **214**) are limited to half-rail voltage swings (i.e., they are limited to range from  $-V_{dd}$  to ground, or from ground to  $V_{dd}$ ). Potential gate oxide reliability problems invoked when the gate control voltages are allowed to swing a full rail (i.e., from  $-V_{dd}$  to  $V_{dd}$ ) are thereby reduced or eliminated.

As shown in FIG. **12**, the charge pump clock generation circuit **802** includes four modified level shifters **804**, **806**, **808** and **810**, coupled together in a feedback configuration. In one embodiment of the modified charge pump, the four modified level shifters are implemented by the modified level shifter **600** described above with reference to FIG. **10**. FIG. **12** shows the level shifters using the symbolic representation **601** of the level shifter **600** of FIG. **10**. In this embodiment, the level shifters **804**, **806**, **808**, and **810** perform identically to the level shifter **600** of FIG. **10**. The two non-overlapping clock signals, "Clk1", and "Clk2" (and their inverse signals, "Clk1\_" and "Clk2\_", respectively) are input to the "in\_" inputs of the level shifters as shown in FIG. **12**. The two input clock signals, "Clk1" and "Clk2", are identical to the non-overlapping clock signals described above with reference to FIGS. **5a-5c**. As shown above with reference to FIG. **5c**, the two non-overlapping clock signals vary in voltage amplitude from  $-V_{dd}$  to  $+V_{dd}$ . In one embodiment, the clock signals vary from  $-3$  VDC to  $+3$  VDC.

The four modified level shifters generate the half-rail clock control signals that are used to control the charge pump **206'**. Specifically, as shown in FIG. **12**, the four level shifters generate the "CLK1POS\_", "CLK1NEG\_", "CLK2POS", and "CLK2NEG" control signals that are input to the charge pump transistor gate control nodes **250**, **252**, **254** and **256**, respectively. In the embodiment shown in FIG. **12**, the level shifters **806** and **808** generate the four transistor gate control signals "CLK1POS\_", "CLK1NEG\_", "CLK2POS", and "CLK2NEG". The level shifter **806** generates the "CLK1POS\_" and "CLK1NEG\_" gate control signals, while the level shifter **808** generates the "CLK2POS", and "CLK2NEG" gate control signals. More specifically, as shown in FIG. **12**, the "out\_pos" output of the level shifter **806** ("CLK1POS\_") is coupled to control the transistor gate input **250** of the transistor **208**. The "out\_neg" output of the level shifter **806** ("CLK1NEG\_") is coupled to control the transistor gate input **252** of the transistor **210**. Similarly, the "out\_pos" output of the level shifter **808** ("CLK2POS") is coupled to control the transistor gate input **254** of the transistor **214**. Finally, the "out\_neg" output of the level shifter **808** ("CLK2NEG") is coupled to control the transistor gate input

**256** of the transistor **214**. The clock generation circuit **802** functions to prevent excessive voltages across the gate oxides of the charge pump transistors.

Those skilled in the transistor design arts shall recognize that other control configurations can be used without departing from the spirit or scope of the present method and apparatus. For example, the other two level shifters (**804**, **810**) can be used to generate the control signals in an alternative embodiment of the modified charge pump. Also, as described above with reference to the charge pump circuit **206**, alternative transistor configurations (N-channel and P-channel) can be used to implement the modified charge pump **206'** of the present method and apparatus.

As shown in FIG. **12**, the four level shifters **804**, **806**, **808** and **810** are coupled together in level shifter pairs (**804** with **806**, and **808** with **810**) in a feedback configuration that is very similar to the feedback topology of the level shifter described above with reference to FIG. **6a**. For example, the "out" output node of the level shifter **804** is provided as feedback to the "out" node of its associated pair level shifter **806**. Similarly, the "out\_" output node of the level shifter **806** is provided as feedback to the "out\_" node of its associated pair level shifter **804**. Similarly, the "out\_" output node of the level shifter **808** is provided as feedback to the "out" node of its associated pair level shifter **810**. The "out\_" output node of the level shifter **810** is provided as feedback to the "out" node of its associated pair level shifter **808**. The feedback configuration is used by the clock generation circuit **802** in the generation of the four transistor gate control signals "CLK1POS\_", "CLK1NEG\_", "CLK2POS", and "CLK2NEG".

#### Summary

A novel RF switch is provided wherein the switch is fabricated using an SOI CMOS process. Fabricating the switch on an SOI substrate results in lack of substrate bias and allows the integration of key CMOS circuit building blocks with the RF switch elements. Integration of the CMOS building blocks with RF switch elements provides a fully integrated RF switch solution that requires use of only a single external power supply (i.e., the negative power supply voltage is generated internally by a charge pump circuit integrated with the RF switch). This results in improvements in RF switch isolation, insertion loss and compression. In one embodiment, the RF switch has a 1 dB compression point exceeding approximately 1 Watt, an insertion loss of less than approximately 0.5 dB, and switch isolation as high as approximately 40 dB. The inventive switch also provides improvements in switching times.

A number of embodiments of the present method and apparatus have been described. Nevertheless, it will be understood that various modifications may be made without departing from the spirit and scope of the method and apparatus.

Accordingly, it is to be understood that the present method and apparatus is not to be limited by the specific illustrated embodiments, but only by the scope of the appended claims.

What is claimed is:

1. A circuit, comprising:

- (a) a first port configured to receive a first RF signal;
- (b) a second port configured to receive a second RF signal;
- (c) an RF common port;
- (d) a first switch transistor grouping having a first node coupled to the first port and a second node coupled to the RF common port, wherein the first switch transistor grouping has a control node configured to receive a switch control signal (SW);
- (e) a second switch transistor grouping having a first node coupled to the second port and a second node coupled to

27

- the RF common port, wherein the second switch transistor grouping has a control node configured to receive an inverse (SW\_) of the switch control signal (SW);
- (f) a first shunt transistor grouping having a first node coupled to the second port and a second node coupled to ground, wherein the first shunt transistor grouping has a control node configured to receive the switch control signal (SW); and
- (g) a second shunt transistor grouping having a first node coupled to the first port and a second node coupled to ground, wherein the second shunt transistor grouping has a control node configured to receive the inverse (SW\_) of the switch control signal (SW),
- wherein the first switch transistor, the second switch transistor, the first shunt transistor, and the second shunt transistor are fabricated on a silicon-on-insulator (SOI) substrate, and wherein the SOI substrate comprises a thin-film substrate.
2. The circuit of claim 1, wherein the transistor groupings comprise a plurality of MOSFET transistors arranged in a stacked configuration.
3. The circuit of claim 1, wherein the circuit has an associated 1 dB compression point, and wherein the 1 dB compression point is increased using a stacked MOSFET transistor configuration.
4. A switch circuit, comprising:
- (a) the circuit as set forth in claim 1;
- (b) a control logic block, coupled to the circuit of claim 1, wherein the control logic block is configured to output the switch control signal (SW) and the inverse switch control signal (SW\_); and
- (c) a negative voltage generator, coupled to the control logic block, wherein the negative voltage generator is configured to receive a clocking input signal and a positive power supply voltage from an external power supply, and wherein the negative voltage generator is configured to output a negative power supply voltage.
5. The circuit of claim 4, wherein the circuit is integrated in an integrated circuit (IC) with a plurality of digital and analog circuits.
6. The circuit of claim 4, further including:
- (a) an oscillator, wherein the oscillator is configured to output clocking input signals;
- (b) a charge pump, coupled to the oscillator, wherein the oscillator is configured to input the clocking input signals, and wherein the charge pump is configured to output a negative power supply voltage;
- (c) a logic circuit block, coupled to the charge pump, wherein the logic circuit block is configured to output control signals for use in controlling the switch and shunt transistor groupings;
- (d) a level-shifting circuit, coupled to the logic circuit block and the circuit, wherein the level-shifting circuit is configured to reduce gate-to-drain, gate-to-source, and drain-to-source voltages of MOSFET transistors used to implement the transistor groupings; and
- (e) an RF buffer circuit, coupled to the circuit, wherein the RF buffer circuit is configured to isolate RF signal energy from the charge pump and the logic circuit blocks.
7. The circuit of claim 6, wherein the charge pump comprises:
- (a) at least two P-channel MOSFET transistors;
- (b) at least two N-channel MOSFET transistors, wherein each N-channel MOSFET transistor is coupled in series

28

- with a respective and associated P-channel MOSFET transistor thereby forming a respective leg of the charge pump;
- (c) at least one coupling capacitor coupling each leg of the charge pump coupled to a successive leg; and
- (d) an output capacitor, coupled to an output leg of the charge pump;
- wherein the charge pump is configured to generate the negative power supply voltage by alternately charging and discharging the coupling and output capacitors using non-overlapping input clocking signals to drive the P-channel and N-channel MOSFET transistors.
8. The circuit of claim 7, wherein the non-overlapping input clocking signals comprise two non-overlapping clock control signals, and wherein a first non-overlapping clock control signal controls the P-channel transistors, and wherein a second non-overlapping clock control signal controls the N-channel transistors.
9. The circuit of claim 7, wherein the P-channel and N-channel transistors comprise single-threshold transistors.
10. The circuit of claim 7, wherein a pulse shift circuit is configured to generate the non-overlapping input clocking signals.
11. The circuit of claim 7, wherein the non-overlapping input clocking signals are derived from the oscillator clocking input signals.
12. The circuit of claim 7, wherein the oscillator comprises a relaxation oscillator.
13. The circuit of claim 7, wherein the non-overlapping input clocking signals vary in voltage amplitude from -Vdd to +Vdd.
14. The circuit of claim 6, wherein the level-shifting circuit comprises a plurality of inverters coupled together in a feedback configuration.
15. The circuit of claim 14, wherein the inverters comprise differential inverters having a first differential input, a second differential input, a logic input and a logic output, and wherein the level-shifting circuit comprises:
- (a) an input inverter group comprising two input differential inverters, wherein a first input differential inverter is configured to receive a logic input signal (input) and to output a first logic input signal (in), and wherein a second input differential inverter is configured to receive the first logic input signal (in) and to output an inverse (in\_) of the first logic input signal;
- (b) a first inverter group comprising three differential inverters, wherein the logic output of a first inverter of the first inverter group is coupled to the first logic input signal (in), the logic output of the first inverter is coupled to a first differential input of an output inverter of the first inverter group, the logic output of a second inverter of the first inverter group is coupled to a second differential input of the output inverter of the first inverter group, and wherein the output inverter of the first inverter group is configured to output a first output signal (out); and
- (c) a second inverter group comprising three differential inverters, wherein the logic output of a first inverter of the second inverter group is coupled to the inverse (in\_) of the first logic input signal, the logic output of the first inverter of the second inverter group is coupled to a first differential input of an output inverter of the second inverter group, the logic output of a second inverter of the second inverter group is coupled to a second differential input of the output inverter of the second inverter group, and wherein the output inverter of the second inverter group is configured to output a second output signal (out\_);

wherein the circuit is configured to provide the first output signal (out) as feedback and input to the logic input of the second inverter of the second inverter group, and wherein the circuit is configured to provide the second output signal (out\_) as feedback and input to the logic input of the second inverter of the first inverter group. 5

16. The circuit of claim 15, wherein the switch and shunt transistor groupings are configured to be controlled by the first and second output signals.

17. The circuit of claim 14, wherein the level-shifting circuit is configured to shift the DC level of the logic input signal (input) without affecting the frequency response of the input signal. 10

\* \* \* \* \*